2020

Quantification and Modeling of Bladder Biomechanics Mechanisms Linking Spontaneous Rhythmic Contractions and Dynamic Elasticity to Detrusor Overactivity

Zachary E. Cullingsworth
Virginia Commonwealth University

Virginia Commonwealth University

College of Engineering

Department of Mechanical and Nuclear Engineering

Dissertation:

Quantification and Modeling of Bladder Biomechanics Mechanisms Linking Spontaneous Rhythmic Contractions and Dynamic Elasticity to Detrusor Overactivity

Zachary E. Cullingsworth, MS

Mechanical and Nuclear Engineering

Advisor:

John E. Speich, PhD

Professor of Mechanical and Nuclear Engineering

Contents

Acknowledgements

I would like to thank my family and friends for their support and encouragement through the years as I have worked towards this goal. In addition, I would like to thank members of my lab for their contributions to my work. Specifically, I would like to thank Dr. Anna Nagle for her many MATLAB tips, conference travel advice and research mentorship, Dr. Rui Li for insights in conducting statistical analysis, the Urology residents that have helped me in conducting pig bladder experiments and the many undergraduate and medical students that assisted throughout the entire process.

I am also grateful to have had Dr. Adam Klausner serve as one of my key research mentors. He has provided significant insights into not only the clinical implications and importance of this research, but also ways improving the presentation of my work, whether orally or in written form. Additionally, I am thankful to the National Institute of Health for their financial support.

Finally, I am thankful for my advisor, Dr. John Speich. He has supported and encouraged me throughout my graduate education journey. I owe all my research accomplishments and awards to his belief in the quality of my work and advice on how to best share that with the field, whether through conference abstracts, presentations or journal papers. Through these individuals, my personal and professional growth over the past four years has been more than I could have ever expected.

List of Abbreviations

CCap – Cystometric capacity

DE – Dynamic elasticity

DO – Detrusor overactivity

DSM – Detrusor smooth muscle

FFT – Fast Fourier transform

ICIq-OAB – International Consultation on Continence Overactive Bladder questionnaire

OAB – Overactive bladder

P_{abd} – Abdominal pressure (cm-H_2O)

P_{ves} – Vesical pressure (cm-H_2O)

S&I – Significant and independent

SRC – Spontaneous rhythmic contractions

UD – Urodynamics

List of Figures

List of Tables

Abstract

Overactive bladder (**OAB**) is a chronic filling phase condition affecting approximately 20% of adults in the United States. It is a complex disorder with often difficult to assess causes. Detrusor overactivity (**DO**) is the presence of isolated, sporadic or periodic non-voiding contractions in the detrusor (bladder) muscle during filling and is present in some individuals with OAB. DO is currently identified visually during an invasive procedure called a urodynamics (**UD**) study that involves urethral and rectal pressure catheters and filling and voiding of the bladder to evaluate its function. UD studies do not currently provide objective metrics for the diagnosis of DO. In addition, UD provides limited subtyping of DO, and an incomplete understanding of the biomechanical mechanisms that contribute to OAB in some individuals.

Aim 1 of this study was to develop objective tools to quantify, subgroup and better understand rhythmic DO. Using fast Fourier transforms, an objective algorithm for quantification of rhythmic DO was developed and implemented on retrospective bladder pressure data. During the retrospective study, the automated algorithm objectively identified a subgroup of participants with DO, quantified frequency and amplitude of the rhythmic DO, and provided a visual model for verification against the original data. The algorithm was then refined and applied during a prospective study in which participants were grouped by OAB symptoms and by the presence or absence of rhythmic DO. During the prospective study, rhythmic DO was characterized throughout filling and the amplitude of rhythmic activity correlated with OAB symptoms. The results indicate that high amplitude rhythmic DO may represent a clinically significant OAB subtype.

Aim 2 focused on dynamic elasticity (**DE**), which is a biomechanical bladder property that was identified in humans during a previous pilot UD study. DE may contribute to acute regulation of bladder wall tension during filling. The present research characterized dynamic elasticity in a

larger group of participants, including those with and without OAB symptoms. A conceptual model linking DO and dynamic elasticity was developed to describe how the presence or absence DO may affect the regulation of bladder wall tension through the mechanisms of dynamic elasticity. This study identified a significant association between the presence of dynamic elasticity and the absence of DO, which supports the conceptual model and explains how DO could contribute to increased bladder wall tension during bladder filling and therefore contribute to OAB.

Aim 2 also contributed to the development of an ex vivo pig bladder model to study dynamic elasticity. A study comparing an invasive catheter filling method with a less invasive external compression method of manipulating dynamic elasticity was completed in the pig model. The pig bladder studies showed that dynamic elasticity could be quantified in this model, and non-invasive compression produced similar changes in dynamic elasticity as the invasive UD method used clinically.

In summary, novel tools to detect and quantify DO in a more objective fashion were developed and used to characterize a rhythm-mediated DO subtype and provide evidence that high amplitude rhythmic DO may be clinically significant. Dynamic elasticity was characterized in individuals with and without OAB and in an isolated pig bladder model, and a novel dynamic elasticity index was defined. Furthermore, the conceptual model linking detrusor overactivity and dynamic elasticity was tested, and a significant association between dynamic elasticity and the absence of DO was identified, indicating that DO may alter the bladder's ability to regulate wall tension through dynamic elasticity. These new techniques for quantifying DO and characterizing dynamic elasticity provided important insight into the regulation of bladder wall biomechanics through dynamic elasticity and how this regulation may be altered by DO in individuals with OAB.

Chapter 1 - Introduction and Motivation

1.1 Anatomy and Bladder Function

The upper urinary tract consists of a pair of bean-shaped kidneys. These organs filter the blood of toxins, regulate minerals in the blood and maintain fluid balance by removing excess water. As it is filtered from the blood, this mixture, known as urine, is transported through muscular tubes, called ureters, to the lower urinary tract where it finally enters the bladder. It is stored in the bladder during the collection, or filling, phase before eventually being evacuated through the urethra during voiding[1].

The urothelium is the innermost mucosal layer of the human bladder and is made up of five to seven epithelial cell layers. The lamina propria is the submucosal layer made up of collagen and provides support to the bladder wall. The detrusor is the muscular layer of the bladder and is characterized by three alternating layers of smooth muscle fibers[2].

These layers allow the bladder to perform several important functions during the collection phase. The urothelium helps maintain watertight containment preventing dangerous urine from seeping into different layers. The lamina propria and detrusor enable the bladder to maintain an efficient shape while being compliant to allow low pressure filling which prevents harmful reflux to the kidneys. When voiding, the detrusor smooth muscle contracts to provide the force needed to adequately empty. The bladder wall also provides filling sensation information to the brain through tension or strain sensors[3].

Three specific mechanical parameters directly affect the detrusor wall tension and therefore sensation, as shown in the model in Figure 1.1. Those parameters are the geometry of the bladder; its dynamic elasticity, a material property that gives it the ability to acutely regulate wall tension;

and spontaneous, non-voiding, often rhythmic contractions of the detrusor (bladder) smooth muscle[4–6]. These parameters affecting the load on the bladder tension sensor shown in Figure 1.1 are described in detail in Chapter 2. Afferent nerves sense changes in bladder wall tension and the neural system processes activity from the brain and spinal cord to provide the sensation of bladder fullness and the desire or urgency to void[7]. A defect in one or more of these parameters could lead to bladder dysfunction, such as altered sensation during filling. This project will focus on developing objective tools to quantify and relate the parameters of spontaneous rhythmic contractions and dynamic elasticity.

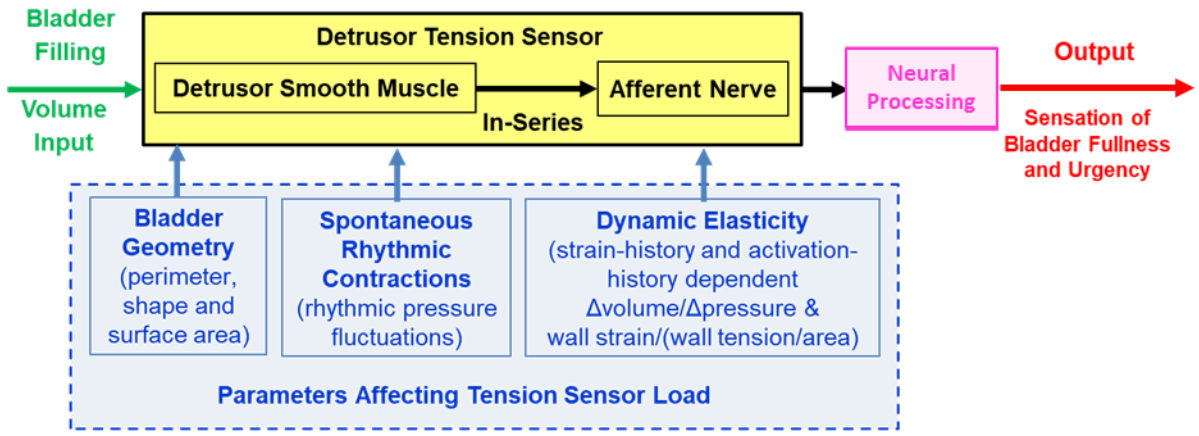

Figure 1.1: Detrusor tension sensor model. Tension sensor model showing mechanical factors affecting bladder sensation.

1.2 Overactive Bladder

Overactive bladder (**OAB**) is a chronic filling-phase condition that affects about one in five adults in the United States[8]. It is defined as elevated urinary urgency, often without identifiable causes and is usually associated with increased daytime frequency or nighttime nocturia, which means an individual has to wake one or more times throughout the night to void[9].

OAB has many potential, but difficult to identify, causes. A change in the smooth muscle making up the detrusor wall could cause a change in wall tension for a given volume, altering the

degree of sensation associated with that volume. This change could be due to mechanical defects in the muscle, inflammation, aging or bladder outlet obstruction. Neurogenic factors due to damage to the brain or spinal cord could lead to changes in the bladder wall. Events in the past could influence individuals psychologically causing them to perceive sensation incorrectly, or OAB could be due to lifestyle factors such as excessive hydration or caffeine intake causing an overproduction of urine. Metabolic factors or certain medications they are taking could also affect urine production.

OAB is complex and has a large societal impact. Psychological effects are caused by this condition, with almost a third of people reporting that OAB symptoms also give them feelings of depression. It is important to note, however, that is unclear whether the OAB symptoms lead to depression or whether similar neurochemical abnormalities are present that cause both OAB and depression[10]. There is also a physical impact it can have on individual. Due to increased frequency of voiding and rushing to get somewhere to void, those with OAB have an increased risk of falling of up to 30%[8].

1.3 Challenges Assessing OAB

Despite OAB's prevalence and its high impact, both physically and psychologically, there is only a limited understanding of this condition. The current gold standard for bladder filling and voiding evaluation, a urodynamic (**UD**) study[9,11], measures bladder pressure during filling. Bladder wall tension affecting the load on the tension-sensitive nerves in the bladder wall responsible for sensation is affected by bladder wall geometry and material properties in addition to bladder pressure[3,12]. As a result, measuring pressure during a UD study does not fully characterize detrusor wall tension during bladder filling. However, for a given volume and geometry, an increase in pressure would correlate with an increase in wall tension, such as during a non-voiding bladder

contraction. As a result, pressure measurements during UD studies are used to identify non-voiding contractions during filling; however, this process involves subjective, visual interpretation of pressure signals and more objective and quantitative techniques are needed. UD studies can also quantify large, clinically significant increases in pressure between empty and full volumes, which identify bladders with low compliance due to chronic disorders such as bladder wall hypertrophy resulting from bladder outlet obstruction[9,13–15]. However, in the absence of subjective, visually identifiable pressure increases caused by non-voiding contractions, a single UD fill does not identify acutely regulated changes in bladder wall material properties from one fill to the next which may contribute to OAB[16]. Thus, current UD studies can be ineffective at fully diagnosing the causes of OAB, and there exists a lack of objective metrics to sub-categorize different forms of OAB that prevents more specific diagnoses such as identifying OAB that is mediated by changes in bladder shape, acute changes in bladder wall elasticity or elevated spontaneous rhythmic contractions[3,17,18].

A UD study is an invasive and potentially painful and embarrassing test that causes participants anxiety[19]. In addition, these tests provide only subjective bladder sensation information, and while objective pressure data is obtained, often these data must be visually interpreted. This leads to the potential for bias when diagnosing the condition. Though highly trained, urodynamicists must interpret the results, and they are sometimes unable to make definitive diagnoses due to inconclusive results.

The lack of objective metrics and subgroups for OAB also affects treatment. The severity of the condition cannot currently be objectively graded in individual patients. By not understanding the specific cause of a particular case of OAB, the current treatment options can be ineffective if they do not match the particular cause[8]. Potential causes of the ineffectiveness of these treatments

are a lack of identified subgroups for targeted prescription of specific treatments and an inability to objectively quantify treatment effectiveness. The goal of the present project was to develop tools to objectively detect and quantify changes in bladder pressure during UD studies that can be used to evaluate and subgroup OAB.

This dissertation has six chapters, including the introduction and motivation in Chapter 1. The remaining chapters are organized as follows. In Chapter 2, important background information and relevant literature are discussed. Chapter 3 describes the research objectives including the specific aims of this dissertation. Chapter 4 concentrates on Aim 1, the objective quantification of spontaneous rhythmic bladder contractions. Chapter 5 focuses on Aim 2, the characterization of bladder dynamic elasticity. The final chapter, Chapter 6, discusses the conclusions from this research, as well as potential future directions.

Chapter 2 - Background

This chapter discusses relevant background information necessary to understand and motivate the research objectives and is organized into four subsections. The first subsection discusses urodynamics studies which are used clinically to evaluate bladder function and were used extensively to collect the data analyzed in this research. The second subsection discusses spontaneous rhythmic bladder contractions, including their proposed role in bladder biomechanics. The second subsection also discusses methods for detecting and measuring spontaneous rhythmic contractions, which is the focus of the first specific aim of this dissertation. The third subsection discusses the material property of the bladder known as dynamic elasticity, or reversible strain softening, which is one focus of the second aim of this dissertation. The final subsection will discuss a potential link between spontaneous rhythmic contractions and dynamic elasticity which is another focus of the second specific aim.

2.1 Urodynamics Studies

The current gold standard for bladder evaluation and assessment of the function or dysfunction of the lower urinary tract, including the identification of detrusor overactivity is a UD study[9]. These studies are used to evaluate detrusor muscle function by measuring bladder pressure during filling and pressure and flow during voiding.

A standard UD study involves a catheter being placed into the bladder through the urethra. This catheter measures bladder pressure through one of three common arrangements, a water-filled catheter with external transducer or an air-filled catheter with either an external transducer or a catheter-tip transducer. These transducers must be accurate enough to adequately measure variation between 1-2.5 cm-H2O to sufficiently detect physiological changes across a range of -

30-250 cm-H_2O. A UD system must also have an analog to digital convertor capable of recording bladder pressure and flow with sampling frequency of at least 3 Hz according to the International Continence Society Guidelines on Urodynamic Equipment Performance, while UD practices suggest a sampling frequency of 10 Hz[20,21]. The UD systems used in this research collect data with an air-filled catheter that transmits pressure directly to the external transducer at a sampling frequency of 10 Hz. The urethral catheter allows for infusion of saline through an infusion pump. This infusion pump requires an adjustable infusion rate, and the system records infusion rate as well as infused volume. The final function of the urethral catheter is to permit the withdrawal of saline or urine throughout the study[20].

A second catheter is placed into the rectum or other abdominal cavity to measure abdominal pressure during the UD study. This pressure is important to differentiate pressure fluctuations caused by bladder activity from those caused by other bodily processes. Electromyography measurements are also taken during a UD study to record pelvic floor or sphincter muscle activity[20].

While it is the current gold standard, a UD study is an invasive test involving catheters in the bladder and another cavity, and in some cases needles for electromyography measurement. This invasive test currently focuses on measuring detrusor pressure, which is the difference between the vesical pressure measured by the bladder catheter and the abdominal pressure measured by the rectal catheter. Detrusor pressure is objective data that is clinically useful for identifying detrusor overactivity, as described in Chapter 1, but pressure alone cannot fully characterize changes in detrusor wall tension because UD studies do not measure bladder geometric parameters which are needed to relate the pressure to wall tension[16].

2.2 Bladder Contractile Activity

This subsection includes background information pertaining to bladder contractile activity during filling, including a bladder disorder identified during UD known as detrusor overactivity. Fast Fourier transform (**FFT**) methods used to quantify contractile activity throughout this research are discussed, along with the steps taken to prepare data for analysis and why they are necessary. In addition, a specific type of detrusor overactivity, spontaneous rhythmic contractions, that is the subject of the first specific aim of this research is discussed.

2.2.1 Detrusor Overactivity

Detrusor overactivity is a urodynamic observation identified through involuntary contractions of the detrusor. These involuntary contractions can occur in several forms[9]. They can be rhythmic, meaning they produce periodic pressure fluctuations throughout filling (Fig 2.1A). DO can also be isolated or sporadic non-voiding contractions during filling (Fig 2.1B)[22] or DO can be terminal, characterized by a single non-voiding contraction near capacity resulting in involuntary bladder voiding[23]. A major focus of this project is the development of signal processing algorithms to quantify rhythmic DO.

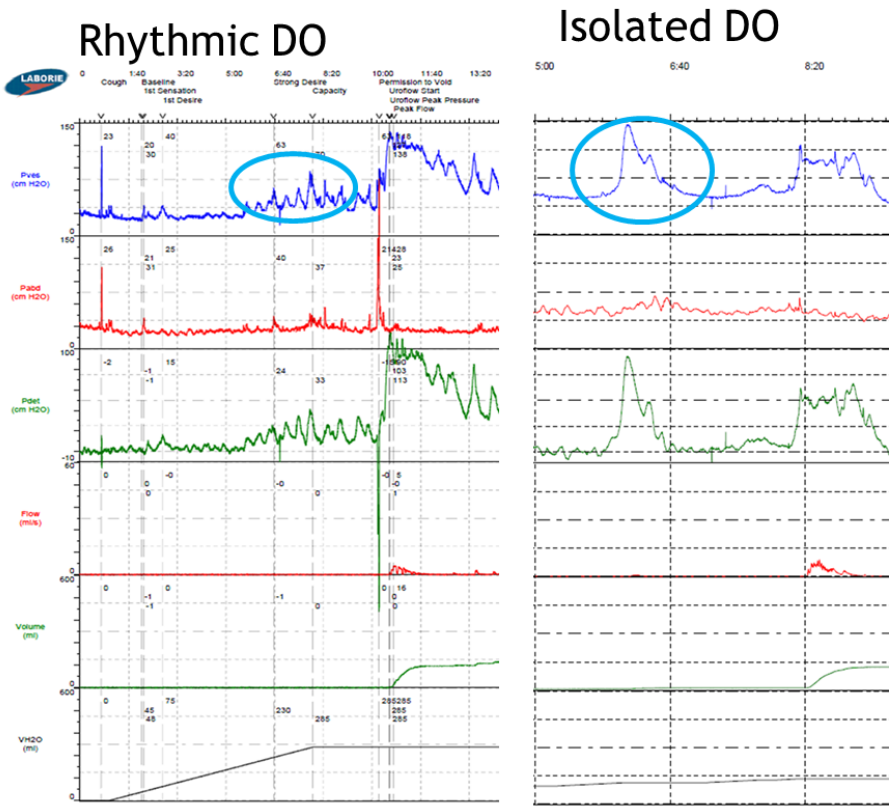

*Figure 2.1: Urodynamic pressure tracing. A urodynamic pressure tracing showing (**A**, blue circle) rhythmic DO and (**B**, blue circle) isolated DO*[24].

2.2.2 Signal Processing

A Fourier Transform is a mathematical function that decomposes a function or signal into a sum of sinusoidal waves of different amplitudes and frequencies that make up that signal. An FFT is a popular form of Fourier Transform that utilizes computers and symmetrical properties of periodic waveforms to reduce calculations (Figure 2.2)[22]. FFT allows a signal to be analyzed across a spectrum of frequencies to determine what frequency content makes up the signal. While not considered in this research, it is important to note that FFT also reports phase information. FFT also allows data quantification based on what underlying waveforms make up the entire signal. The example of FFT analysis shown in Figure 2.2 was performed using MATLAB (R2016A, MathWorks, Natick, MA), which was used throughout this project. The ideal sine wave in panel

A has a frequency of 5.0 Hz and an amplitude of 1.0. The FFT output in panel B has a peak at the expected frequency of 5.0 Hz and an amplitude of 1.0.

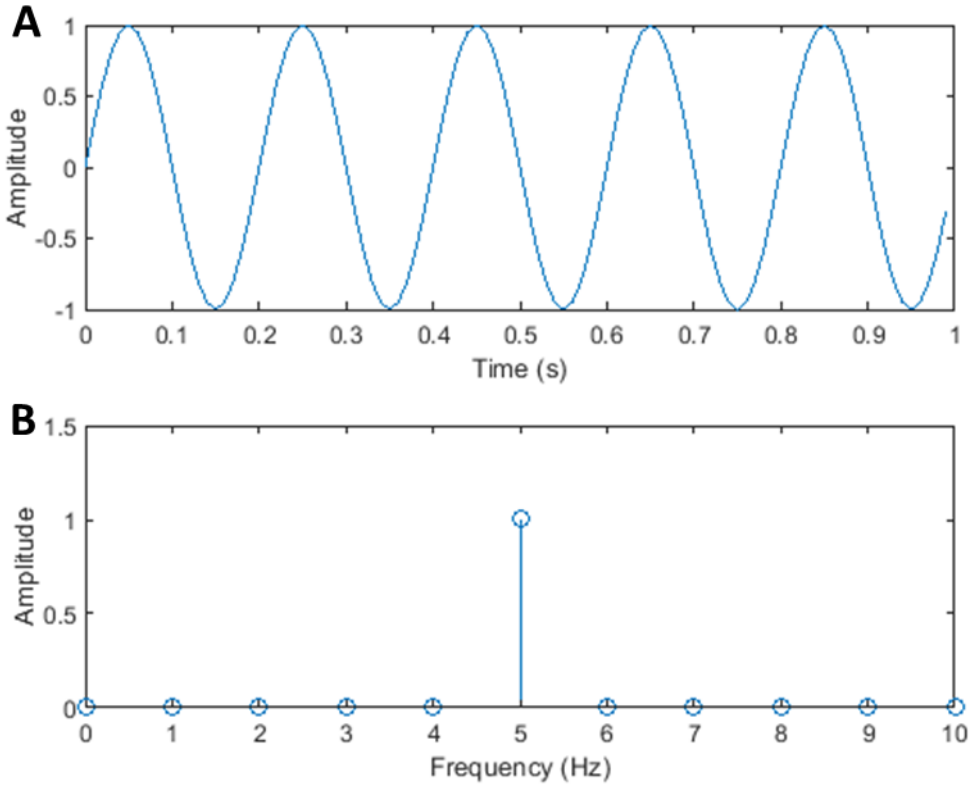

*Figure 2.2: Ideal fast Fourier transform. (**A**) An ideal sine wave and (**B**) corresponding FFT output demonstrating the conversion from the time to frequency domain that occurs during FFT analysis.*

Analog signals represent a continuous physical variable that varies with time. When analyzing data using a digital computer for processing, the analog signal must be converted to digital form that is an adequate representation. Transducers convert an analog signal into a digital signal that follows the variations with time by collecting a value from the signal at discrete time intervals. Collection of instantaneous values at discrete times is known as sampling.

The Nyquist Sampling Theorem states that to adequately represent a signal, it must be sampled at a rate higher than twice the frequency of interest[25]. If data is not sampled adequately, aliasing can occur. Aliasing is the result of under-sampling that produces an incorrect representation of the signal (Figure 2.3). For example, if data is collected at a sampling rate of 10Hz, then according to the Nyquist Sampling Theorem, the highest frequency that could adequately be reproduced would be 5Hz (300 cycles/min)[25].

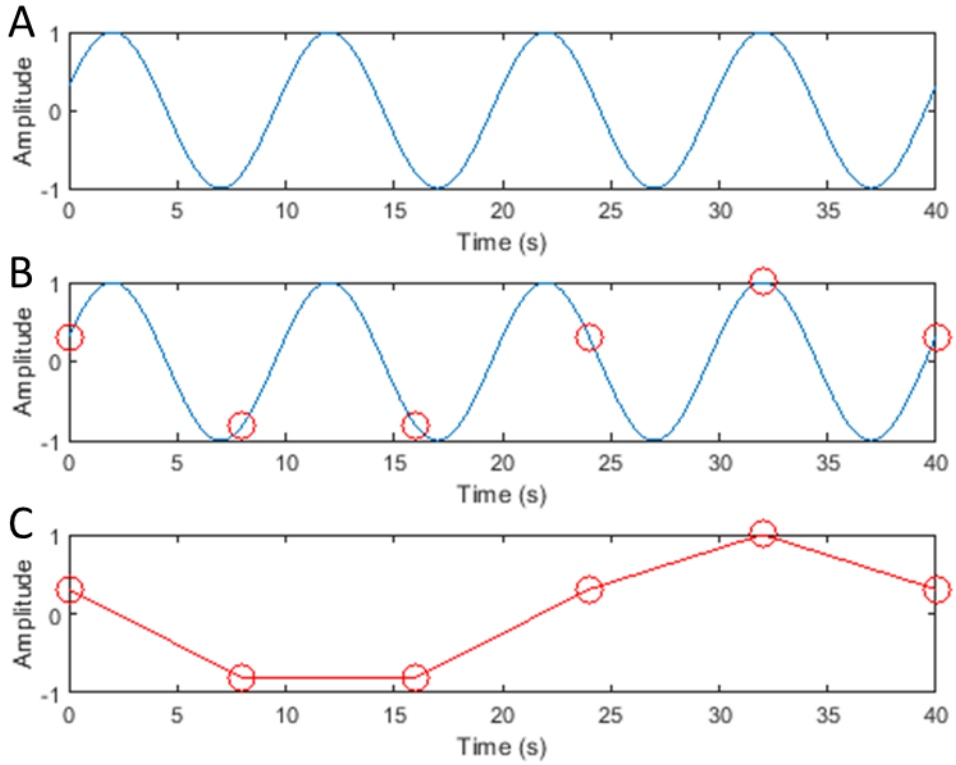

*Figure 2.3: Effects of under-sampling a signal. An example demonstration of the effects of under-sampling showing (**A**) the original signal with frequency 0.1 Hz, (**B**) points being sampled at a rate of 0.15 Hz (red circles) which is too low to preserve the original signal and (**C**) the recreated signal*

Once data has been collected and recorded, it must still undergo further preparation before FFT analysis. For this research, data preparation occurs in three steps (Figure 2.4). The first is

filtration using a 10-point smoothing filter that passes low frequencies and attenuates higher frequencies, which was chosen because the frequencies of interest are much lower than the sampling frequency (1.75-8 cycles/min vs. 600 cycles/min respectively).

The next step in the data preparation was to remove any steady state pressure offset from the signals. The effect of any steady state offset is reduced by linearly detrending the data. This process fits a line to the signal and then subtracts that line from the signal to remove the linear trend and allow for more accurate frequency spectra.

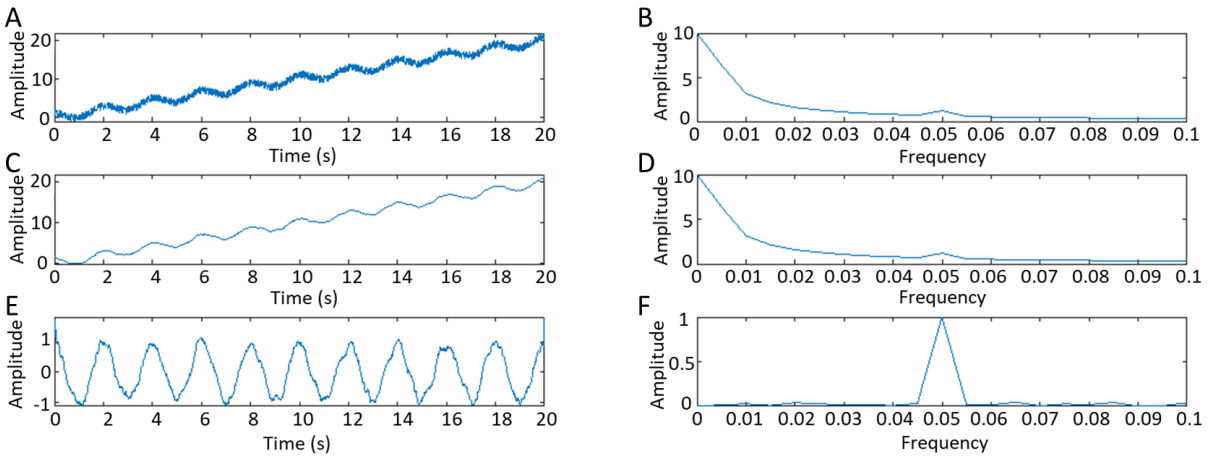

*Figure 2.4: Data preparation steps for FFT analysis. (**A**) A raw noisy signal with a linear trend and (**B**) corresponding FFT output for that signal. (**C**) The signal after applying a 10-point smoothing filter and (**D**) corresponding FFT output. (**E**) The signal after being linearly detrended and (**F**) corresponding FFT output which shows a clear distinct peak with a smaller scale to clearly see the peak.*

When analyzing data using a Fourier Transform, the analysis assumes a signal of infinite length. Using sampled data of finite-length is possible, but the transform will simulate infinite length by continuing from the first point after the last point. In many practical applications, these values are not equal leading to the introduction of noise in the frequency spectrum due to the discontinuity. To smooth any discontinuities at the beginning and end of the sampled data, a Hann

or Hanning window was applied by multiplying the sampled signal by a tapered cosine window [26]. Both Hamming and Hanning windows were considered for this work and the later was selected because it more exactly cancels the sidelobes by reaching zero at both ends of the signal when eliminating discontinuities[26]. It is important to note that an amplitude correction factor of 2.0 is necessary when quantifying amplitudes after applying the Hanning window to a signal.

2.2.3 Spontaneous Rhythmic Contractions

During filling, the bladder develops tone and can exhibit local contractions and relaxations[27]. This contractile activity is believed to be myogenic and may be reinforced by signaling from the urothelium and lamina propria[28,29]. Spontaneous rhythmic contractions have been shown in both mammalian[30–32] and human[29,33,34] DSM during the bladder filling phase in the form of phasic non-voiding contractions that are low in amplitude when compared to maximal KCL-induced contractions[35]. They are thought to occur with the role of maintaining bladder tone throughout filling and allowing for an active voiding contraction to occur at any volume[18].

Studies have shown spontaneous rhythmic contractions to be elevated in DSM samples taken from patients with OAB[36] and in bladders with DO[3,34] when compared to normal bladders. Furthermore, these contractions have been shown to increase in amplitude, but not frequency in whole pig bladders with increasing volume[37]. This could suggest rhythmic contractions are a mechanism for the modulation of the detrusor muscle across a broad range of operating volumes and that a disorder involving rhythmic contractions is related to the presence of urgency as well as phasic DO[18,38].

Spontaneous rhythmic contractions have been identified over a range of frequencies[39]. Biers et al showed in human detrusor strips that rhythm in tension tracings occurred between 1.8-

2.6 cycles/minute[40]. Drake et al measured micromotion between sensors placed on a balloon and filled inside the bladder during UD studies and identified frequencies of 2-5 cycles/minutes[3]. Bladder smooth muscle cells have shown action potentials at a frequency of 7.9 per minute[41].

The first study correlating in vitro human urinary bladder pressure waves with those found in human bladder strip analysis showed the potential FFT had as a tool for quantification and characterization of spontaneous rhythmic contractions in data obtained during UD studies[33]. This study by Colhoun et al showed an average frequency of 2.34 cycles/minute when analyzing UD study tracings, which was consistent with the other finding of a mean frequency of 1.97 cycles/minute in human detrusor strips[33]. Peaks in amplitude in the frequency domain were identified visually before further analysis. For the UD data, the peak FFT amplitudes were compared to thresholds corresponding to a large vesical pressure amplitude relative to the rest of the signal (Figure 2.5B, Threshold 1) and also compared to the overall abdominal pressure signal (Figure 2.5B, Threshold 2) to confirm it was not caused by other bodily functions[33]. Aim 1 of the current project was to develop a tool for objective quantification and identification of spontaneous rhythmic contractions and characterized them throughout filling.

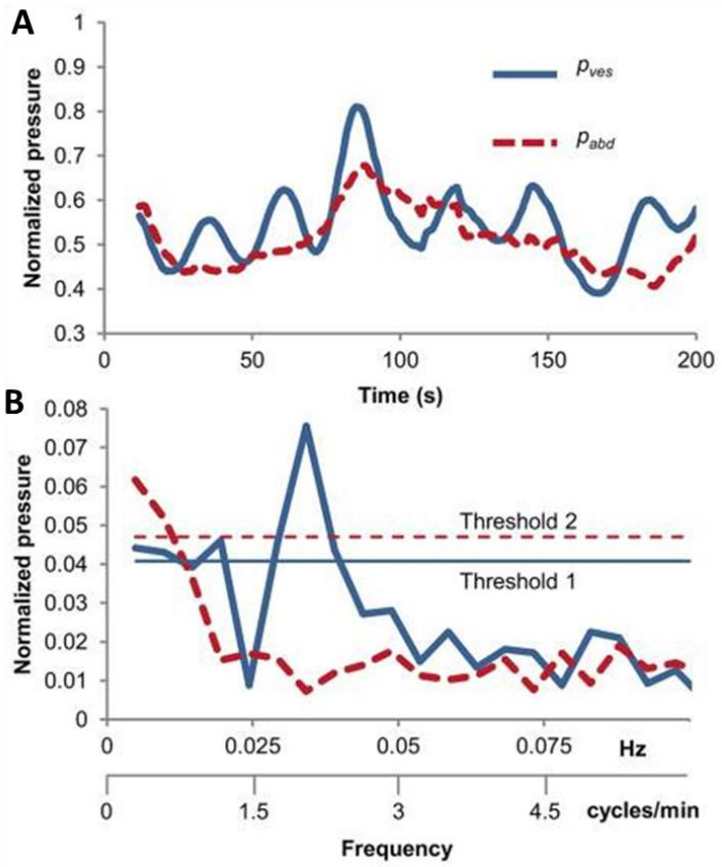

Figure 2.5: Visually identified spontaneous rhythmic contractions and FFT analysis. Pressure tracing of P_{ves} (blue) and P_{abd} (red dashed) signals in the (A) time domain showing pressure fluctuations and (B) corresponding frequency transformation with a peak corresponding to the pressure fluctuations showing spontaneous rhythmic contraction frequency and amplitude[33].

2.3 Dynamic Elasticity of the Bladder

This subsection will cover background information about dynamic elasticity of the bladder. It will describe the material property of strain-induced stress softening. Studies identifying it as reversible in smooth muscle strips and the function of active and passive pressures within the bladder will be discussed. A pilot study quantifying dynamic elasticity clinically will be reviewed including the pilot study protocol and study limitations. Finally, the pig experimental set up used to investigate dynamic elasticity in whole pig bladders will be explained.

2.3.1 Strain-induced Stress Softening

Strain-induced stress softening was originally shown to be a property of rubber known as the Mullins' effect[42]. This "strain softening" is the loss of stiffness or softening in a material after a stretch to a new force[43]. Strain softening results in a lower stress for the same applied strain and explains the phenomonon of preconditioning[44]. The most strain softening is caused by the first loading cycle and then less softening occurs in subsequent cycles of loading and unloading until an equilibrium is reached[45]. Strain softening only appears for strains equal or less than those already applied, and strains beyond that will show a similar stress response as initial loadings[45].

A common analogy for the strain softening effect when considering the bladder is a latex balloon. A previously unstretched balloon is difficult to inflate and has very stiff walls leading to high wall tension. After stretching or inflating it, the next few fills require less pressure with each subsequent fill due to broken polymer chains[42]. In the case of the latex balloon, and typically when considering most materials, strain softening is irreversible[45]. Studies involving smooth muscle, however, have shown this to be reversible after the muscle has been activated[46].

2.3.2 Dynamic Length-Tension Relationship in DSM

Within the bladder, tension can be divided into preload and active components. Preload, or "passive," tension allows the bladder to retain its shape during filling. The preload tension in detrusor smooth muscle was previously attributed to passive structures (collagen and elastin) and tension-maintaining actomyosin cross-links[46,47]. Studies suggest, however, that slowly cycling cross-bridges also contribute to the preload stiffness[48]. These cycling cross-bridges may ensure that the detrusor smooth muscle can operate over a broad range of working lengths[47]. Active tension is caused by the contraction itself and provides the force that drives voiding.

Historically, the preload and active relationships of length and tension were believed to be static. More recently, studies have shown these relationships to be dynamic and have challenged the static assumption in tracheal smooth muscle[49] and bladder smooth muscle[50]. When conducting experiments, smooth muscle tissues usually undergo cyclic stretching to achieve consistent results in a process known as preconditioning[51]. The resulting change in steady-state stiffness in following loadings is thought to be the result of strain softening and is shown schematically in Figure 2.6 (black arrow, green to blue line).

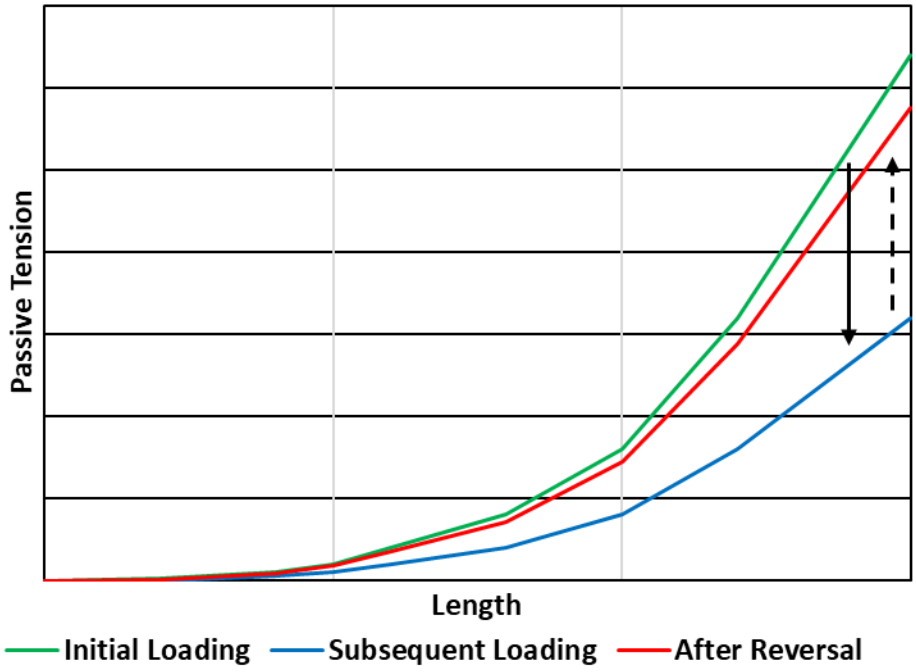

Figure 2.6: Dynamic length-passive tension curves. Passive tension as a function of length for an initial loading (stretch 1, green) and passive tension at the same lengths for subsequent loadings (stretch 2, blue) resulting in strain softening (black arrow, green to blue line). Passive tension after strain softening reversal (stretch 3, red) which in smooth muscle results from muscle activation (dashed arrow, blue to red line).

Rabbit detrusor strips were shown to have irreversible strain softening when undergoing cyclic loading while the tissue remained in a calcium-free solution. These strips were shown to behave in a similar manner to latex strips also undergoing cyclic loading[52]. Both showed peak stiffness during the first loading before dropping and eventually having similar response to subsequent loadings, both documented features of strain softening. After potassium induced contractions, the strips regained stiffness and reversed the strain softening that had occurred(Figure 2.6, dashed arrow, blue line to red line)[46]. Similar findings have been shown in other smooth muscles from rat esophagus[53].

An additional study into this reversible strain softening was conducted to validate the theory of a dynamic relationship between preload length and tension due to muscle strain and activation history[54]. By demonstrating a similar contraction strength (active force) before and after strain softening, but a difference in steady state tension (passive force), this study showed that the passive stiffness of detrusor muscle is adjustable, not static, as well as reversible[52]. Reversible strain softening has been shown in human detrusor strips[55].

2.3.3 Pilot Study of Dynamic Elasticity of the Human Bladder

In addition to human detrusor strips, reversible strain softening has also been identified clinically in human bladders during a limited pilot study that termed the material property "dynamic elasticity". The pilot study used a comparative-fill urodynamics protocol involving a clinical fill and four subsequent fills and compared pressures during each fill to quantify dynamic elasticity (Figures 2.4 and 2.5)[56]. When quantifying dynamic elasticity, the method in which the bladder is emptied contributes directly to the response observed in the following fill.

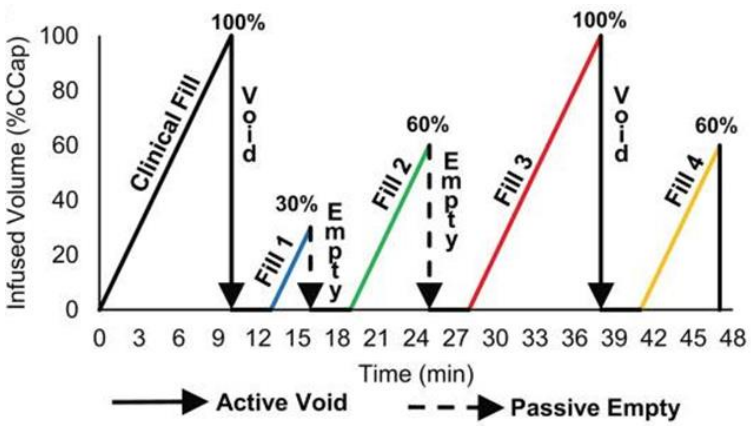

Figure 2.7: Pilot study comparative-fill urodynamics protocol. Comparative-fill urodynamics protocol used to identify dynamic elasticity[56].

The clinical fill was used to determine cystometric capacity (CCap, Figure 2.7, vertical axis) and was followed by an active void to contract the bladder and reset any strain softening. Following an active void, a baseline bladder pressure was measured, during Fill 1 (Figure 2.7, blue line) of the comparative-fill protocol. This fill went to 30% CCap and was followed by a passive emptying of the bladder through syringe aspiration to avoid an active contraction that would be expected to reset strain softening so that the loss of elasticity could be quantified in Fill 2 (Figure 2.7, green line). During Fill 2, the bladder was further strain softened by filling to a volume of 60% CCap. This was followed again by passive emptying, and the additional strain softening from the increased volume could be quantified during Fill 3 (Figure 2.7, red line). After quantifying the additional strain softening during Fill 3, the participant's bladder was filled completely followed by another active void to reset strain softening. The degree of strain softening reversal was quantified during Fill 4 (Figure 2.7, yellow line).

The baseline pressure, which occurred after an active void, was recorded during Fill 1 (Figure 2.8, blue bar). Passively emptying the bladder following Fills 1 and 2 prevented an active contraction from resetting strain softening, and decreased pressures were observed during Fill 2

and Fill 3 (Figure 2.8, green and red bars). Finally, the bladder was actively voided to reset strain softening following Fill 3, and increased pressure was observed during Fill 4(Figure 2.8, yellow bar). Dynamic elasticity is characterized by the decrease in pressure following filling and passive emptying (Figure 2.8, blue vs red bars) and the restoration of filling pressure in a fill after an active void (Figure 2.8, yellow vs red bars).

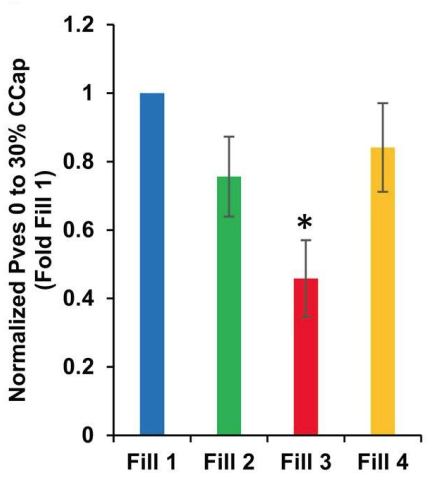

Figure 2.8: Pilot study pressure results demonstrating dynamic elasticity. Results of comparative-fill urodynamics protocol with Fills 1-2 being followed by syringe aspiration and Fill 3 being followed by an active void[56].

While the dynamic elasticity pilot study identified and quantified dynamic elasticity clinically, it had a limited group of participants, all with OAB, and utilized four comparative fills. The present study will analyze comparative-fill UD data from a larger group of participants with and without OAB[56].

2.3.4 Pig Bladder Experiments

Bladders from adult pigs were harvested immediately after slaughter from local abattoirs and the vascular tree, ureters and urethra in tact[57]. The bladders were cannulated and perfused with heparinized Krebs-Henseleit buffer and stored on ice to the lab to be used within 48 hours[58]. Once

in the lab, the vesical arteries were cannulated and perfused with Krebs-Henseleit buffer at a rate of 4 mL/minute while the bladders were stored in a humidified and heated chamber (Figure 2.9)[59]. The urethra was catheterized to permit infusion and monitor vesical pressure using an Aquarius TT urodynamics unit (Laborie Inc., Mississauga, Ontario)[59]. This experimental setup was designed to mimic clinical UD studies while simulating physiological conditions for the whole bladders. This isolated pig bladder model was used to investigate dynamic elasticity in the present study and quantify the effects of compression versus filling on bladder pressure.

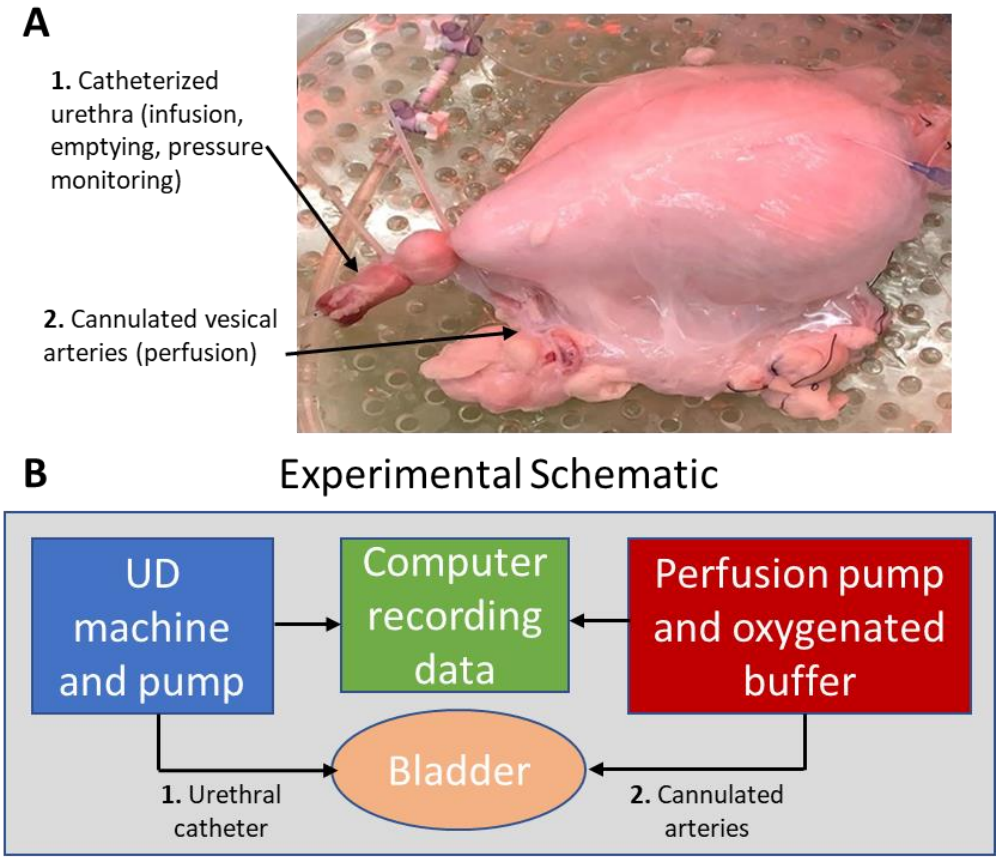

*Figure 2.9: Pig bladder in experimental chamber. (**A**) Photo of an isolated bladder being perfused and heated within experimental chamber. (**B**) Experimental schematic showing the UD and perfusion pump configuration.*

Aim 2 of this project had both basic science and clinical sub-aims. The basic science sub-aims were to investigate dynamic elasticity in an isolated pig bladder model and quantify the effects of compression versus filling on bladder pressure. The clinical sub-aims were to quantify dynamic elasticity in participants with and without OAB using a simplified UD protocol and to test a hypothesized model linking dynamic elasticity and DO.

2.4 Connecting Spontaneous Rhythmic Contractions and Dynamic Elasticity

Because dynamic elasticity is reset via active voiding contractions[18,56], this project tested the hypothesis that spontaneous rhythmic contractions during filling, i.e. DO, also affect dynamic elasticity and that the presence of DO and corresponds to a lack of dynamic elasticity. Any lack of identifiable dynamic elasticity would be expected to be caused by the DO acting as small active forces reestablishing actin-myosin connections throughout filling and preventing the bladder wall from strain softening to adjust its compliance to keep DSM wall tension low throughout filling.

Altered dynamic elasticity could lead to a higher perceived bladder volume that could artificially elevate sensation and cause urgency resulting in overactive bladder. Aims 1 and 2 of this project explored the potential link between spontaneous rhythmic contractions and dynamic elasticity and how elevated spontaneous rhythmic contractions and/or altered dynamic elasticity could contribute to OAB.

Chapter 3 - Research Objectives

3.1 Tension Sensor Model

Three mechanical factors are thought to contribute to perceived sensation by altering DSM wall tension (Figure 3.1). These factors are bladder geometry (perimeter, shape and surface area), rhythmic contractions that cause pressure fluctuations and the dynamic elasticity of the bladder wall, which if altered could raise vesical pressure. This relationship between the DSM and bladder sensation is a function of bladder volume and tension in the muscle affecting the load on the nerves is illustrated in Figure 3.1.

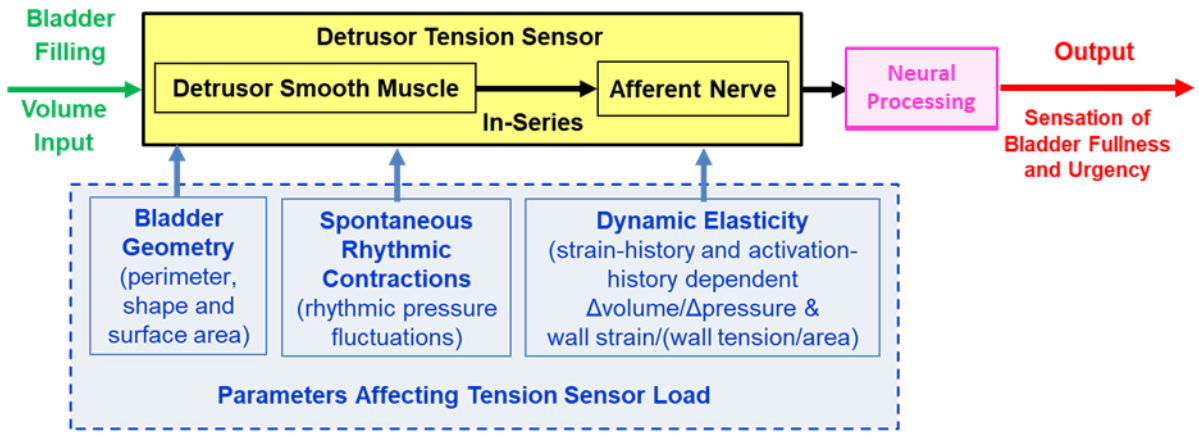

Figure 3.1: Detrusor tension sensor model. Model showing detrusor as a tension sensor and the parameters affecting the load applied to this tension sensor.

3.2 Proposed Model Linking Spontaneous Rhythmic Contractions and Dynamic Elasticity

As the bladder fills and other changes occur in the geometry of the bladder wall due to deformation from normal activity, the bladder undergoes strain softening. A conceptual model outlining the bladder as having a balance of competing forces was proposed (Figure 3.2). The model shows the passive mechanisms that affect the bladder leading to lower wall tension by

breaking actin-myosin connections through normal activity such as filling, moving, coughing or having pressure applied to the bladder, which has been shown to cause detectable strain softening[59]. In order to regulate wall tension and maintain elasticity, the bladder actively reverses these forces through voiding or non-voiding contractions and actin-myosin cross bridge cycling as demonstrated in previous studies[47].

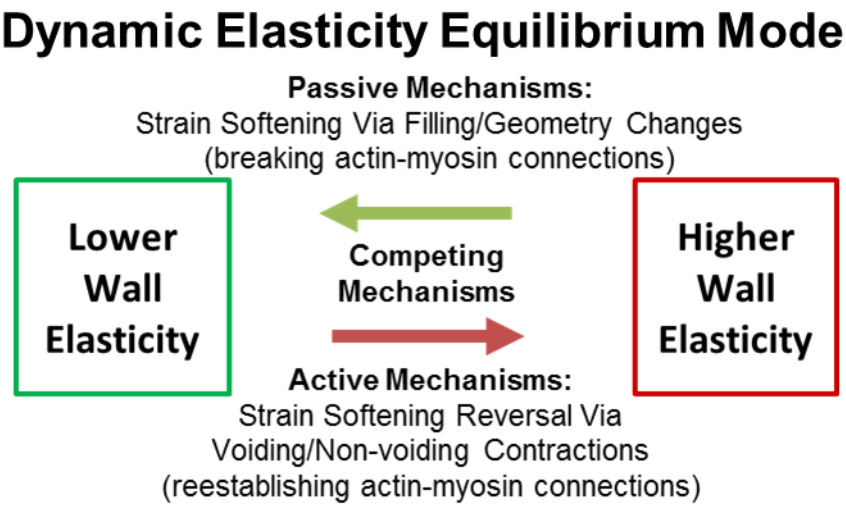

Figure 3.2: Dynamic elasticity equilibrium model. Proposed conceptual model showing the hypothesized competing mechanisms acting on the bladder wall to regulate tension.

This model could explain the purpose of bladder rhythmic contractions and DSM cross-bridge cycling during filling. The model also gives a potential explanation for the reasons DO is linked to overactive bladder. In some people, the contractions directly affect the tension sensors, but the dynamic elasticity equilibrium model gives another mechanism for DO to cause OAB. DO acts as an excessive active mechanism causing an imbalance. The bladder will not sufficiently acutely regulate its wall tension during filling. Even if the DO only occurs at low volumes, it could result in a less elastic, or stiffer, bladder. In conjunction with the tension sensor model, would explain the resulting increase in urgency (Figure 3.3, larger red arrow compared to Figure 3.2).

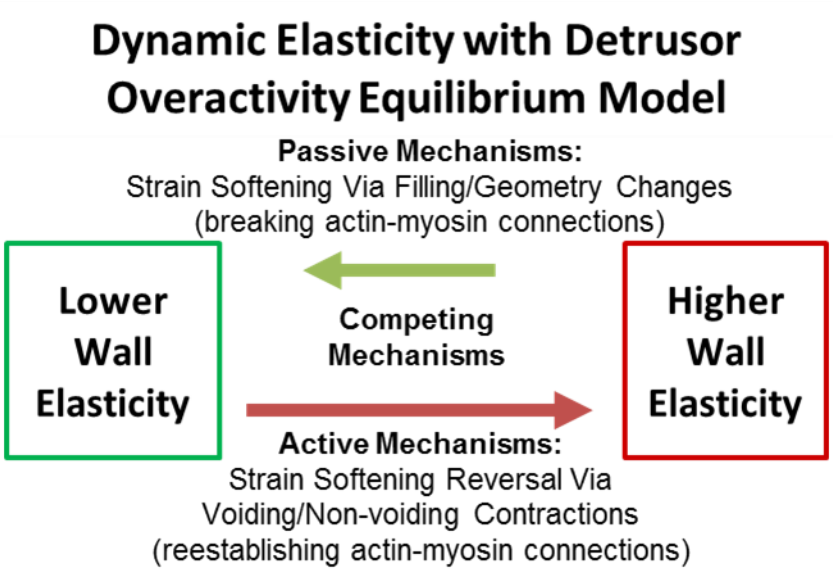

Figure 3.3: Detrusor elasticity equilibrium model for detrusor overactivity. Proposed conceptual model showing the hypothesized competing mechanisms acting on the bladder wall to regulate tension in a bladder with detrusor overactivity, with a larger red arrow representing an imbalance in forces due to increased non-voiding contractions.

3.3 Dissertation Aims

3.3.1 Specific Aim 1 – Objective Quantification of Rhythmic Detrusor Overactivity

Aim 1 was to develop tools to detect and quantify rhythmic detrusor overactivity in a more objective fashion and characterize a spontaneous rhythmic contraction-mediated detrusor overactivity subtype. Spontaneous rhythmic contractions of detrusor smooth muscle often show some degree of rhythmicity[60] and have been identified in muscle strips from animals[27] and humans[29]. These contractions are responsible for localized micromotion during filling which has been associated with increased urgency[3]. In addition, they are elevated in patients with DO[34]. During UD studies, they are identified as vesical pressure fluctuations.

SRC during bladder filling is has been identified visually from clinical UD data to diagnose DO. A recent study quantified SRC manually using Fast Fourier Transforms (**FFT**) on the visually

identified regions[33], but an objective tool for both the identification and quantification was lacking. The first step in identifying and understanding the link between bladder elasticity and spontaneous rhythmic contractions involved the development of such a tool. To achieve this aim, a Fast Fourier Transform algorithm was developed and used to identify and model the rhythmic activity of detrusor smooth muscle using clinical UD data.

This novel tool was first applied to retrospective urodynamics data at high bladder volume to quantify its effectiveness by detecting rhythmic contractions and a identify subgroup of those patients with DO[22]. The next step was applying this tool to both high and low bladder volume regions on prospective data to characterize the changes in rhythmic activity throughout filling.

3.3.2 Specific Aim 2 – Characterization of Dynamic Elasticity

Aim 2 was to quantify dynamic elasticity in participants using a simplified protocol, investigate dynamic elasticity in an animal model and test the hypothesis that detrusor overactivity inhibits dynamic elasticity. Bladder wall tension is influenced by pressure changes during filling, bladder shape and volume. Changes in wall tension are important because they can affect urgency and influence OAB[3,18]. Standard UD studies consider the bladder to have static compliance and it was believed to not change in the absence of a chronic process[23,61]. Recent studies have challenged this concept and introduced the concept of bladder dynamic elasticity[56,62]

Dynamic elasticity is a material property of detrusor smooth muscle that is responsible for acutely regulating bladder wall tension and is reduced due to strain-induced stress softening (strain softening) during filling[63]. The novel technique of comparative-fill urodynamics[56,62] has the potential to identify changes in pressure-volume curves between one fill and the next due to acute changes in dynamic elasticity, assuming a relatively small changes in bladder geometry for a given

volume from one fill to the next, these change in pressure would directly correlated with changes in bladder wall tension[16,18]. Dynamic elasticity is restored by contractile activity during voiding[46]. This specific aim was to address and expand on multiple areas regarding dynamic elasticity in the bladder muscle using data from comparative fill UD studies.

Dynamic elasticity was identified in detrusor strip studies[55] and a limited clinical pilot study[56], and this project expanded the study of DE to an isolated whole bladder model[57–59] which allowed the mechanisms of dynamic elasticity to be studied without outside bodily influences. In addition, this study demonstrated that strain softening can be induced non-invasively through abdominal compression to acutely regulate bladder pressures and this technique has potential therapeutic applications[59]. Furthermore, this study tested the hypothesized link between the competing mechanisms of active and passive forces in the DSM wall in a human UD study to determine whether the clinical problem of DO affects DE.

Chapter 4 – Aim 1: Objective Quantification of Spontaneous Rhythmic Contractions

Aim 1 was to develop tools to detect and quantify rhythmic DO in an objective fashion and characterize a spontaneous rhythmic contraction mediated DO subtype. This aim was broken into two sub-aims which were to:

1) Develop an objective method of quantifying spontaneous rhythmic contractions

2) Quantify changes in rhythmic contraction amplitude throughout filling

4.1 Sub-Aim 1A – Objective method of quantifying spontaneous rhythmic contractions

The purpose of this sub-aim was to develop an objective method to quantify spontaneous rhythmic contraction frequencies and amplitudes in UD without the potential bias of someone visually identifying a real signal initially. Once significant and independent (**S&I**) spontaneous rhythmic contractions (**SRC**) had been identified using an objective algorithm, the presence of S&I SRC was compared with the presence of urologist-diagnosed DO and used to determine if a subgroup of patients with spontaneous rhythmic contraction mediated DO existed. The published study corresponding to this sub-aim is attached in Appendix A[22], and is summarized in this chapter.

4.1.1 Introduction to Objective Quantification of SRC

Human and animal muscle strips have been shown to exhibit spontaneous rhythmic contractions[27,33]. Often these contractions show some degree of rhythmicity[60]. They are elevated in patients with detrusor overactivity and generate afferent nerve activity[31]. During bladder filling, SRC are responsible for localized micromotion which, when elevated, has been associated with urgency[34]. DO is a urodynamic observation identified by the presence of non-voiding detrusor

smooth muscle contractions during the bladder filling phase and often contributes to overactive bladder[16].

DO can occur in various forms and has been observed as isolated or sporadic contractions in some, while in others DO is manifested as spontaneous rhythmic contractions. Previous work has used FFT to quantify visually identified SRC during urodynamic studies and determined the frequency in both UD and bladder muscle strips showed similar agreement[33]. Another study utilized time-frequency analysis, or wavelets, to identify non-voiding bladder activity[64]. The study by Colhoun, et al. required the visual inspection and identification of spontaneous rhythmic contractions before proceeding with FFT analysis[65].

Visually, the diagnosis of DO can be relatively straightforward[9], determining if it corresponds with isolated and unrelated events of coordinated waveforms is more challenging. The present study used retrospective UD data to show the broad application of this technique by using "real-world" UD data to identify and characterize a subgroup of DO patients[22].

4.1.2 Methods for Objective Quantification of SRC

Data from 239 consecutive UD studies performed in the Virginia Commonwealth University Urology Urodynamics Laboratory over a three-year period were collected directly from the Laborie Aquarius TT™ multichannel UD machine (Laborie, Toronto). Of those, 131 unique patients with complete medical records, meeting the required age of 21 and having at least 7 minutes of standard UD filling were considered. Studies from 36 patients with leaks or multiple voiding events were not considering, resulting in a study consisting of 95 patients, shown in Table 4.1, with a terminal or no voiding event. A blinded neurourologist and expert urodynamicist diagnosed DO in these individuals using ICS guidelines[9].

Table 4.1: Patient information for those included in the retrospective study.

	DO	not DO	Total
N	52	43	95
Male	26	14	40
Female	26	29	55
Age (years)	53.4 ± 2.1	51.4 ± 2.2	52.4 ± 1.5
Neurogenic	28	17	45
Idiopathic	24	26	50

An automated FFT algorithm, outlined in Figure 4.1, was developed in MATLAB to analyze a region of interest of these retrospectively collected "real-world" UD studies ending prior to voiding[22]. During standard UD studies, a catheter is inserted into the bladder through the urethra to measure vesical pressure (P_{ves}). Another catheter is inserted into the rectum to record abdominal pressure (P_{abd}) during the test. This is done to verify that any activity in P_{ves} is caused by the bladder and not movement, digestion or other bodily functions[9].

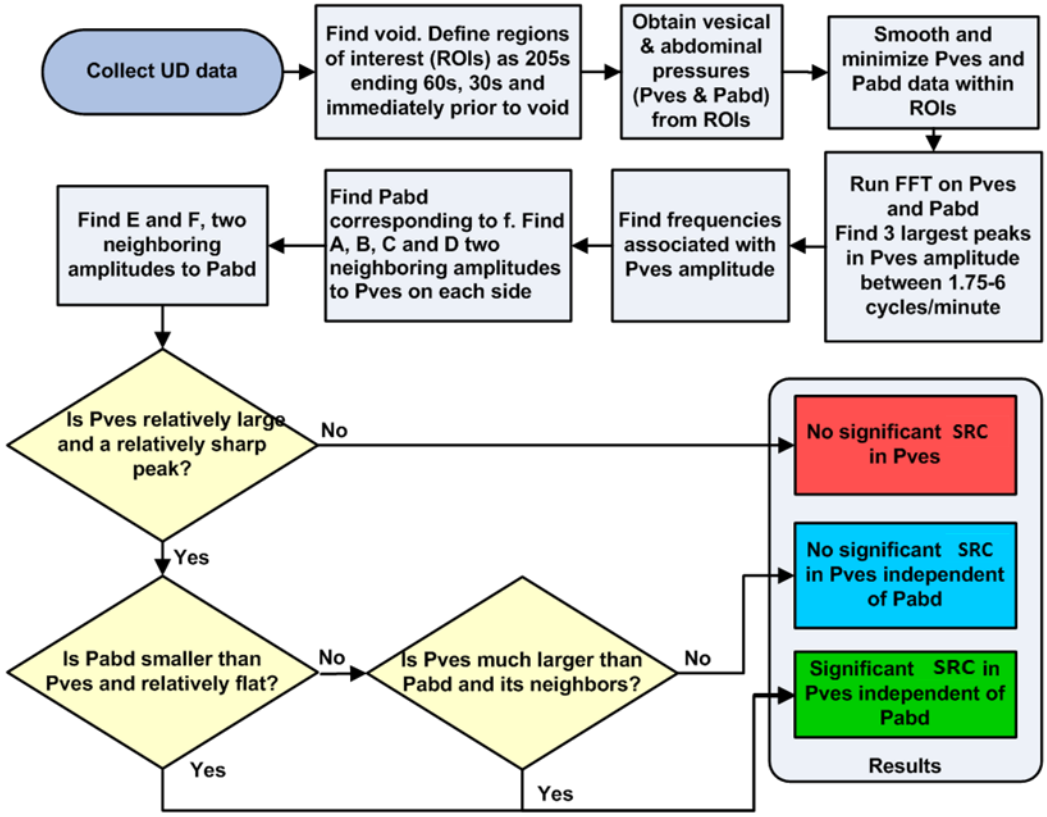

Figure 4.1: Automated FFT spontaneous rhythmic contraction analysis flowchart. Flowchart for the FFT spontaneous rhythmic contractions detection and quantification algorithm including data processing steps, analysis and categorization of results.

The voiding event, if any occurred, was identified using voided volume data. Contractile activity that shows a ramp-up pattern in P_{ves} may occur immediately prior to voiding. This led to the selection and testing of three regions of interest ending at different times before voiding. These regions of interest of 205 seconds were defined as ending 1) at void, 2) 30 seconds prior to void, and 3) 60 seconds prior to void (Figure 4.2). P_{ves} and P_{abd} data were smoothed with a 10-point moving average filter. Data were then shifted by subtracting the minimum value from each signal from every point in the signal to remove some of the effect of any steady state pressure. A Hann window was then applied to the signals to eliminate discontinuities at the beginning and end of the signals because the analysis assumes periodicity[22].

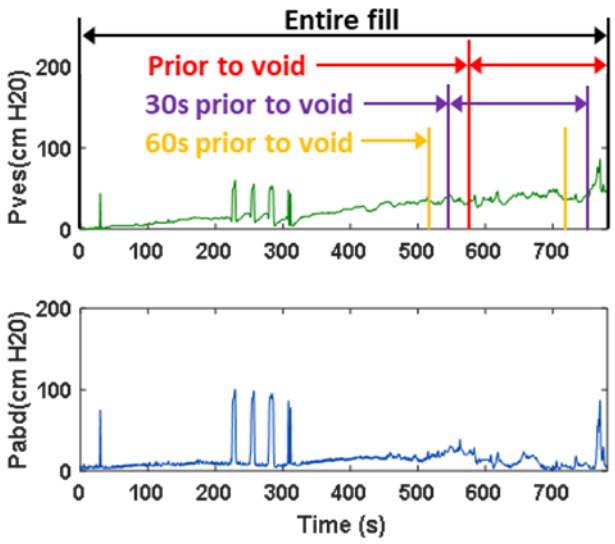

Figure 4.2: Schematic of regions of interest within filling for FFT analysis. Three regions of interest within the entire signal (prior to void, 30s prior to void and 60s prior to void) were defined for analysis with the FFT algorithm.

The algorithm identified the three largest rhythmic amplitude peaks in in the 1.75-6 cycle/minute frequency range. This frequency range was selected for this study based on prior studies that identified bladder rhythmicity occurring between approximately 1.8-5 cycles/minute[3,29]. The UD machine collected data at the standard frequency of 10Hz. According to the Nyquist theorem, this data should be free of aliasing that would obstruct in finding the desired signals. Collecting data at 10Hz would allow accuracy up to 5Hz or 300 cycles/minute, much higher than the anticipated 1.75-6 cycle/minute range[22].

Each peak in P_{ves} found in this range were tested for two criteria. The first test was to determine whether they were significant (above baseline P_{ves} activity) and the second was to determine if they were independent (distinct from any in P_{abd} rhythm). To be considered significant, a P_{ves} peak needed an amplitude of 1.8cm-H_2O and adequate prominence or sharpness. To evaluate sharpness, a slope criterion was established corresponding to a steep grade in the P_{ves}

amplitude in the frequency spectra of at least 20% P_{ves} per frequency step for at least one of the next two slower frequency steps and at least one of the next two faster frequency steps[22].

The independence criteria were important because translated abdominal events produce peaks in both P_{ves} and P_{abd} tracings[33]. In addition, non-translated abdominal activity, such as rectal contractions, can produce peaks that only occur in P_{abd}. In order to assure that the rhythmic activity was caused by the bladder and not being produced by other abdominal activity that could confound analysis, each significant P_{ves} signal was individually compared to the corresponding P_{abd} signal to ensure any bladder activity was independent of abdominal activity. This independence test was performed in multiple steps for each significant P_{ves} peak. First, the P_{ves} amplitude was required to be at least 1.5 times greater than P_{abd} at the same frequency. This identified only relatively large P_{ves} signals. Next, P_{abd} was required to be less than 133% of P_{abd} at either neighboring frequency step, representing a relatively flat signal at that frequency with respect to its neighboring points[22].

A post hoc power analysis determined that a sample size of 52 (participants with DO) and 43 (participants without DO) with a power level of 0.8 and a two-tailed alpha value of 0.05 would result in a power of 0.986. Fisher's exact test was then used to determine if a significant association occurred between DO and the presence of S&I spontaneous rhythmic contractions. Additionally, the patients were grouped by gender and neurogenic (caused by relevant neurological condition) vs. idiopathic (no defined causes)[9] DO to ensure no association existed based on those parameters. Participants with and without S&I SRC were compared by age using a t-test to ensure age was not a significant difference[22].

4.1.3 Results for Objective Quantification of SRC

Ninety-five UD studies met criteria for inclusion and were analyzed with the algorithm. During a blinded visual analysis, a neurourologist/urodynamicist identified 52/95 (55%) patients as having DO. The algorithm was applied to the three defined regions of interest at high volume (ending 0, 30 and 60s prior to the start of voiding). The 30s prior to void region of interest resulted in the FFT algorithm identifying S&I spontaneous rhythmic contractions in 14/52 (27%) patients with DO and 0/43 patients (0%) without DO. This corresponds with 27% sensitivity (reasonable for a subgroup) and 100% specificity. A post hoc power analysis determined that a sample size of 52 (participants with DO) and 43 (participants without DO) with an effect size of 0.8 and a two-tailed alpha value of 0.05 would result in a power of 0.986. It quantified both frequency (3.11±0.34 cycles/min) and amplitude (8.24±1.24 cm-H_2O) of the slowest spontaneous rhythmic contraction frequency identified in this region of interest. When using any of the 3 ranges, 22 of the 52 (42%) patients with DO were correctly identified, while only 1 out of 43 (2%) without were identified resulting in a specificity of 93% and the entire results are shown in Table 4.2[22].

Table 4.2: Results of algorithm when applied to three different regions of interest [22].

Analysis Range	Significant and Independent	Observed DO	No Observed DO	Total	p-value	Sensitivity	Specificity
Prior to void	S&I	16	1	17	0.0003	30.77%	97.67%
	not S&I	36	42	78			
	Total	52	43	95			
30s prior to void	S&I	14	0	14	<0.0001	26.92%	100%
	not S&I	38	43	81			
	Total	52	43	95			
60s prior to void	S&I	13	0	13	0.0002	25%	100%
	not S&I	39	43	82			
	Total	52	43	95			
Any 3 ranges	S&I	22	1	23	<0.0001	45.82%	93.33%
	not S&I	30	42	72			
	Total	52	43	95			

4.1.4 Conclusions for Objective Quantification of SRC

This study developed an automated tool to objectively analyze UD data to determine the presence of and quantify S&I spontaneous rhythmic contractions. It highlighted the feasibility of fast Fourier transform analysis being applied to "real-world" UD studies to automatically characterize the frequency and amplitude of underlying spontaneous rhythmic contractions as well as provide a visual model to verify results as shown in Figure 4.3. Additionally, it identified and quantified a potential subgroup of patients with specifically SRC-mediated DO[22].

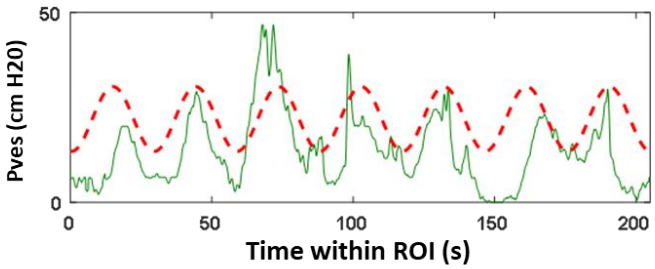

Figure 4.3: Visual confirmation of FFT model compared to original pressure signal. Identified signal showing the original vesical pressure signal (green) and a reconstructed modeled signal (red)[22].

When compared to the previous study that applied fast Fourier transform analysis to human UD studies[33], the present study provides an objective tool that eliminates any bias from first visually inspecting pressure tracings for spontaneous rhythmic contractions. The automated algorithm also performs the analysis in under 5 seconds allowing for real-time data interpretation[22].

This study was limited by the potential of selection bias since studies with multiple voids or leaks being excluded. While the algorithm used an automated process to determine DO, these results were compared to the determination made by a urodynamicist which may have made a subjective diagnosis[22].

This study demonstrated the first use of an automated FFT algorithm for identification and quantification of a DO subgroup with SRC in humans. This algorithm has the potential for real-time data interpretation using data that is already being collected and identified a potential subgroup of patients with spontaneous rhythmic contractions-associated DO[22]. The quantification of SRC amplitude may be a valuable tool because it could be used to measure the effectiveness of specific treatments on outcomes for this subgroup of patients.

4.2 Sub-Aim 1B - Quantify changes in rhythmic contraction amplitude throughout filling

4.2.1 Introduction to quantifying changes in rhythmic contractions throughout filling

Once a tool to identify and quantify spontaneous rhythmic contractions at high volumes had been developed[22], the focus was then shifted to refining the tool parameters and using the tool to characterize changes in spontaneous rhythmic contractions throughout filling. The goals were 1) to further quantify spontaneous rhythmic contractions throughout filling, 2) to determine if participants with normal functioning bladders (no or low OAB symptoms) show spontaneous rhythmic contractions and 3) to determine if the volume at which the DO is detected shows a correlation with OAB symptoms. For this prospective study, a validated International Consultation on Continence Overactive Bladder questionnaire (ICIq-OAB) was completed by each participant to identify OAB symptoms and form groups with no/low OAB and high OAB for comparison. Furthermore, the prospective urodynamics studies were blindly reviewed by a urodynamicist to identify DO and distinguish rhythmic DO from sporadic, isolated, or terminal DO. The performance of the algorithm was optimized to maximize the sensitivity of identifying rhythmic DO based on the presence of rhythmic DO identified by the urodyanmicist. Using the updated

algorithm, significant and independent rhythmic DO amplitudes and frequencies were correlated with OAB symptom severity and characterized as a function of percent bladder capacity.

4.2.2 Methods for quantifying changes in rhythmic contractions throughout filling

The previously developed algorithm was refined and applied to prospectively collected data. Instead of analyzing only three 205-second regions of interest at high volumes, the entire filling phase from the start of the UD pump to the last stop of the UD pump before a void occurred was analyzed iteratively. Typical UD studies fill at 10% bladder capacity and are expected to collect about 10 minutes of filling data[66]. During the initial retrospective study, 205 second regions of interest were used because that corresponded to 2^{11} data points, or about 3.5 minutes of pressure data[22]. Using 2^{10} data points, or 102 seconds, would have yielded almost 3 complete cycles at 1.75 cycles/minute, the lowest frequency of interest. The next highest multiple of two was chosen instead because only three regions of interest were being analyzed and the retrospective study wanted to analyze as much "high volume" data as possible[22].

For the present prospective study that iteratively analyzed the entire filling phase, two signal lengths were tested, a smaller P_{ves} peak threshold was used, and the significance and independence criteria were refined. For signal length, in addition to the 205 second range, the smaller, but still appropriate 102 second signal length was tested to more precisely identify the volume regions where SRC occurs during filling. The original minimum P_{ves} amplitude of 1.8cm-H2O was tested in addition to a smaller 1.0cm-H2O based on minimum urodynamic equipment standards[20]. The significance and independence criteria that were optimized included the slope criteria, the independence peak criteria, and the ratio of the P_{ves} peak to the P_{abd} peak. In the original study, a slope of 20%P_{ves} per frequency step was used to test for significance. While optimizing

the parameters, five slopes were tested (10%, 12.5%, 15%, 17.5% and the original 20%). The first independence criteria requiring the P_{ves} amplitude to be 1.5 times as large as the P_{abd} amplitude at the same frequency was adjusted and tested at five different values (1.0, 1.2, 1.25, 1.3 and the original 1.5). The second independence criteria requiring the P_{abd} amplitude to be less than 133% of its neighboring peaks was iterated through seven values (100%, 125%, the original 133%, 150%, 166%, 175% and 200%). All of these combinations were tested with the goal of maximizing sensitivity.

From the start of filling with the UD pump, the first region of interest extended 205 seconds forward. Each subsequent overlapping region started 30 seconds later and extended 205 seconds forward. This sequence of overlapping regions of interest was repeated until the end of the region of interest passed the final pump stop before voiding. At this point, the end of the region of interest was set at the pump stop time and extended backwards 205 seconds. It is important to note that each individual region of interest was processed individually after being segmented and not the entire signal as a whole. In addition to decreasing the pressure data signal length, the frequency range of interest was expanding from 1.75-6 cycle/min to 1.75-8 cycle/min to identify any higher frequency bladder activity based on studies revealing that the bladder smooth muscle cells exhibit spontaneous action potentials at a frequency of 7.9±4.2 per minute while remaining below average human breathing[41].

Another improvement in the algorithm was the method of preparing data with respect to any steady state offset. In the prior retrospective study, the minimum value of the signal was subtracted from each point in the signal (Figure 4.4 A vs. B), while in the current iteration of the algorithm used for the prospective study, the data were linearly detrended (Figure 4.4 A vs. C) before having a Hanning window applied and undergoing FFT analysis. While this may seem to

be a subtle and insignificant change, the signals in the example in Figure 4.4 show that the effect of detrending on the FFT output is that the steady state value (Figure 4.4, D-F at 0 cycle/min) is removed and the noise at low frequencies making up the underlying trend is diminished (Figure 4.4, 0-3 cycle/min of D and E vs. F). The improved clarity of the frequency spectrum due to the detrending technique is shown in Figure 4.4 with D, E and F corresponding to the respective signals in A, B and C.

Because of the many overlapping volume ranges being analyzed and the large variation in bladder capacity from one participant to another, each region of interest was classified as "First Half" if at least half of the region lay in the first half of the fill based on volume (midpoint volume of the region of interest < capacity at voiding/2) and any region above that threshold was classified as "Second Half". Participants with SRC identified in both "First Half of Filling" and "Second Half of Filling" were classified as "Throughout Filling". Any significant rhythm detected in P_{ves} between 1.75-8 cycles/minute was recorded and quantified and then compared to the P_{abd} signal as in the previous study[22] to determine if it was independent of other rhythmic activity in the body to isolate the bladder as the cause. The volume at which S&I SRC occurred was recorded and the participant was flagged as having S&I SRC in the First Half, Second Half or Throughout filling.

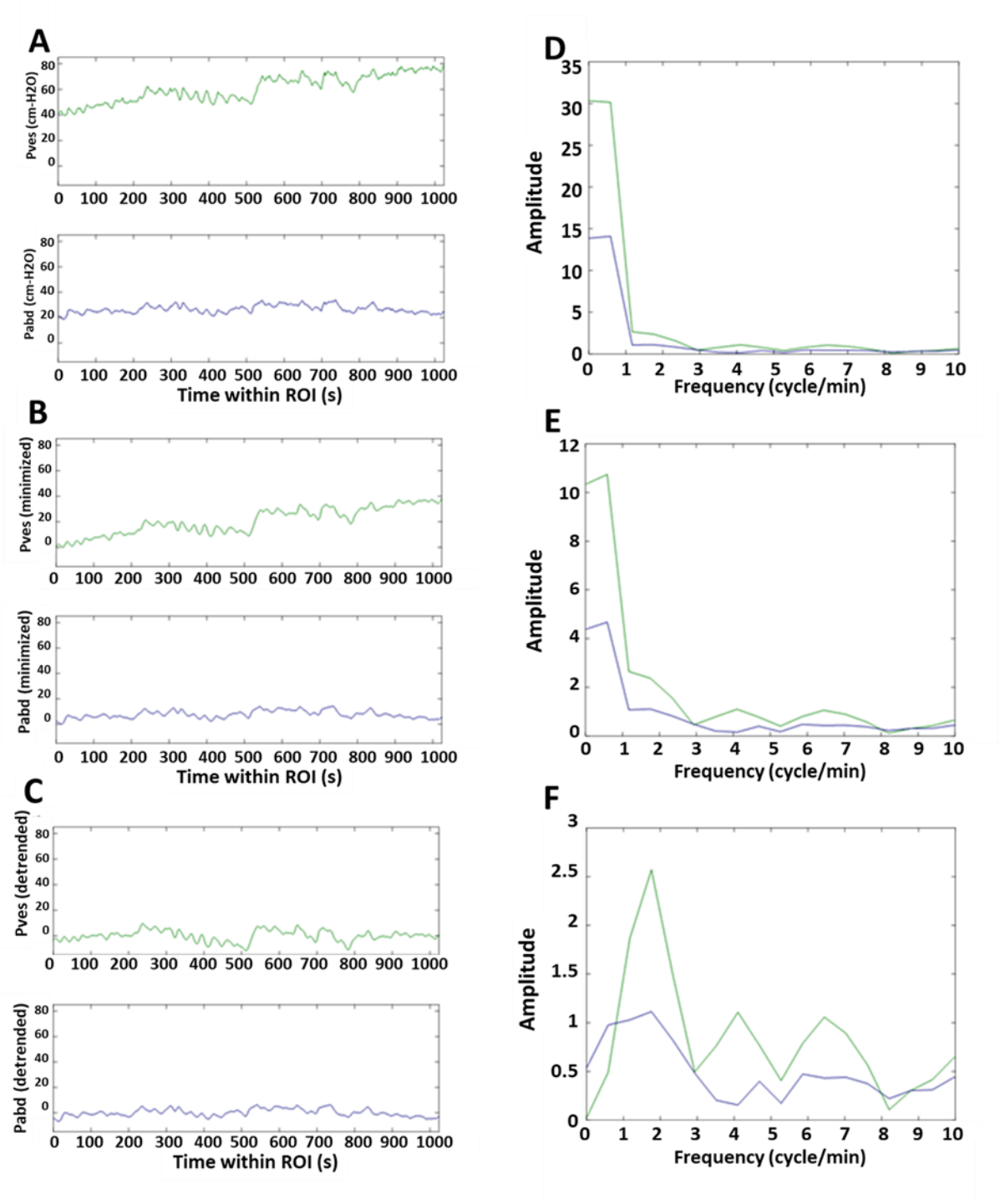

*Figure 4.4: Example of data preparation and FFT output. Pressure data being prepared for analysis: (**A**) raw data, (**B**) data minimized (prior algorithm) and (**C**) data after detrending (current algorithm). Corresponding frequency spectrums for: (**D**) raw data, (**E**) delta pressure (prior algorithm) and (**F**) detrended data (current algorithm).*

4.2.3 Results for quantifying changes in rhythmic contractions throughout filling

Prospective participants were enrolled in this study and completed an OAB survey to determine their symptoms. Complete data sets without relevant artifacts were available for 133 individuals. From this group, 29 (22%) individuals were identified with rhythmic DO in the blinded analysis by a urologist (Table 4.3).

The results of the original and refined algorithms are provided in Tables 4.4 and 4.5. The combination of refined parameters that yielded the highest sensitivity was as follows: the original signal length of 205 seconds, a minimum amplitude of 1.0cm-H_2O, a slope of 15% per frequency step, a P_{ves} value greater than 1.25 times the P_{abd} value and the original criteria of P_{abd} less than 133% of its neighboring points. From the group of 133 participants, the original algorithm identified 28 (21%) individuals with significant and independent SRC (Table 4.4) and the refined algorithm identified 60 (45%) (Table 4.5). Then, participants with S&I SRC were grouped as either no/low OAB (ICIq-OAB 5a=0-1, n=23) or high OAB (5a=2-4, n=37) symptoms and the results are provided in Table 4.4 for the original algorithm parameters as compared to the results for the refined parameters shown in Table 4.5. By refining the parameters, seven additional participants with rhythmic DO were detected by the algorithm, improving the sensitivity to 82%. Maximizing sensitivity was the criteria for refining the algorithm because the expected application of this tool is to supplement a urologist's review of the patient's data, and therefore quantifying all rhythmic DO identified by the urologist was the most important objective. Also, because the tool could potentially identify real rhythmic DO that is not identified visually by a urologist, a specificity of less than 100% for the algorithm was expected and not considered to be a weakness. Furthermore, because this tool will overlay a model of any rhythmic DO identified onto the actual data for the

urologist to review, as shown in Figure 4.3, they will be able to determine whether the signal identified by the algorithm is clinically relevant or an artifact.

Table 4.3: All Participant Characteristics by Significant and Independent SRC – Refined Algorithm.

	S&I	not S&I	Total
n	60	73	133
Rhythmic DO	24	5	29
Age	55.0±2.5	54.2±2.2	54.5±1.6
Male	16	25	41
Female	44	48	92
High OAB	37	36	73
No/low OAB	23	37	60

Table 4.4: Significant and Independent Against Rhythmic DO – Original Algorithm.

	SI	no SI	Total
RDO	16	13	29
no RDO	12	92	104
Total	28	105	133
Sensitivity	55%		
Specificity	88%		
p-value	<0.0001		

Table 4.5: Significant and Independent Against Rhythmic DO – Refined Algorithm

	SI	no SI	Total
RDO	24	5	29
no RDO	36	68	104
Total	60	73	133
Sensitivity	83%		
Specificity	65%		
p-value	<0.0001		

The highest amplitude of rhythmic activity was recorded for each participant, along with the corresponding volume which was used to calculate the percentage of capacity at which it occurred. S&I SRC amplitude was found to be statistically higher, in participants with high OAB compared to those with no/low OAB, 6.86 cm-H_2O and 3.01 cm-H_2O respectively (Figure 4.5A,

p=0.02), while frequency was not different in participants with high OAB and no/low OAB, 3.47 cycle/min and 3.46 cycle/min respectively (Figure 4.5B, p=0.97).

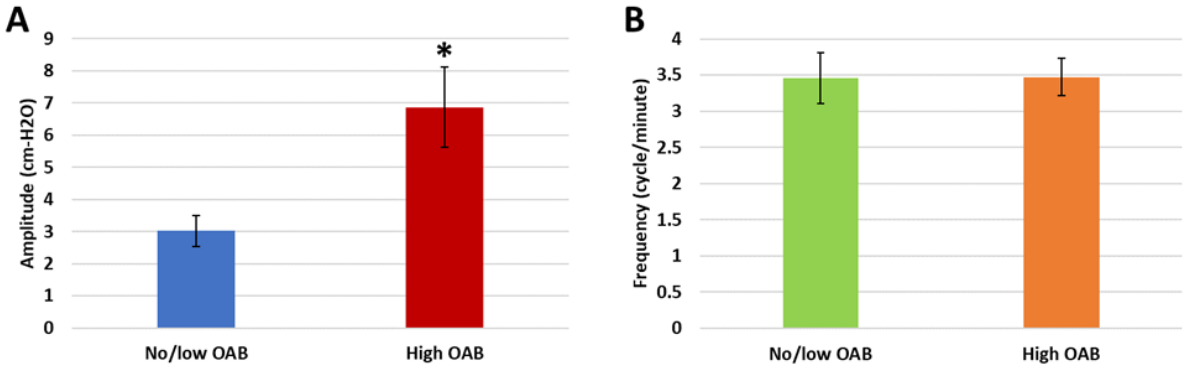

*Figure 4.5: Average peak SRC amplitude and corresponding frequency of groups by OAB. (**A**) Average amplitude of no/low OAB (blue) vs. high OAB (red) SRC (* denoting significant difference) and (**B**) average frequency of no/low OAB (green) and high OAB (orange) SRC.*

In addition to quantifying amplitude and frequency in individuals with and without OAB, this analysis compared the location of the detected S&I SRC by capacity. It was found that 41% of all participants were identified with S&I SRC in the first half compared to 59% in the second half regardless of their OAB symptoms (Figure 4.6, all points to the left and right of the black vertical line, respectively).

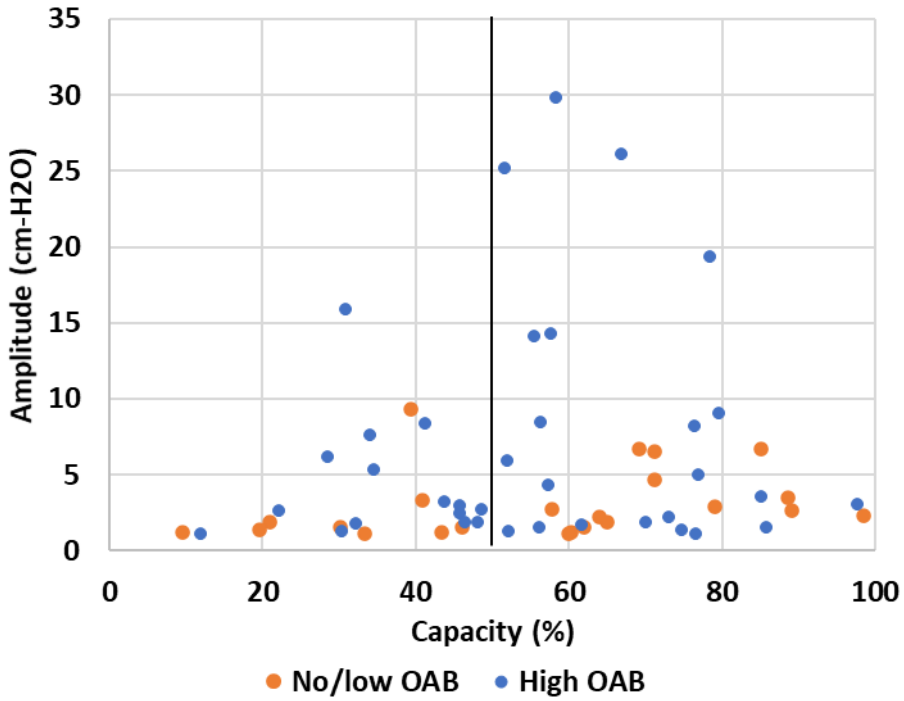

Figure 4.6: Peak significant and independent SRC amplitude versus percent capacity. Scatter plot showing the highest SRC amplitude for each participant with S&I SRC as a function of percent capacity for the no/low OAB group (orange) and high OAB group (blue).

An additional analysis was performed using the slowest S&I SRC frequency found for each participant instead of the highest amplitude. The SRC amplitudes selected by the slowest S&I SRC frequency identified throughout filling are shown in Figure 4.7, noting the similar axis scale as Figure 4.6 for direct comparison. This analysis yielded similar results and the S&I SRC amplitude was statistically greater in participants with high OAB compared to those with no/low OAB (Figure 4.8, panel A, yellow bar compared to red). This shows consistency in the results and in the differences in amplitudes between the high and no/low OAB groups, and highlights the need for quantification of SRC amplitude. Prior work focused on quantifying just frequency[3]. Further quantifying frequency can be simply be done manually by counting peaks[67], while quantifying

amplitude can be more difficult in complex waveforms or those with underlying trends, highlighting the need for the analysis tools developed in this project.

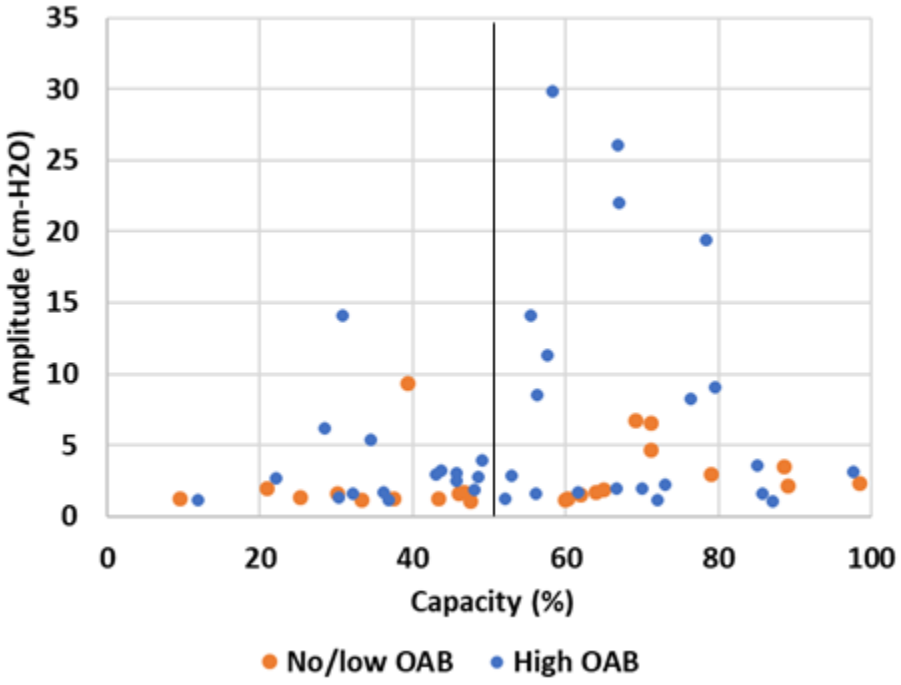

Figure 4.7: Amplitude of S&I SRC with lowest frequency versus percent capacity. Scatter plot of amplitudes throughout filling when determining points using slowest frequency instead of highest amplitude.

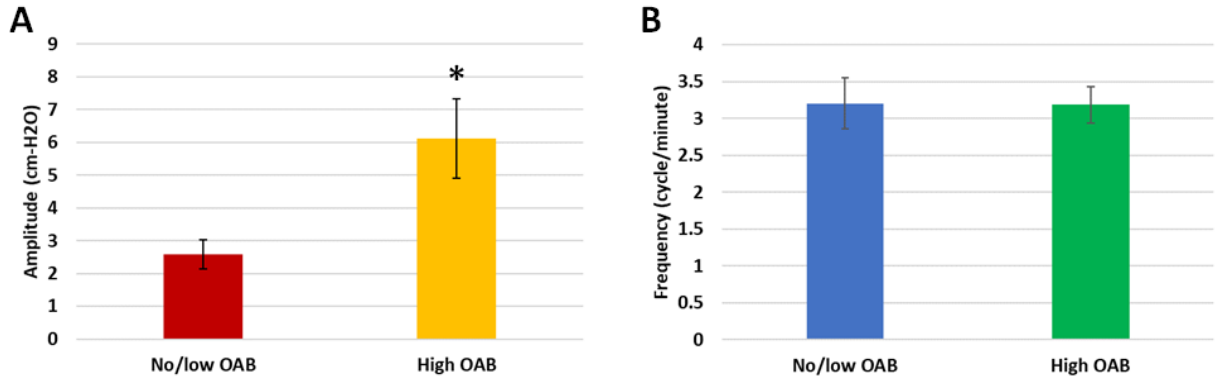

Figure 4.8: Average SRC amplitude and frequency for slowest S&I frequency grouped by OAB. Comparison of (A) amplitude and (B) frequency when using the slowest frequency significant and independent SRC.

4.2.4 Discussion for quantifying changes in rhythmic contractions throughout filling

The outcome of this prospective study was the determination that the rhythmic DO amplitude may have some effect of the participants OAB symptoms since it was shown to be higher in those with higher OAB symptom scores. If a DO threshold amplitude of 7cm-H_2O is established, only 1/23 (4%) of the participants with no/low OAB while 12/37 (33%) of those with high OAB had an amplitude higher than that threshold (Figure 4.9, Table 4.5, p-value = 0.0108). While S&I SRC was found across a variety of participants, those with no/low OAB typically had smaller amplitudes. While some studies have been conducted concerning algorithms to detect bladder contractions as they occur for bladder stimulation[68], the algorithm developed in present study acts as a tool to detect significant and independent rhythmic bladder contractions over an entire UD study to aid clinicians in accurate diagnosis and quantification of severity. These results are similar to previous work suggesting the amplitude of DO contractions may contribute to OAB severity[69] and are consistent with a pre-clinical animal study[60] and another clinical study using time-frequency analysis[64]. The new algorithm could represent a clinically feasible step towards development of measures to quantify DO severity.

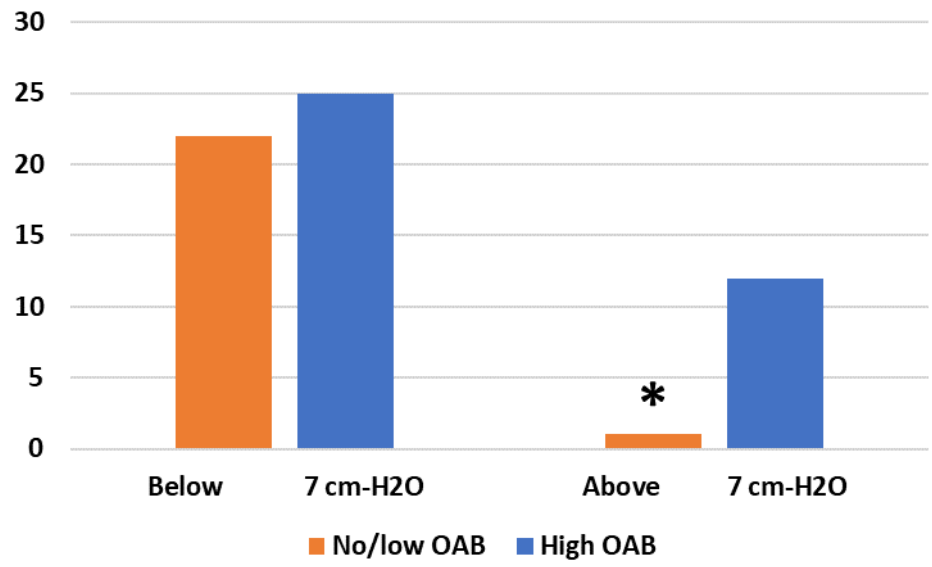

Figure 4.9: Number of participants identified with SRC by amplitude threshold for the no/low OAB group (orange) and high OAB group (blue) (denoting significant difference, p=0.0108).*

Table 4.6: Contingency table of no/low OAB and High OAB by S&I SRC amplitude threshold.

	Below 7 cm-H2O	Above 7 cm-H2O	Total
No/low OAB	22	1	23
High OAB	25	12	37
Total	47	13	60

4.2.4 Conclusions for quantifying changes in rhythmic contractions throughout filling

This study quantified SRC in participants in both frequency and amplitude. It determined that participants with high OAB symptoms showed an elevated amplitude of SRC when compared to those with no/low OAB symptoms while frequency remained similar in both groups. The clinical relevance of this study is the finding that the amplitude of rhythmic DO identified by the algorithm correlates with the severity of OAB symptoms.

Chapter 5 – Aim 2: Characterization of Dynamic Elasticity

Aim 2 investigated and characterized dynamic elasticity (**DE**). This aim was broken into the following four sub-aims:

1) Develop an isolated bladder pig model to study the biomechanical mechanisms affecting dynamic elasticity
2) Quantify dynamic elasticity in participants with and without overactive bladder using comparative-fill urodynamics data
3) Test the hypothesis that dynamic elasticity is inhibited by detrusor overactivity using prospective urodynamics data to confirm Dynamic Elastic Equilibrium Model in Figure 3.2
4) Develop a method to induce dynamic elasticity non-invasively using compression for potential diagnostic and therapeutic applications

5.1 Sub-Aim 2A – Develop isolated pig model to study mechanisms of dynamic elasticity

In order to further study the mechanisms of dynamic elasticity in DSM without influence from other bodily organs and functions, an isolated pig model using whole pig bladders was developed. This study was the basis of the first sub-aim of the dynamic elasticity study of this research and is summarized in this subsection.

5.1.1 Introduction to Pig Bladder Dynamic Elasticity Study

An isolated whole pig bladder model was used to show that the vesical pressure of a whole bladder would significantly decrease following strain softening via filling and passive emptying by syringe aspiration[56]. The study also showed that by inducing voiding contractions that the

decrease in vesical pressure was reversed during the next fill as in previous muscle strips studies[46,47] and the clinical pilot study[56]. This confirmed that dynamic elasticity could be recreated in an isolated environment and that it was an intrinsic mechanical property of the bladder.

5.1.2 Methods for the Pig Bladder Dynamic Elasticity Study

Following previously established methodology[57,58], pig bladders were used in this study. Bladders with the vascular tree and a portion of the aorta were harvested from a local abattoir immediately after slaughter and the vascular system was flushed with Krebs-Henseleit buffer. After transport to the lab in cold buffer, the superior vesical arteries were cannulated and perfused with oxygenated physiologic-temperature Krebs-Henseleit buffer at 4 mL/min (Figure 5.1A). The urethra was catheterized to allow infusion, monitor invervesical pressure and permit voiding. The bladders then underwent a urodynamics protocol with an initial setup fill followed by four comparative test fills (1-3). During these fills, the bladder was filled to 250mL, assumed to be 50% of a total capacity of 500mL, followed by either passive emptying through syringe aspiration or potassium induced contractions to mimic active voiding (Figure 5.1B).

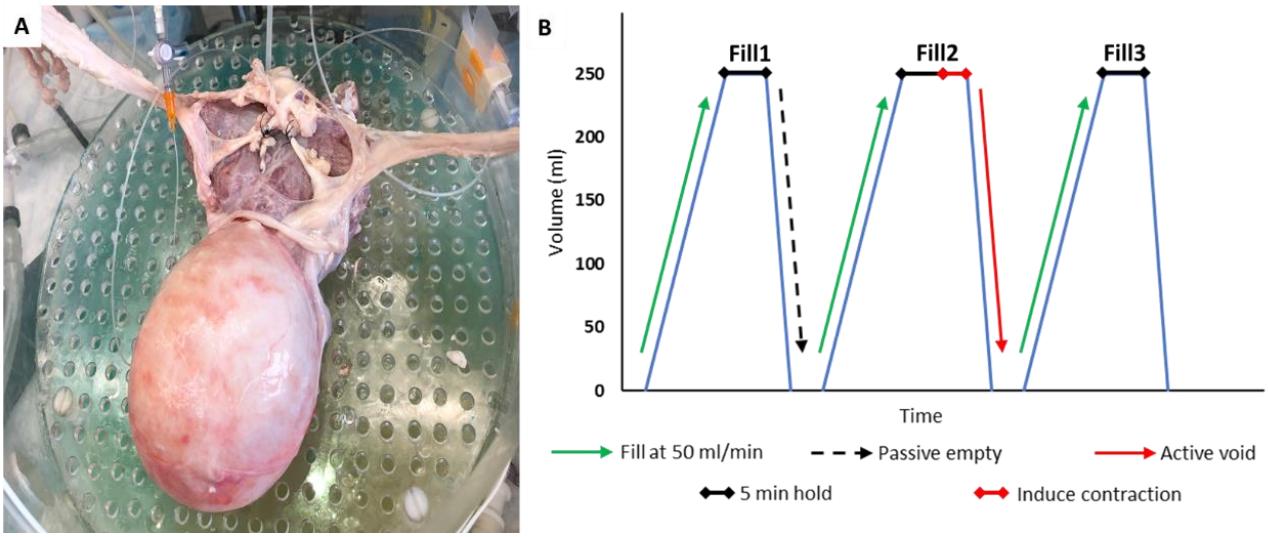

*Figure 5.1: Isolated pig bladder photo and dynamic elasticity protocol. (**A**) Photo of pig bladder in experimental chamber and (**B**) comparative-fill urodynamics protocol. Fill1 is before strain softening, Fill2 is after strain softening and passive emptying and Fill3 is after an active void.*

The setup fill was followed by an active void to empty the bladder and reset any strain softening that occurred before the start of the experiment. Filling data "after active voiding" was recorded in Fill1 as the baseline filling pressure. Fill1 was expected to cause strain softening that could be observed during Fill2, and the bladder was passively emptied following Fill1 to prevent any potential reversal strain softening by way of an active contraction. Filling data was recorded "after passive emptying" during Fill2 and was expected to be less than during Fill1. The bladder was actively voided after Fill2, and this was expected to reverse any strain softening caused by Fill2. Filling data "after active voiding" was recorded in Fill3 and was expected to be greater than "after passive emptying" and similar to baseline filling "after active voiding". The average pressure throughout each fill was calculated and dynamic elasticity was quantified as the change in average pressure between fills divided by the change in percent capacity of filling, assumed to be 50%[56,70].

5.1.3 Results of the Pig Bladder Dynamic Elasticity Study

This comparative-fill urodynamics protocol was performed on six male pig bladders. A quantifiable drop in filling pressure occurred due to strain softening that was regained during subsequent filling following active voiding. The average pressure during Fill2 was significantly lower than the average pressure during Fill1, while Fill1 and Fill3 showed no significant difference (Figure 5.2, p-values of 0.01 and 0.37, respectively). Dynamic elasticity was lost due to strain softening (-0.11 cm-H_2O/%capacity) which was calculated by the change in pressure divided by the assumed change in capacity of 50%, but a comparable amount was regained following active voiding (0.12 cm-H_2O/%capacity).

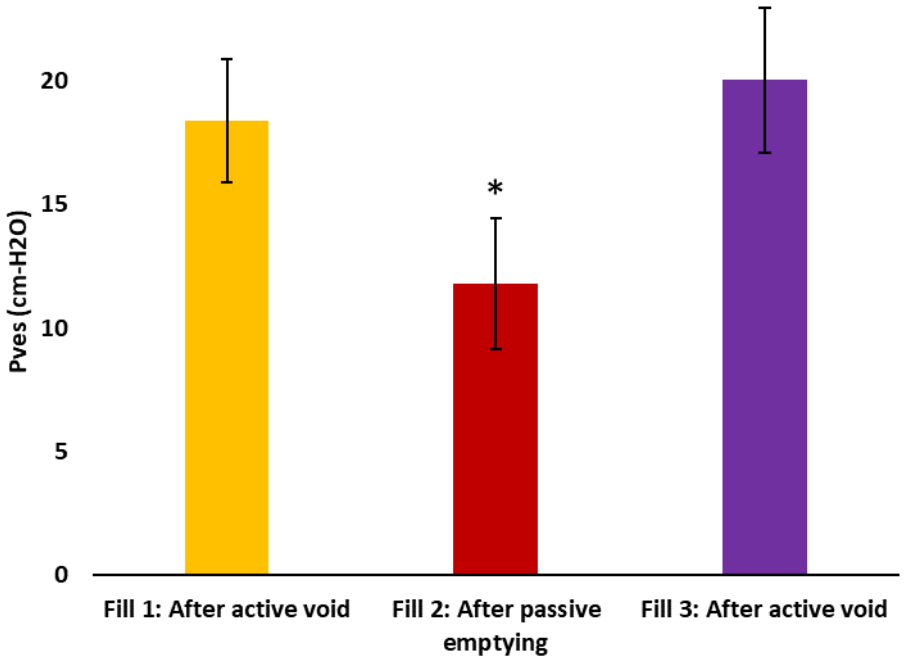

*Figure 5.2: Results demonstrating dynamic elasticity in isolated pig bladders. Average vesical pressure during Fill1-3 with * indicating significant difference from Fill1.*

5.1.4 Conclusions from the Pig Bladder Dynamic Elasticity Study

This study demonstrated that dynamic elasticity could be identified in pig bladders in an isolated environment. The results showed that dynamic elasticity could be quantified in this environment using the same methodology as previously shown in individuals with overactive bladder[56]. Dynamic elasticity regulation would affect bladder wall tension during filling, and consequently affect the stimulation of tension-sensitive nerves responsible for the bladder fullness sensation[3].

A defect in the regulation of dynamic elasticity could contribute to overactive bladder by altering this sensation[18]. More detailed investigations of this bladder material property can be conducted using this isolated pig bladder model to isolate such factors as incomplete voiding, non-voiding contractions, and bladder ischemia that could affect dynamic elasticity[35,53,54]. This would lead to a better understanding of this material property and its effects on bladder biomechanics. Improved knowledge of the role of dynamic elasticity in bladder function and the mechanisms responsible for this property could have diagnostic and therapeutic implications in the management of bladder pathology.

5.2 Sub-Aim 2B – Dynamic elasticity in participants with and without overactive bladder

A pilot clinical study investigating dynamic elasticity was conducted previously[56]. This study focused on whether determining individuals displayed bladder dynamic elasticity and if it could be quantified. While this study revealed dynamic elasticity, it only included five participants, all of which had OAB[56]. One goal of the present study was to further determine whether dynamic elasticity is present in human bladders. This study included a larger group of participants and included those with and without OAB. Participants with and without urgency based on ICIq-OAB

surveys were prospectively enrolled in an IRB-approved comparative-fill UD protocol for this study.

5.2.1 Introduction to the Clinical Dynamic Elasticity Study

A comparative-fill UD protocol differs from a traditional UD protocol in that multiply fill-void cycles are performed and compared during a single visit. Comparative fill UD allows a bladder material property known as dynamic elasticity to be measured. Dynamic elasticity is shown by a reduction in pressure during fills due to strain softening when the bladder is not allowed to actively void and to reset the effects of strain softening. After an active voiding contraction, a restoration in pressure is observed in the subsequent fill demonstrating the reversibility of strain softening in the bladder[56].

5.2.2 Participant Enrollment

Participants over the age of 21 were prospectively enrolled both with and without OAB into the comparative-fill urodynamics protocol. These participants were categorized as having either no/low urgency (ICIq-OAB 5a = 0-1) or high urgency (ICIq-OAB 5a = 2-4). The presence or absence of DO based on urodynamics was also used to characterize participants, as this is more objective than patient reported survey scores.

To determine the minimum number of participants needed for this study, a power analysis was performed based on results of the previous pilot study[56]. Linear interpolation of the normalized data for strain softening to 30% capacity and 60% capacity in the pilot study indicated an expected difference in means of 32% for strain softening to 40% capacity. The power analysis determined

that a sample size of 8 participants per group was needed to identify a statistical difference between groups with a power level of 0.8 and a two-tailed alpha value of 0.05.

5.2.3 Dynamic Elasticity Detection

To determine the presence or absence of dynamic elasticity, multiple urodynamic fills from a single session were compared for each participant. This allowed each individual to act as their own control. An initial "setup fill" to determine cystometric capacity was followed by three consecutive fills were completed by each participant. Each of these fills was followed by either an active void or passive emptying[62]. The fills are described as follows (Figure 5.3):

- Fill 1 – Before strain softening: This fill occurs after the active void following the setup fill which should have reset any strain softening. This fill acts as a baseline for comparison during the next fills. Following this fill to 40% capacity, the bladder is passively emptied through syringe aspiration.
- Fill 2 – After strain softening: This fill occurs after a passive emptying of the bladder so it should show a drop in pressure indicating that the bladder had been strain softened. The bladder is filled to 100% capacity during this fill, but for the comparison, only the pressure from 0-40% capacity is measured. After the participant reaches 100% capacity, they actively void their bladder.
- Fill 3 – After active void: Following the active void at the end of Fill 2, the bladder should have reversed any strain softening that had occurred. Fill 3 is used to determine the degree of strain softening reversal that occurred.

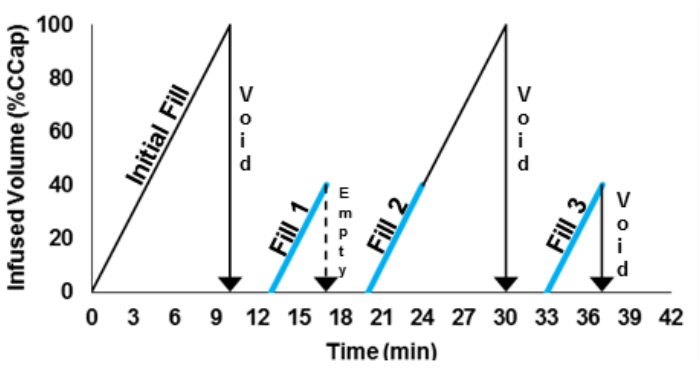

Figure 5.3: Comparative-fill urodynamics protocol to identify dynamic elasticity. Fill 1: before strain softening. Fill 2: after strain softening and passive emptying. Fill 3: after active void[62].

The average pressures from Fills 1-3 were compared to determine if the participant demonstrated dynamic elasticity. A participant was classified as showing dynamic elasticity if the pressure after strain softening was lower than before strain softening and if it showed a return towards the baseline value after active voiding. All other participants were classified as not showing dynamic elasticity[62].

5.2.4 Results from the Entire Dynamic Elasticity Study Population

Of the 43 consecutive studies completed, 28 of them were included in the analysis (Table 5.1) while the other 15 were excluded, including 7 of the 22 no/low OAB participants, due to high post-void residuals which could potentially affect the amount of strain softening reversed following an active void. The group of 28 participants showed the expected trend of reduced pressure in Fill 2 compared to Fills 1 and 3, but did not show statistical significance (Fig. 5.4, p=0.17). These results suggest that either not all bladders exhibited DE during testing or that the protocol used in this study does not adequately detect DE in all participants[62].

Table 5.1: Patients Characteristics Grouped by OAB.

	No/low OAB	High OAB	p-value
Participants	15	13	-
Female	11	10	-
Male	4	2	-
Age (years)	28±3	49±5	<0.01
3-Day Diary Max Voided Volume (ml)	558±49	523±60	0.66
Cystometric Capacity (ml)	611±58	501±91	0.29

OAB = Overactive Bladder, No/low OAB: 5a = 0-1, High OAB: 5a = 2-4

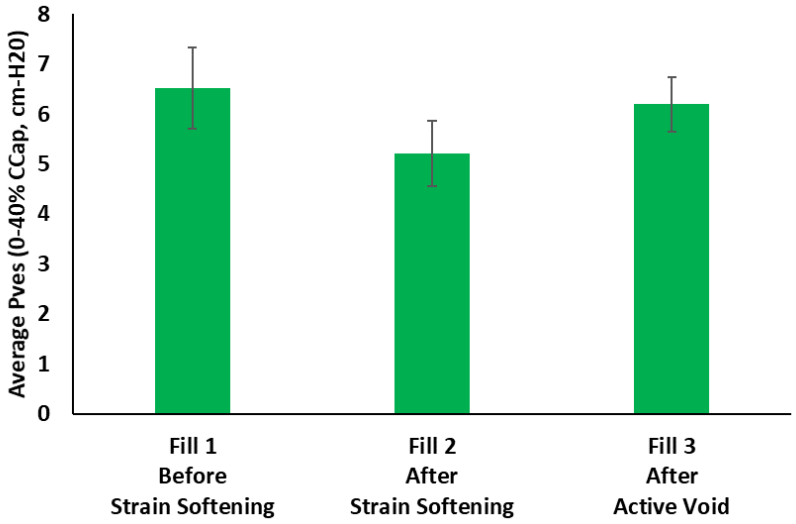

Figure 5.4: Pressure during each comparative UD fill for all participants. Average pressures during each fill of comparative-fill urodynamics protocol (n = 28).

5.2.5 Results of Dynamic Elasticity Grouped by OAB

To further investigate the dynamic elasticity property, participants were grouped as having "No/low OAB" (5a = 0-1, n = 15) and "High OAB" (5a = 2-4, n = 13) and comparative-fill UD results were compared based on this grouping. When comparing void diaries and cystometric capacity of the two groups, no differences were found. The ages were different between the groups, but OAB symptoms appear to increase with age[71], so this does not represent a novel finding when grouping participants by OAB. While dynamic elasticity was identified during the pilot study with 5 participants with OAB[56], the drop in pressure when grouping the current participants by their

level of OAB was not statistically significant (Figure 5.5, p=0.14 Fill1 vs Fill2). Additionally, a pressure drop after passive voiding was only shown in 18/28 participants[62].

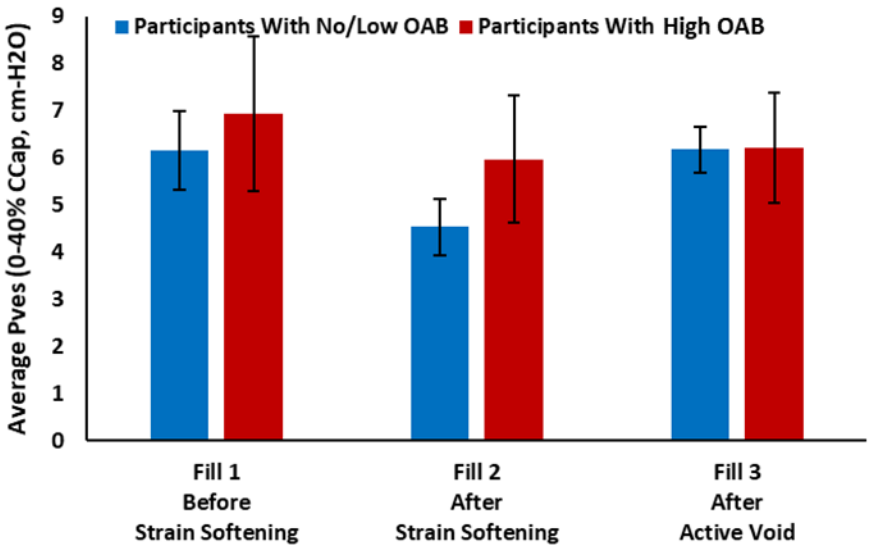

Figure 5.5: Pressure during each comparative UD fill grouped by OAB. Results of comparative-fill studies when grouping participants by No/Low OAB (n=15) and High OAB (n=13).

While strain softening has been shown in other materials[42] and even detrusor strips[50], it was not shown in some of the participants suggesting that something was preventing it from occurring or it was not being measured adequately. Further studies were required to determine what factors might be affecting the dynamic elasticity of the bladder.

5.3 Sub-Aim 2C – Test the Dynamic Elasticity Equilibrium Model

This sub-aim describes a published study linking dynamic elasticity and detrusor overactivity through the Dynamic Elasticity Equilibrium Model previously shown in Figure 3.2[62]. The journal paper is attached in Appendix B and is summarized in this subsection[62].

5.3.1 Introduction to the Dynamic Elasticity Equilibrium Model Study

Dynamic elasticity was identified in 18/28 participants in the study. Grouping the participants by OAB did not correlate with the presence or absence of dynamic elasticity. Since contractions reverse strain softening[55], this sub-aim tested the hypothesis that spontaneous rhythmic contractions may affect DE.

Spontaneous rhythmic contractions are elevated in the detrusor of patients with DO when compared to urodynamically normal bladders[34]. Elevated spontaneous rhythmic contractions, or micromotions[38], have also been associated with urgency[3,18].

5.3.2 Dynamic Elasticity Equilibrium Model

These studies suggest a link between dynamic elasticity and DO and were the motivation behind the construction of the conceptional biomechanical model (Figure 5.6) which is similar to the model proposed by van Duyl[72]. According to the model, dynamic elasticity is lowered by passive forces such as stretching that occurs during filling. This decreased tension is restored through active contractions of the bladder muscle. In urodynamically normal bladders, these active and passive mechanisms should be appropriately balanced such that they aid in maintaining optimal biomechanical conditions[62].

Bladders with elevated contractile activity (DO), may have altered dynamic elasticity regulation leading them to exhibit less dynamic elasticity. Normal bladders are expected to have balanced mechanisms as shown in Figure 5.6. Bladders with DO do not fit this model because the active mechanisms are increased and do not show a drop in pressure due to strain softening. To test the DE Model in Figure 5.6, participants were grouped by the presence or absence of DO instead of by OAB symptoms to determine the effect DO has on the bladder's ability to regulate wall tension through dynamic elasticity[62].

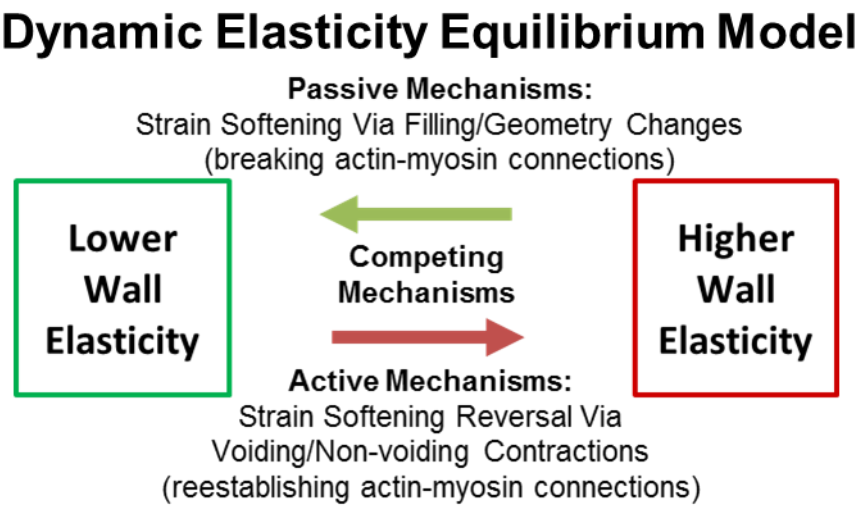

Figure 5.6: Dynamic elasticity equilibrium model. Conceptual model potentially explaining lack of pressure drop in some participants[62].

5.3.3 Results of the Dynamic Elasticity Equilibrium Model Study

Participants characteristics are listed in Table 5.1 for the groups with and without DO. Those groups were not found to be different based on age (t-test, p=0.73) and maximum voided volume during the 3-day void diary completed prior to the study (p=0.76, one participant with DO did not complete a void diary). The groups did show a difference when comparing the capacities

based on the setup fill and those without DO in this study were found to have larger cystometric capacities during UD studies (p=0.03)[62].

Table 5.2: Patient Characteristics Grouped by DO.

	DO+	DO-	p-value
Participants	15	13	-
Female	10	11	-
Male	5	2	-
High Urgency	10	3	-
No Urgency	5	10	-
Age (years)	39±5	36±5	0.73
3-Day Diary Max Voided Volume (ml)	554±60	530±35	0.76
Cystometric Capacity (ml)	443±74	667±61	0.03

DO = Detrusor Overactivity, + = positive, - = negative.

A significant drop in pressure was found in participants without DO after strain softening, while those with DO did not show such drop (Figure 5.7, green bars p-value = 0.004 and yellow bars p-value = 0.0862, respectively). The group without DO then showed a return towards the baseline value following the active void (Figure 5.7)[62].

A dynamic elasticity index to quantify the degree of bladder dynamic elasticity in a single number was defined as:

$$Dynamic\ elasticity\ index = \frac{\left((P_{ves}1 - P_{ves}2) + (P_{ves}3 - P_{ves}2)\right)}{40\%\ capacity}$$

where $P_{ves}1$ is the average pressure from 0-40% capacity during Fill 1, $P_{ves}2$ is the average pressure from 0-40% capacity during Fill 2 and $P_{ves}3$ is the average pressure from 0-40% capacity during Fill 3. By the definition of the dynamic elasticity index, a higher index would correspond to more dynamic elasticity or a larger loss of elasticity from strain softening and more restoration of elasticity due to an active void reversing strain softening. A threshold corresponding to 1.0 cm-

H_2O over 40% capacity was defined to divide the groups into higher dynamic elasticity (index ≥ 0.025cm-H_2O/%capacity, Figure 5.8, above red line) and reduced dynamic elasticity (index < 0.025cm-H_2O/%capacity, Figure 5.8, below red line). Participants without DO (9 out of 15, 60%) showed a dynamic elasticity index less than 0.025cm-H2O, while only 2 out of 13 (15%) of participants with DO showed an index below that threshold resulting in a significant association between reduced dynamic elasticity and DO (p-value = 0.024)[62].

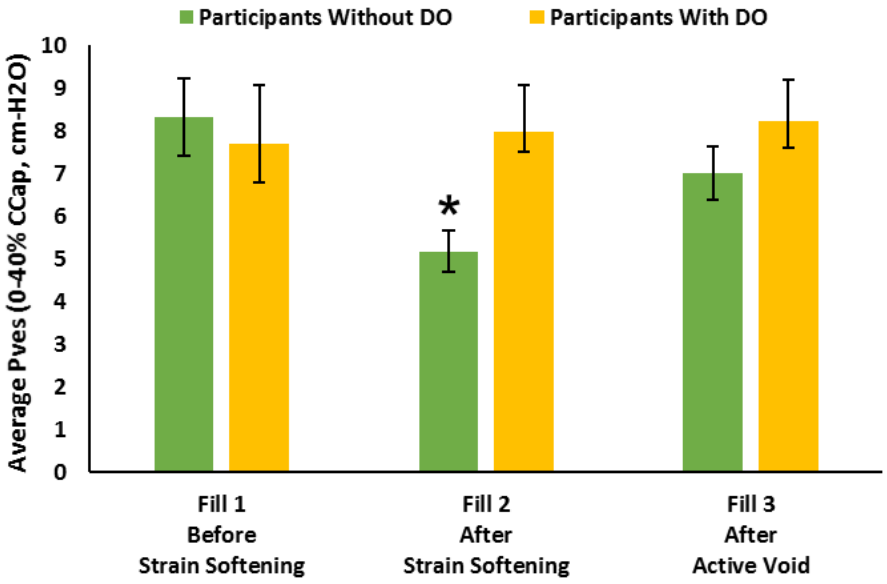

Figure 5.7: Pressure during each comparative UD fill grouped by DO. Average bladder pressures between 0-40% capacity for participants without (green) and with (yellow) DO. Participants without DO showed a significant drop in pressure between Fills 1-2 (p=0.004), while those with DO did not. After active voiding the participants without DO showed a return toward the baseline value of Fill 1[62].

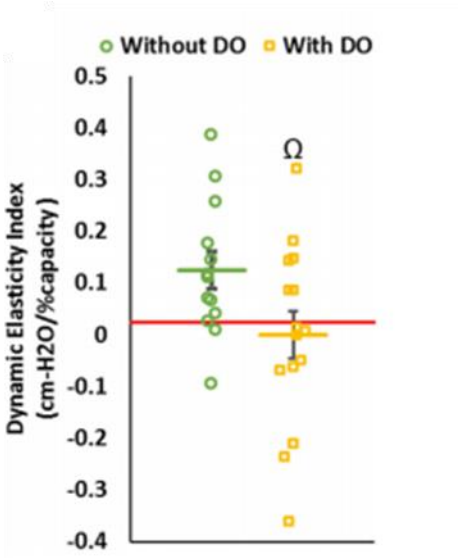

Figure 5.8: Dynamic elasticity index results. The average dynamic elasticity index was significantly less in participants with DO (yellow line, p=0.045, Ω) compared to those without DO (green line). A threshold was selected at 0.025 cm-H2O/%capacity (red line) to distinguish between those with reduced dynamic elasticity and those with greater dynamic elasticity[62].

Dynamic elasticity was identified mainly in individuals without DO, which supports the conceptually model proposed. This model describes the relationship between passive mechanisms, such as the bladder wall stretching during filling, which lower wall tension and active mechanisms, such as voiding contractions or DO, which increase wall tension. It may identify the purpose of SRC, which was shown in Chapter 4 to be present throughout filling even in some individuals without OAB symptoms. Additionally, the dynamic elasticity equilibrium model could explain the contribution DO has to OAB in that it creates an imbalance of active vs. passive mechanisms (Figure 5.6)[62].

5.3.4 Conclusions of Dynamic Elasticity Equilibrium Model Study

This study simplified the comparative-fill protocol by measuring and comparing pressure between the same volumes (0-40%) and removing an extra fill. A limitation of the study was the lack of objective metrics to identify DO. Many participants were also excluded due to high post-void residuals, but this group also included several patients showing no/low OAB symptoms[62].

In summary, the study described in this sub-aim tested the conceptual model for dynamic elasticity with competing active and passive mechanisms presented in Figure 5.6. An association between DO and an absence of dynamic elasticity was found. This absence suggests that DO may cause an imbalance in the competing mechanisms affecting the bladders ability to regulate wall tension which is an important step in understanding the factors likely contributing to OAB in some individuals[62].

5.4 Sub-Aim 2D – Induce dynamic elasticity non-invasively using compression

This sub-aim describes a published study on an innovative protocol involving external compression of the bladder to induce dynamic elasticity non-invasively in the previously described isolated pig bladder model[57,58]. The journal paper is attached in Appendix C, and is summarized in this section[59].

5.4.1 Introduction to the Compression Study

Prior studies have identified reversible strain-softening of the bladder, termed dynamic elasticity, during UD studies[56,62]. This biomechanical property of the bladder is responsible for acute regulation of bladder wall tension during filling. Those studies required invasive UD protocols, including the placement of a urethral catheter to facilitate passive emptying. UD studies have inherent risks[19] and any strain softening caused by UD filling is expected to be reversed

during the next void. The present study aimed to strain-soften the bladder using non-invasive compression techniques to reduce intravesical pressure and possibly urinary urgency which may represent an essential step in potential therapies.

5.4.2 Balloon Study Methods

Latex balloons were infused using a urodynamics unit (Aquarius TT, Laborie, Ontario) and catheter similar to how an actual UD study would be performed clinically to determine if strain softening could be accomplished through compression. Each balloon was either filled to a volume of 3000 mL then emptied to 1500 mL before measuring pressure ("Fill" protocol, Figure 5.9 A and C) or filled to 1500 mL then pressed by hand to a similar pressure as the balloons during the Fill protocol experienced at 3000 mL ("Press" protocol, Figure 5.9 B and D)[59].

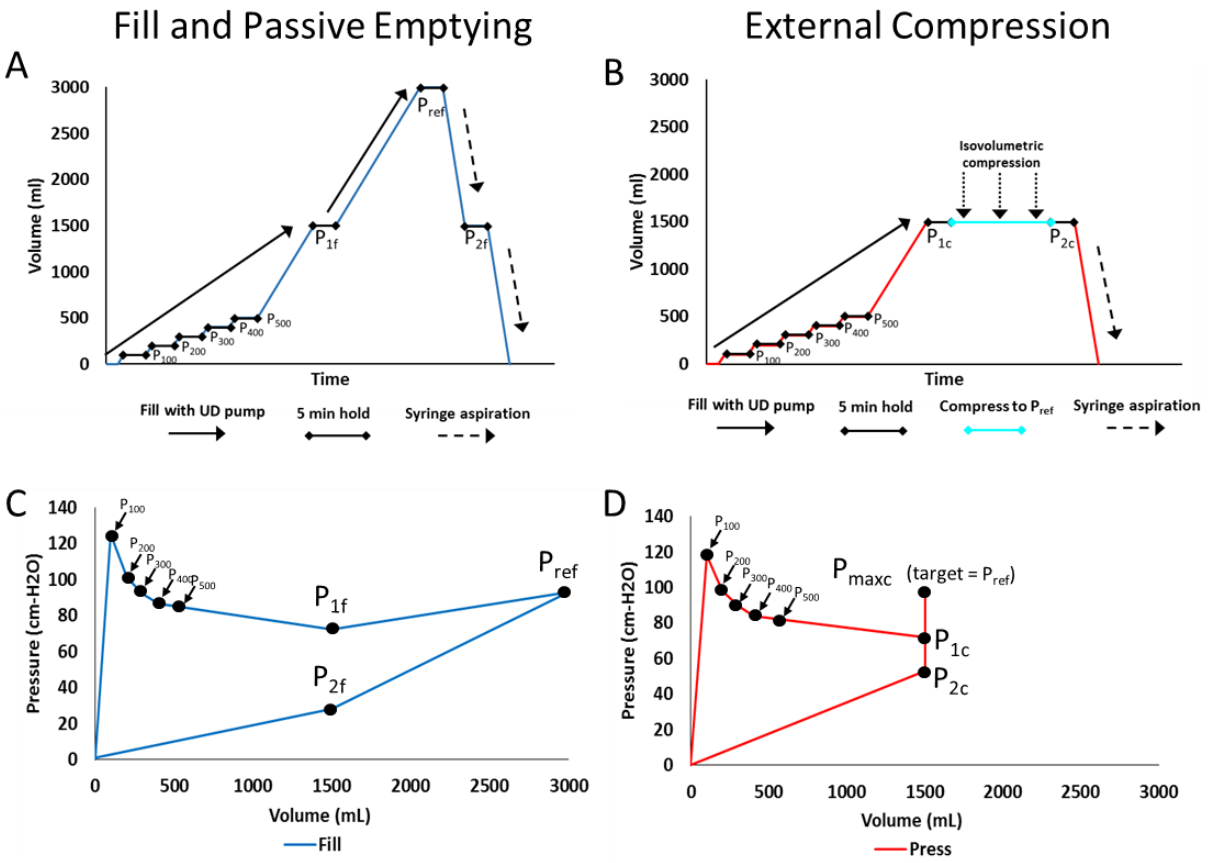

Figure 5.9: Fill and compression protocols for quantifying strain softening. Protocols for balloon experiments showing time and volume for fill and compression (A and B respectively) and volume and pressure for fill and compression (C and D respectively) [59].

Both Fill and Press protocols were applied to separate balloons and new balloons were used for each protocol. At 1500 mL after a 5-minute equilibration period, pressures from both groups were recorded and compared. Those that underwent the Fill protocol showed a comparable degree of strain-softening as those in the Press protocol validating the concept before it was applied to pig bladders[59].

5.4.3 Pig Bladder Methods

Pig bladders from adult male and female pigs were obtained immediately after harvest and cannulated with heparinized Krebs-Henseleit buffer for transport to the lab. Once in the lab, excess tissue was removed and vesical arteries were cannulated to allow perfusion of oxygenated Krebs-Henseleit buffer at 4 mL/minute. The urethra was cannulated to allow infusion, voiding and monitoring of vesical pressure throughout filling or compression and the bladder was stored in a custom chamber to regulate temperature (Figure 5.10)[59].

Figure 5.10: Isolated pig bladder in experimental chamber. The chamber regulates humidity and temperature while the bladder is perfused to simulate physiologic conditions[59].

A similar protocol was applied to the bladders as the balloons underwent. A fill and empty protocol ("Fill") began by filling the bladder to 250 mL, allowing it to reach a stable pressure, then recording that pressure. The bladder was then filled to 500 mL, allowed to reach a steady state and record the pressure before being syringe aspirated to 250 mL and recording the pressure there after equilibration to quantify the pressure drop to strain softening. The compress-release protocol

("Press") filled the bladder to 250 mL and allowed to reach steady state before isovolumetric compression by hand to the same pressure reached at 500 mL during the previous Fill protocol. The pressure after compression was then recorded to compare the degree of strain softening from each method. Each bladder underwent 2 cycles of Fill then Press protocols. This allowed a maximal filling pressure value to be determined for each individual bladder so that subsequent compression could be applied to reach the same target pressure. It also demonstrated repeatability and that the compression protocol had not damaged the bladders[59].

5.4.4 Results from the Balloon and Pig Compression Studies

The balloon study involved ten balloons (n = 5, Fill and n = 5, Press, Figure 5.11, blue and red, respectively) and both protocols showed a significant drop in pressure due to the strain softening caused. A total of eight (n = 8) pig bladders underwent the Fill then Press protocols. A significant drop in pressure before and after filling was achieved. A similarly significant drop in pressure occurred when the bladders were compressed instead. After the active void following each protocol, the pressures showed no significant differences, indicating the strain softening was reversed (Figure 5.12)[59].

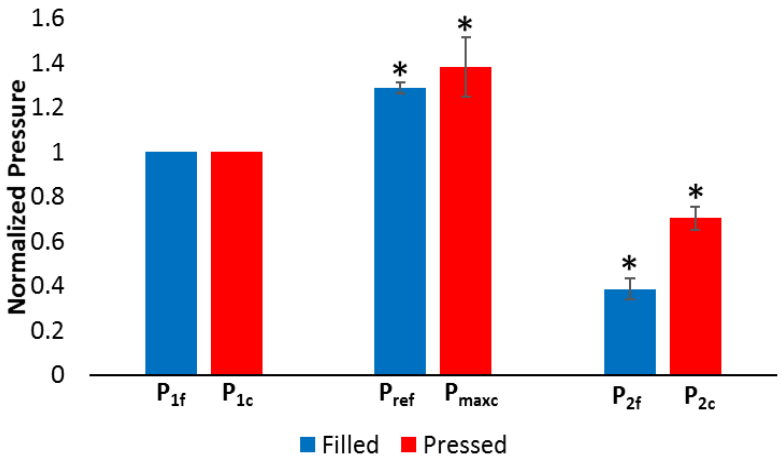

Figure 5.11: Balloon stain softening results for filling versus compression. Normalized pressure of balloons when filled (blue) and compressed (red) [59].

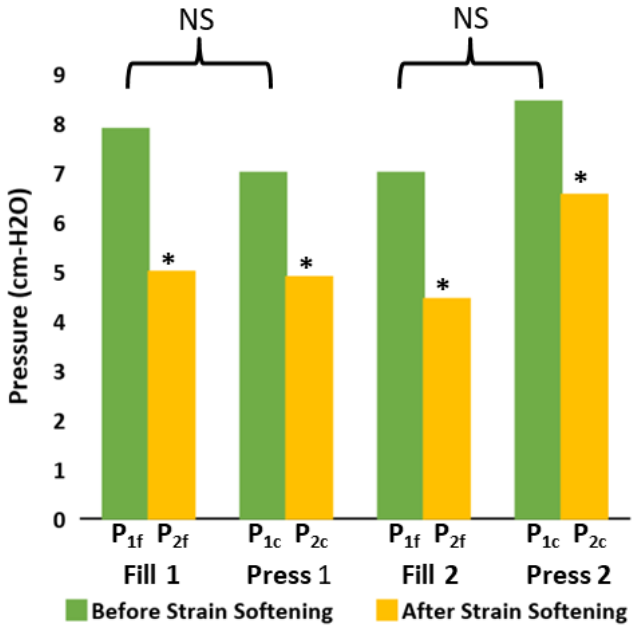

Figure 5.12: Pig bladder strain softening results for filling versus comparison. Average pressures for pig bladder experiments before strain softening (green) and after strain softening (yellow) and each fill and compression experiments[59].

This study showed that it was feasible to adjust bladder wall tension through non-invasive methods, in this case compression. This could potentially be used as a therapeutic tool to reduce bladder wall tension and therefore sensation which could prolong the filling phase and reduce

urgency associated with OAB. It also shows the potential the isolated pig model developed has when considering the study of dynamic elasticity and other related mechanisms within the bladder[59].

5.4.5 Limitations of Compression Study

This study used an ex-vivo pig model which may not be representative of human bladder function. Reversible strain softening has been identified in multiple mammalian species warranting further studies. External compression may also increase the need to void in vivo. This suggests further studies would be required to find the magnitude and timing of compression to effectively treat symptoms[59].

5.4.6 Conclusions of Compression Study

In summary, this study described in this sub-aim showed that strain softening could be demonstrated using both filling and isovolumetric compression. This strain softening was acutely reversible. This novel, noninvasive technique has the potential for diagnostic and therapeutic applications. The reduction of intravesical pressure may prolong filling and lead to a reduction in OAB symptoms[59].

Chapter 6 – Summary and Conclusions

6.1 Research Summary

OAB is a complex issue affecting many people, and many of the mechanisms that cause it are not understood. Therefore, new diagnostic tools improved subtyping are needed. This dissertation investigated the mechanisms regulating bladder biomechanics as a potential factor contributing to OAB. Additionally, methodologies were developed to objectively detect and quantify different types of DO.

6.2 Specific Contributions

This research provided the following specific contributions:

- Developed a novel tool for quantification of spontaneous rhythmic contractions in clinical UD data[22]
- Identified a DO subgroup with spontaneous rhythmic contractions[22]
- Applied the quantification tool to prospective data throughout filling to characterize changes in rhythmic contractions as volume increases in individuals with and without OAB symptoms
- Identified dynamic elasticity in an isolated pig bladder model to enable further study individual biomechanical factors
- Quantified dynamic elasticity in individuals with and without OAB for the first time[62]
- Defined a dynamic elasticity index to quantify degree of dynamic elasticity with a single value[62]
- Linked dynamic elasticity to DO and developed a model of competing biomechanical mechanisms acting to acutely regulate bladder elasticity[62]

- Induced dynamic elasticity non-invasively through a novel external compression protocol in an isolated pig bladder model[59]

Through the contributions of sub-aim 1A, this dissertation project showed the potential for subtyping of an SRC-mediated form of DO through automated, real-time analysis. Sub-aim 1B investigated changes in rhythm, both amplitude and frequency, throughout the filling phase and patients with and without OAB symptoms. The results of sub-aim 1B indicate that the amplitude of rhythmic activity correlates with OAB symptoms and that high amplitude rhythmic DO may represent a clinically significant OAB subtype.

With regards to dynamic elasticity, sub-aim 2A showed that it could be studied in an ex-vivo pig model to isolate biomechanical factors for further study. Sub-aim 2B provided a simplified protocol for quantifying dynamic elasticity. Sub-aim 2C linked DO to dynamic elasticity and established a model of competing biomechanical mechanisms that regulate dynamic elasticity. Sub-aim 2D developed a novel technique to non-invasively induce strain softening using external compression, providing a necessary step toward future studies involving diagnostic and therapeutic tools for OAB.

These contributions have provided improved understanding of the biomechanical factors influencing OAB which could allow for more effective treatment and diagnostics. In addition, this work could provide the necessary background information for the development of additional objective and non-invasive tools surrounding OAB.

6.3 Future Directions

Improvements to the spontaneous rhythmic contraction quantification algorithm could be made that allow it to detect clinically relevant DO using only data obtained from bladder pressure tracings, eliminating the need for a second invasive catheter placement in the rectum. This stems from the idea that the bladder acts as a tension sensor and any increase in tension in the bladder wall, even those caused by other bodily activity, could have clinical relevance in the sensation feedback. Studies involving machine learning could be conducted to either optimize the current algorithm parameters or develop new parameters entirely now that the underlaying mechanisms have been investigated.

Further studies are needed involving dynamic elasticity to completely confirm the equilibrium model and how it is influenced by detrusor overactivity. Further studies should incorporate participants with underactive bladder, which may have the opposite effect on dynamic elasticity compared to DO. Additional studies are also needed to determine the exact feasibility of isovolumetric compression as a therapeutic tool. Specific studies are needed to determine 1) if it is possible to apply sufficient compression without generating an uncontrollable desire to void, 2) the magnitude of acute compression that is necessary to provide a meaningful decrease in pressure and sensation, and 3) the optimal timing of these compressions for relevantly prolonging the filling phase.

References

1. Drake RL (Richard L, Vogl W, Mitchell AWM, Gray H. *Gray's Anatomy for Students*.

2. Bouhout S, Rousseau A, Chabaud S, Morissette A, Bolduc S. Potential of Different Tissue Engineering Strategies in the Bladder Reconstruction. In: *Regenerative Medicine and Tissue Engineering*. ; 2013. doi:10.5772/55838

3. Drake MJ, Harvey IJ, Gillespie JI, Van Duyl WA. Localized contractions in the normal human bladder and in urinary urgency. *BJU Int*. 2005;95(7):1002-1005. doi:10.1111/j.1464-410X.2005.05455.x

4. Speich JE, Southern JB, Henderson S, Wilson CW, Klausner AP, Ratz PH. Adjustable passive stiffness in mouse bladder: regulated by Rho kinase and elevated following partial bladder outlet obstruction. *Am J Physiol Ren Physiol*. 2012;302(8):F967-76. doi:ajprenal.00177.2011 [pii] 10.1152/ajprenal.00177.2011

5. Southern JB, Frazier JR, Miner AS, Speich JE, Klausner AP, Ratz PH. Elevated steady-state bladder preload activates myosin phosphorylation: detrusor smooth muscle is a preload tension sensor. *Am J Physiol Ren Physiol*. 2012;303(11):F1517-26. doi:10.1152/ajprenal.00278.2012

6. Almasri AM, Ratz PH, Bhatia H, Klausner AP, Speich JE. Rhythmic contraction generates adjustable passive stiffness in rabbit detrusor. *J Appl Physiol*. 2010;108(3):544-553. doi:01079.2009 [pii] 10.1152/japplphysiol.01079.2009

References

7. Yoshimura N, Chancellor MB. Neurophysiology of lower urinary tract function and dysfunction. *Rev Urol*. 2003;5 Suppl 8(Suppl 8):S3-S10. http://www.ncbi.nlm.nih.gov/pubmed/16985987. Accessed May 26, 2020.

8. Hashim H, Abrams P. Overactive bladder: an update. *Curr Opin Urol*. 2007;17(4):231-236. doi:10.1097/MOU.0b013e32819ed7f9

9. Abrams P, Cardozo L, Fall M, et al. The standardisation of terminology of lower urinary tract function: report from the Standardisation Sub-committee of the International Continence Society. *Neurourol Urodyn*. 2002;21(2):167-178. http://www.ncbi.nlm.nih.gov/pubmed/11857671.

10. Dolat MET, Klausner AP. UROPSYCHIATRY: The Relationship Between Overactive Bladder and Psychiatric Disorders. *Curr Bladder Dysfunct Rep*. 2013;8(1):69-76. doi:10.1007/s11884-012-0164-5

11. Gormley EA, Lightner DJ, Faraday M, Vasavada SP, American Urological A, Society of Urodynamics FPM. Diagnosis and treatment of overactive bladder (non-neurogenic) in adults: AUA/SUFU guideline amendment. *J Urol*. 2015;193(5):1572-1580. doi:10.1016/j.juro.2015.01.087

12. Kanai A, Andersson KE. Bladder afferent signaling: recent findings. *J Urol*. 2010;183(4):1288-1295. doi:10.1016/j.juro.2009.12.060

13. Mahfouz W, Al Afraa T, Campeau L, Corcos J. Normal urodynamic parameters in women: part II--invasive urodynamics. *Int Urogynecol J*. 2012;23(3):269-277. doi:10.1007/s00192-011-1585-y

References

14. Frenkl TL, Railkar R, Palcza J, et al. Variability of urodynamic parameters in patients with overactive bladder. *Neurourol Urodyn*. 2011;30(8):1565-1569. doi:10.1002/nau.21081

15. Drake MJ, Hedlund P, Harvey IJ, Pandita RK, Andersson KE, Gillespie JI. Partial outlet obstruction enhances modular autonomous activity in the isolated rat bladder. *J Urol*. 2003;170(1):276-279. doi:10.1097/01.ju.0000069722.35137.e0

16. Habteyes FG, Komari SO, Nagle AS, et al. Modeling the influence of acute changes in bladder elasticity on pressure and wall tension during filling. *J Mech Behav Biomed Mater*. 2017;71:192-200. doi:10.1016/j.jmbbm.2017.02.020

17. Eastham JE, Gillespie JI. The concept of peripheral modulation of bladder sensation. *Organogenesis*. 2013;9(3):224-233. doi:10.4161/org.25895

18. Coolsaet BLRA, Van Duyl WA, Van Os-Bossagh P, De Bakker H V. New concepts in relation to urge and detrusor activity. *Neurourol Urodyn*. 1993;12(5):463-471. doi:10.1002/nau.1930120504

19. Solomon ER, Ridgeway B. Interventions to decrease pain and anxiety in patients undergoing urodynamic testing: A randomized controlled trial. *Neurourol Urodyn*. 2016;35(8):975-979. doi:10.1002/nau.22840

20. Gammie A, Clarkson B, Constantinou C, et al. International continence society guidelines on urodynamic equipment performance. *Neurourol Urodyn*. 2014;33(4):370-379. doi:10.1002/nau.22546

References

21. Schfer W, Abrams P, Liao L, et al. Good Urodynamic Practices: Uroflowmetry, filling cystometry, and pressure-flow studies. *Neurourol Urodyn*. 2002;21(3):261-274. doi:10.1002/nau.10066

22. Cullingsworth ZE, Kelly BB, Deebel NA, et al. Automated quantification of low amplitude rhythmic contractions (LARC) during real-world urodynamics identifies a potential detrusor overactivity subgroup. *PLoS One*. 2018;13(8):e0201594. doi:10.1371/journal.pone.0201594

23. Abrams P, Cardozo L, Fall M, et al. The standardisation of terminology of lower urinary tract function: report from the Standardisation Sub-committee of the International Continence Society. *Neurourol Urodyn*. 2002;21(2):167-178. doi:10.1002/nau.10052 [pii]

24. Cullingsworth ZE, Kelly BB, Deebel NA, et al. Automated quantification of low amplitude rhythmic contractions (LARC) during real-world urodynamics identifies a potential detrusor overactivity subgroup. *PLoS One*. 2018;13(8):e0201594. doi:10.1371/journal.pone.0201594

25. Lessard CS (Charles S. *Signal Processing of Random Physiological Signals*. Morgan & Claypool Publishers; 2006.

26. Harris FJ. On the Use of Windows for Harmonic Analysis with the Discrete Fourier Transform. *Proc IEEE*. 1978;66(1):51-83. doi:10.1109/PROC.1978.10837

27. Shenfeld OZ, McCammon KA, Blackmore PF, Ratz PH. Rapid effects of estrogen and progesterone on tone and spontaneous rhythmic contractions of the rabbit bladder. *Urol Res*. 1999;27(5):386-392. http://www.ncbi.nlm.nih.gov/pubmed/10550529.

References

28. Andersson KE. Detrusor myocyte activity and afferent signaling. *Neurourol Urodyn*. 2010;29(1):97-106. doi:10.1002/nau.20784

29. Brading AF. A myogenic basis for the overactive bladder. *Urology*. 1997;50(6A Suppl):57-73. http://www.ncbi.nlm.nih.gov/pubmed/9426752.

30. Szell EA, Somogyi GT, de Groat WC, Szigeti GP. Developmental changes in spontaneous smooth muscle activity in the neonatal rat urinary bladder. *Am J Physiol Regul Integr Comp Physiol*. 2003;285(4):R809-16. doi:10.1152/ajpregu.00641.2002

31. McCarthy CJ, Zabbarova I V, Brumovsky PR, Roppolo JR, Gebhart GF, Kanai AJ. Spontaneous contractions evoke afferent nerve firing in mouse bladders with detrusor overactivity. *J Urol*. 2009;181(3):1459-1466. doi:10.1016/j.juro.2008.10.139

32. Chacko S, Cortes E, Drake MJ, Fry CH. Does altered myogenic activity contribute to OAB symptoms from detrusor overactivity? ICI-RS 2013. *Neurourol Urodyn*. 2014;33(5):577-580. doi:10.1002/nau.22599

33. Colhoun AF, Speich JE, Cooley LF, et al. Low amplitude rhythmic contraction frequency in human detrusor strips correlates with phasic intravesical pressure waves. *World J Urol*. 2017;35(8):1255-1260. doi:10.1007/s00345-016-1994-0

34. Kinder RB, Mundy AR. Pathophysiology of idiopathic detrusor instability and detrusor hyper-reflexia. An in vitro study of human detrusor muscle. *Br J Urol*. 1987;60(6):509-515. http://www.ncbi.nlm.nih.gov/pubmed/3427334.

35. Komari SO, Headley PC, Klausner AP, Ratz PH, Speich JE. Evidence for a common mechanism for spontaneous rhythmic contraction and myogenic contraction induced by quick stretch in detrusor smooth muscle. *Physiol Rep*. 2013;1(6):e00168. doi:10.1002/phy2.168

36. Sui G, Fry CH, Malone-Lee J, Wu C. Aberrant Ca2+ oscillations in smooth muscle cells from overactive human bladders. *Cell Calcium*. 2009;45(5):456-464. doi:10.1016/j.ceca.2009.03.001

37. Lentle RG, Reynolds GW, Janssen PW, Hulls CM, King QM, Chambers JP. Characterisation of the contractile dynamics of the resting ex vivo urinary bladder of the pig. *BJU Int*. 2015;116(6):973-983. doi:10.1111/bju.13132

38. Drake MJ, Kanai A, Bijos DA, et al. The potential role of unregulated autonomous bladder micromotions in urinary storage and voiding dysfunction; overactive bladder and detrusor underactivity. *BJU Int*. 2017;119(1):22-29. doi:10.1111/bju.13598

39. Potjer RM, Constantinou CE. Frequency of spontaneous contractions in longitudinal and transverse bladder strips. *Am J Physiol - Regul Integr Comp Physiol*. 1989;257(4). doi:10.1152/ajpregu.1989.257.4.r781

40. Biers SM, Reynard JM, Doore T, Brading AF. The functional effects of a c-kit tyrosine inhibitor on guinea-pig and human detrusor. *BJU Int*. 2006;97(3):612-616. doi:10.1111/j.1464-410X.2005.05988.x

41. Hashitani H, Brading AF, Suzuki H. Correlation between spontaneous electrical, calcium and mechanical activity in detrusor smooth muscle of the guinea-pig bladder. *Br J Pharmacol*. 2004;141(1):183-193. doi:10.1038/sj.bjp.0705602

42. Mullins L, Tobin NR, Harwood JAC, Payne AR. Stress softening in rubber vulcanizates -- 3. *J Appl Polym Sci*. 1966;10(2):315-324. doi:10.1002/app.1966.070100212

43. Mullins L. Effect of Stretching on the Properties of Rubber. *Rubber Chem Technol*. 1948;21(2):281-300. doi:10.5254/1.3546914

44. Carew EO, Barber JE, Vesely I. Role of preconditioning and recovery time in repeated testing of aortic valve tissues: validation through quasilinear viscoelastic theory. *Ann Biomed Eng*. 2000;28(9):1093-1100. doi:10.1114/1.1310221

45. Diani J, Fayolle B, Gilormini P, Diani J, Fayolle B, Gilormini P. A review on the Mullins effect A review on the Mullins effect. European Polymer A review on the Mullins' effect. doi:10.1016/j.eurpolymj.2008.11.017ï

46. Speich JE, Borgsmiller L, Call C, Mohr R, Ratz PH. ROK-induced cross-link formation stiffens passive muscle: reversible strain-induced stress softening in rabbit detrusor. *Am J Physiol Cell Physiol*. 2005;289(1):C12-21. http://www.ncbi.nlm.nih.gov/entrez/query.fcgi?cmd=Retrieve&db=PubMed&dopt=Citation&list_uids=15716326.

47. Ratz PH, Speich JE. Evidence that actomyosin cross bridges contribute to "passive" tension in detrusor smooth muscle. *Am J Physiol Ren Physiol*. 2010;298(6):F1424-35. doi:ajprenal.00635.2009 [pii] 10.1152/ajprenal.00635.2009

48. Neal CJ, Lin JB, Hurley T, et al. Slowly cycling Rho kinase-dependent actomyosin cross-bridge "slippage" explains intrinsic high compliance of detrusor smooth muscle. *Am J Physiol Ren Physiol*. 2017;313(1):F126-F134. doi:10.1152/ajprenal.00633.2016

References

49. Ford LE, Seow CY, Pratusevich VR. Plasticity in smooth muscle, a hypothesis. *Can J Physiol Pharmacol*. 1994;72(11):1320-1324. doi:10.1139/y94-190

50. Colhoun AF, Speich JE, Dolat MT, et al. Acute length adaptation and adjustable preload in the human detrusor. *Neurourol Urodyn*. 2016;35(7):792-797. doi:10.1002/nau.22820

51. Fung YC (Yuan-cheng), Fung YC (Yuan-cheng), 1919-. *Biomechanics : Mechanical Properties of Living Tissues*. Springer-Verlag; 1993.

52. Speich JE, Almasri AM, Bhatia H, Klausner AP, Ratz PH. Adaptation of the length-active tension relationship in rabbit detrusor. *Am J Physiol Ren Physiol*. 2009;297(4):F1119-28. doi:10.1152/ajprenal.00298.2009

53. Jiang H, Liao D, Zhao J, Wang G, Gregersen H. Contractions reverse stress softening in rat esophagus. *Ann Biomed Eng*. 2014;42(8):1717-1728. doi:10.1007/s10439-014-1015-7

54. Almasri AM, Ratz PH, Speich JE. Length adaptation of the passive-to-active tension ratio in rabbit detrusor. *Ann Biomed Eng*. 2010;38(8):2594-2605. doi:10.1007/s10439-010-0021-7

55. Colhoun AF, Speich JE, Dolat MT, et al. Acute length adaptation and adjustable preload in the human detrusor. *Neurourol Urodyn*. 2015. doi:10.1002/nau.22820

56. Colhoun AF, Klausner AP, Nagle AS, et al. A pilot study to measure dynamic elasticity of the bladder during urodynamics. *Neurourol Urodyn*. 2017;36(4):1086-1090. doi:10.1002/nau.23043

57. Vince R, Tracey A, Deebel NA, et al. Effects of vesical and perfusion pressure on perfusate flow, and flow on vesical pressure, in the isolated perfused working pig bladder reveal a potential mechanism for the regulation of detrusor compliance. *Neurourol Urodyn*. 2018;37(2):642-649. doi:10.1002/nau.23362

58. Anele UA, Ratz PH, Colhoun AF, et al. Potential vascular mechanisms in an ex vivo functional pig bladder model. *Neurourol Urodyn*. 2018;37(8):2425-2433. doi:10.1002/nau.23710

59. Balthazar A, Cullingsworth ZE, Nandanan N, et al. An external compress-release protocol induces dynamic elasticity in the porcine bladder: A novel technique for the treatment of overactive bladder? *Neurourol Urodyn*. 2019. doi:10.1002/nau.23992

60. Byrne MD, Klausner AP, Speich JE, Southern JB, Habibi JR, Ratz PH. Fourier transform analysis of rabbit detrusor autonomous contractions reveals length dependent increases in tone and slow wave development at long lengths. *J Urol*. 2013;190(1):334-340. doi:10.1016/j.juro.2013.02.071

61. Metcalfe PD, Wang J, Jiao H, et al. Bladder outlet obstruction: progression from inflammation to fibrosis. *BJU Int*. 2010;106(11):1686-1694. doi:10.1111/j.1464-410X.2010.09445.x

62. Cullingsworth ZE, Klausner AP, Li R, et al. Comparative-fill urodynamics in individuals with and without detrusor overactivity supports a conceptual model for dynamic elasticity regulation. *Neurourol Urodyn*. 2020;39(2):707-714. doi:10.1002/nau.24255

63. Colhoun AF, Klausner AP, Nagle AS, et al. A pilot study to measure dynamic elasticity of the bladder during urodynamics. *Neurourol Urodyn*. 2016. doi:10.1002/nau.23043

64. Niederhauser T, Gafner ES, Cantieni T, et al. Detection and quantification of overactive bladder activity in patients: Can we make it better and automatic? *Neurourol Urodyn*. 2018;37(2):823-831. doi:10.1002/nau.23357

65. Nagle AS, Speich JE, De Wachter SG, et al. Non-invasive characterization of real-time bladder sensation using accelerated hydration and a novel sensation meter: An initial experience. *Neurourol Urodyn*. 2016. doi:10.1002/nau.23137

66. Drake MJ, Doumouchtsis SK, Hashim H, Gammie A. Fundamentals of urodynamic practice, based on International Continence Society good urodynamic practices recommendations. *Neurourol Urodyn*. 2018;37:S50-S60. doi:10.1002/nau.23773

67. Klausner AP, King AB, Byrne MD, et al. A new and automated method for objective analysis of detrusor rhythm during the filling phase. *World J Urol*. 2014;32(1):85-90. doi:10.1007/s00345-013-1084-5

68. Karam R, Bhunia S, Majerus S, Brose SW, Damaser MS, Bourbeau D. Real-time, autonomous bladder event classification and closed-loop control from single-channel pressure data. In: *Proceedings of the Annual International Conference of the IEEE Engineering in Medicine and Biology Society, EMBS*. Vol 2016-October. Institute of Electrical and Electronics Engineers Inc.; 2016:5789-5792. doi:10.1109/EMBC.2016.7592043

69. Miller KL, Dubeau CE, Bergmann M, Griffiths DJ, Resnick NM. Quest For A Detrusor Overactivity Index. *J Urol*. 2002;167(2 Pt 1):578-585. doi:10.1097/00005392-200202000-00028

References

70. Anele UA, Ratz PH, Colhoun AF, et al. Potential vascular mechanisms in an ex vivo functional pig bladder model. *Neurourol Urodyn*. 2018. doi:10.1002/nau.23710

71. Eapen RS, Radomski SB. Review of the epidemiology of overactive bladder. *Res Reports Urol*. 2016;8:71-76. doi:10.2147/RRU.S102441

72. van Duyl WA. A model for both the passive and active properties of urinary bladder tissue related to bladder function. *Neurourol Urodyn*. 1985;4(4):275-283. doi:10.1002/nau.1930040404

Appendix A – PloS ONE FFT Algorithm Paper

PLOS ONE

RESEARCH ARTICLE

Automated quantification of low amplitude rhythmic contractions (LARC) during real-world urodynamics identifies a potential detrusor overactivity subgroup

Zachary E. Cullingsworth[1], Brooks B. Kelly[2], Nicholas A. Deebel[2], Andrew F. Colhoun[2], Anna S. Nagle[1], Adam P. Klausner[2,3], John E. Speich[1]*

1 Department of Mechanical and Nuclear Engineering, Virginia Commonwealth University School of Engineering, Richmond, Virginia, United States of America, **2** Department of Surgery/Division of Urology, Virginia Commonwealth University School of Medicine, Richmond, Virginia, United States of America, **3** Department of Surgery/Division of Urology Hunter Holmes McGuire Veterans Affairs Medical Center, Richmond, Virginia, United States of America

* jespeich@vcu.edu

OPEN ACCESS

Citation: Cullingsworth ZE, Kelly BB, Deebel NA, Colhoun AF, Nagle AS, Klausner AP, et al. (2018) Automated quantification of low amplitude rhythmic contractions (LARC) during real-world urodynamics identifies a potential detrusor overactivity subgroup. PLoS ONE 13(8): e0201594. https://doi.org/10.1371/journal.pone.0201594

Editor: Adrian Stuart Wagg, University of Alberta, CANADA

Received: January 23, 2018

Accepted: July 18, 2018

Published: August 15, 2018

Data Availability Statement: All relevant data are within the paper and its Supporting Information files.

Funding: This work was supported by grant number R01DK101719 from the National Institutes of Health (https://www.niddk.nih.gov/) awarded to APK and JES. The funder had no role in study design, data collection and analysis, decision to publish, or preparation of the manuscript.

Abstract

Objectives

Detrusor overactivity (DO) is characterized by non-voiding detrusor smooth muscle contractions during the bladder filling phase and often contributes to overactive bladder. In some patients DO is observed as isolated or sporadic contractions, while in others DO is manifested as low amplitude rhythmic contractions (LARC). The aim of this study was to develop an objective method to quantify LARC frequencies and amplitudes in urodynamic studies (UDS) and identify a subgroup DO of patients with LARC.

Methods

An automated Fast Fourier Transform (FFT) algorithm was developed to analyze a 205-second region of interest of retrospectively collected "real-world" UDS ending 30 seconds before voiding. The algorithm was designed to identify the three largest rhythmic amplitude peaks in vesical pressure (P_{ves}) in the 1.75–6 cycle/minute frequency range. These peak P_{ves} amplitudes were analyzed to determine whether they were 1) significant (above baseline P_{ves} activity) and 2) independent (distinct from any in abdominal pressure (P_{abd}) rhythm).

Results

95 UDS met criteria for inclusion and were analyzed with the FFT algorithm. During a blinded visual analysis, a neurourologist/urodynamicist identified 52/95 (55%) patients as having DO. The FFT algorithm identified significant and independent (S&I) LARC in 14/52 (27%) patients with DO and 0/43 patients (0%) without DO, resulting in 100% specificity and a significant association (Fischer's exact test, $p<0.0001$). The average slowest S&I LARC frequency in this DO subgroup was 3.20±0.34 cycles/min with an amplitude of 8.40±1.30

Appendix

Competing interests: The authors have declared that no competing interests exist.

cm-H_2O. This algorithm can analyze individual UDS in under 5 seconds, allowing real-time interpretation.

Conclusions

An FFT algorithm can be applied to "real-world" UDS to automatically characterize the frequency and amplitude of underlying LARC. This algorithm identified a potential subgroup of DO patients with LARC.

Introduction

Isolated detrusor smooth muscle strips from animals [1–3] and humans [4–6] exhibit spontaneous contractions, which often show some degree of rhythmicity [7] and have low amplitudes relative to maximal KCl-induced contractions [8]. These low amplitude rhythmic contractions (LARC) generate afferent nerve activity [1] and are elevated in the detrusor from patients with DO [6]. LARC are responsible for localized micromotion during bladder filling, and elevated micromotion has been associated with urgency [9]. In preclinical investigations, LARC have been identified in detrusor smooth muscle strips from various mammalian species [1–6] as well as in isolated whole bladders [10–13]. Although there may not be a one-to-one correlation between contractile events observed in preclinical studies and pressure fluctuations seen during UDS, the term LARC has been used for both types of events [4]. The reason is that isolated changes in vesical pressure (P_{ves}) during urodynamics must be due to underlying bladder contractions. Therefore, for this study, the term LARC refers to rhythmic contractile events that are distinct from isolated or sporadic (i.e. non-rhythmic) contractions during bladder filling.

In humans, LARC has been identified in isolated human detrusor strips[4–6] and studies using catheter-mounted electrodes have shown increased LARC in women with elevated urinary urgency.[9] However, one critical research objective has been to develop methodologies to identify and characterize LARC during human urodynamic studies (UDS). To this end, recent investigations have used Fast Fourier Transforms (FFT), a mathematical technique in which complex waveforms are broken down and presented as underlying frequencies with scaled amplitudes, to characterize LARC in UDS. The first study used FFT to quantify visually identified LARC during UDS and showed a similar underlying frequency in both UDS and in isolated human detrusor strips.[4] Another study, which used a form of FFT called wavelet analysis, showed that the technique might be used to improve and automate the diagnosis of DO.[14]

Although the diagnosis of DO is relatively straightforward and based on visual identification of involuntary contractions [15], determining whether DO represents isolated, unrelated events, as opposed to coordinated rhythmic waveforms, is much more challenging, especially at amplitudes <5 cm-H_2O [15]. We hypothesize that among the group of individuals with visually identifiable DO there is a subgroup with quantifiable LARC. The aims of the present study were 1) to develop an automated and objective FFT algorithm to identify and quantify LARC in UDS pressure data and 2) to implement the algorithm on data from patients with and without DO to determine the algorithm's sensitivity and specificity.

For this initial investigation, we chose to use retrospectively collected UDS data (multiple indications and replete with artifacts and technical irregularities) in order to show broad applicability of our technique in "real-world" UDS. This method could ultimately be used to identify and characterize a subgroup of DO patients with LARC.

Appendix

Methods

Patient information

This study was approved by the Virginia Commonwealth University Institutional Review Board. Retrospective data from 239 consecutive UDS performed in the VCU Urology Urodynamics Laboratory over a three-year period were extracted directly from a Laborie Aquarius TT™ multichannel UDS system (Laborie, Toronto). Data from 131 patients at least 21 years of age with complete medical records, vesical and abdominal pressure data, and at least 7 minutes of UDS filling were considered for analysis (see example in Fig 1). Studies from 36 patients with leaks or multiple voiding events were not included because the algorithm was designed to analyze a single fill-void cycle. Therefore, data from 95 studies with either a terminal voiding event or no voiding event were analyzed. The UDS pressure data were retrospectively analyzed by a neurourologist and expert urodynamicist who was blinded to other patient information. DO was diagnosed in 52 individuals based on ICS guidelines.[15] Patient characteristics as well as DO and algorithm results were then unblinded and summarized in Table 1.

FFT analysis of pressure data

Multichannel UDS data were loaded into an automated MATLAB (R2016A, MathWorks, Natick, MA) algorithm developed to analyze the data as described in the flow chart in Fig 2. A step-by-step example of the data analysis is provided in Fig 2 with panel labels A-G corresponding to the steps in the flow chart. The actual data from the UDS machine example (Fig 1) was utilized for the generation of Fig 2. The beginning of the voiding event, if any, was identified by analyzing the voided volume data (Fig 2A, blue line). A ROI was defined as the 205 seconds ending 30 seconds before the beginning of the voiding event (Fig 2A, green region). The 205-second duration was chosen because it represents 2048, or 2^{11}, data points collected at 10 Hz, permitting consistent bin width and windowing during FFT analysis. The algorithm was implemented on three 205-second ROIs ending 1) at void, 2) 30 seconds prior to void, and 3) 60 seconds prior to void (Fig 3A, red, purple, and yellow, respectively). The reason for varying this time from the onset of voiding was because some voiding contractions (i.e. not filling phase activity) can precede the onset of voiding and because there can be some delay in the detection of voiding between the time urine leaves the urethral meatus to the time it hits the flowmeter.

P_{ves} and P_{abd} data for the ROI in its raw form (Fig 2B) were shifted by subtracting the minimum value for each signal from all data in the ROI. P_{ves} and P_{abd} data were subsequently smoothed using a 10-point moving average (Fig 2C). A Hanning window was applied to P_{ves} and P_{abd} data to eliminate discontinuities at the beginning and end of the ROI when making the signal periodic. FFT analysis was performed independently on the P_{ves} and P_{abd} data in the ROI to convert the signals to the frequency domain (Fig 2D). Normalized pressure amplitudes corresponding to frequencies within a range of 1.75–6.0 cycles/min were analyzed (Fig 2E) based on previous studies showing bladder rhythmic activity occurring between 1.8 and 5 cycles/min.[4, 5, 9].

Significant and independent LARC

The results of the FFT analysis were used to identify LARC in P_{ves} signals with "significant" amplitude peaks at frequencies within the 1.75–6.0 cycles/min range that were "independent" of any amplitude peaks in P_{abd}. Within range of 1.75–6 cycles/min, the three largest amplitude peaks in P_{ves} and corresponding frequencies were identified (Fig 2D, P_{ves}1-3). For each P_{ves} peak (Fig 2E, P_{ves}1), the two neighboring points on each side (Fig 2F, points J and K on left

Appendix

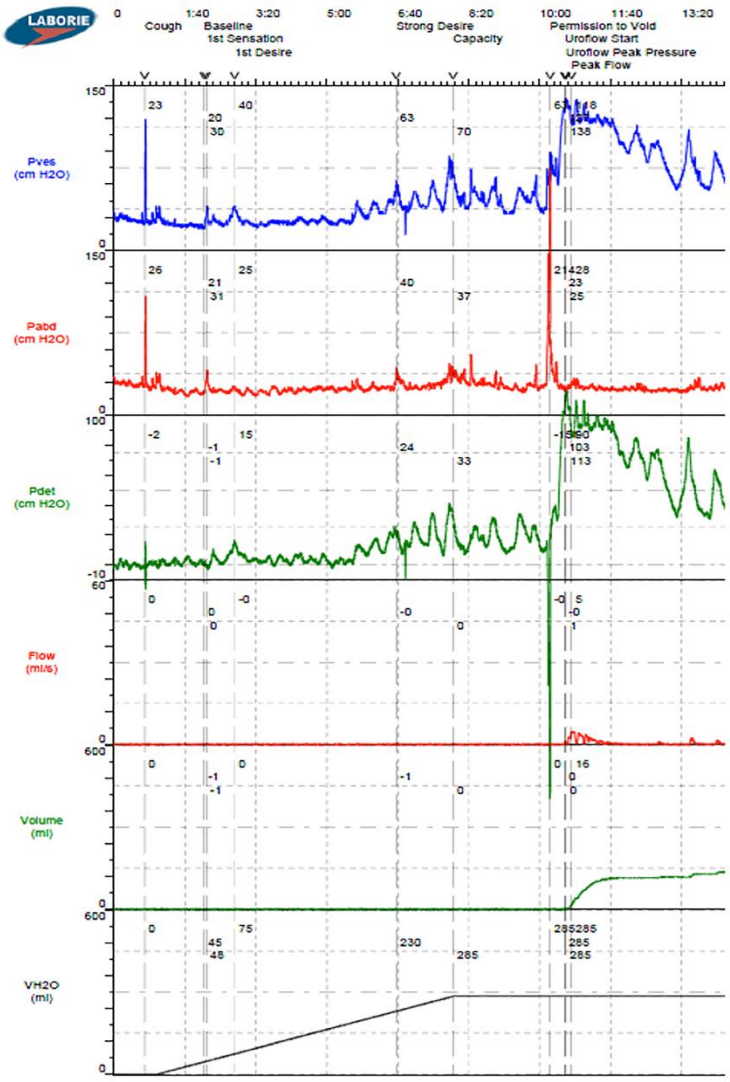

Fig 1. Example multichannel urodynamics output for P_{ves}, P_{abd}, detrusor pressure ($P_{det} = P_{ves} - P_{abd}$), infused volume (VH2O), voided volume (volume) and void flow rate (flow).

https://doi.org/10.1371/journal.pone.0201594.g001

and points L and M on the right) were analyzed to test for significance (Fig 2F). In addition, in order to show independence from $P_{abd,}$ the corresponding P_{abd} point (Fig 2G, P_{abd}I) was compared with one neighboring P_{abd} point on each side (Fig 2G, points Q and R).

Appendix

Table 1. Patient information. P-values showing no significant association between Male vs. Female and NDO vs. IDO (Fisher's exact test), and no significant difference in ages of S&I and DO vs. Others (t-test).

	Urologist Determination			Algorithm Determination*		
	DO	not DO	Total	S&I and DO	Others	p
N	52	43	95	14	38	
Male	26	14	40	5	35	0.8
Female	26	29	55	9	46	
Age (years)	53.4 ± 2.1	51.4 ± 2.2	52.4 ± 1.5	50.1 ± 4.1	52.9 ± 1.6	0.52
Neurogenic	28	17	45	8	37	0.56
Idiopathic	24	26	50	6	44	

*Using 30 seconds prior to void ROI

https://doi.org/10.1371/journal.pone.0201594.t001

LARC significance criteria

Two threshold criteria were established to determine whether each P_{ves} peak was significant. First, to eliminate P_{ves} peaks with very small amplitudes, the normalized P_{ves} amplitude was required to be greater than a threshold of 1.8 cm-H_2O. Second, to determine whether a P_{ves} peak was of adequate prominence (sharpness), a slope criterion was established (Fig 2F, red shaded region). This slope corresponded to a steep grade (20% P_{ves} per frequency step) in order to demonstrate a sharp increase from the adjacent frequency point. To meet this criterion, point J and/or K and point L and/or M must appear in the red shaded region in Fig 2F.

LARC independence criteria

Three thresholds were established to determine whether a significant P_{ves} peak was independent of the corresponding P_{abd} data. First, P_{ves} was required to be greater than a threshold value of 1.5 times P_{abd} and its two nearest neighboring values. This threshold was designed to identify a P_{ves} value that was relatively large compared to P_{abd}. This threshold was also designed to check that the LARC in the bladder was not due to bowel contractions. Second, P_{abd} was required to be less than a threshold of 133% of its nearest neighboring values. This threshold was designed to determine that P_{abd} was less than or relatively flat compared to its neighbors and also to check that LARC in the bladder was not due to bowel contractions. Third, as a separate independence criteria, P_{ves} was considered independent of P_{abd} if P_{ves} was greater than a threshold value of two times both P_{abd} and its two nearest neighbors, regardless of any peak in P_{abd}. This threshold was designed to check that significant bladder LARC was not caused by much a smaller corresponding rhythmic pressure changes noted in the bowel.

The threshold values for significance and independence of P_{ves} were determined by inspecting ~15 studies to determine values that identified signals with visible LARC. Once appropriate values were identified, the automated algorithm was implemented to analyze the entire set of 95 studies. The algorithm grouped the patients into three categories: those with 1) no significant rhythm found in P_{ves}, 2) significant rhythm in P_{ves} that was not independent of P_{abd}, or 3) significant rhythm in P_{ves} that was independent of P_{abd} (S&I). A patient was classified as having S&I LARC if any one or more of the three peak P_{ves} frequencies was found to be S&I.

Statistical analysis

Fisher's exact test was used to determine whether there was a significant association between the two groups (DO and not DO) and the two outcomes (S&I and not S&I) (Table 2). This test was also used to determine any association between male vs. females and between neurogenic

Appendix

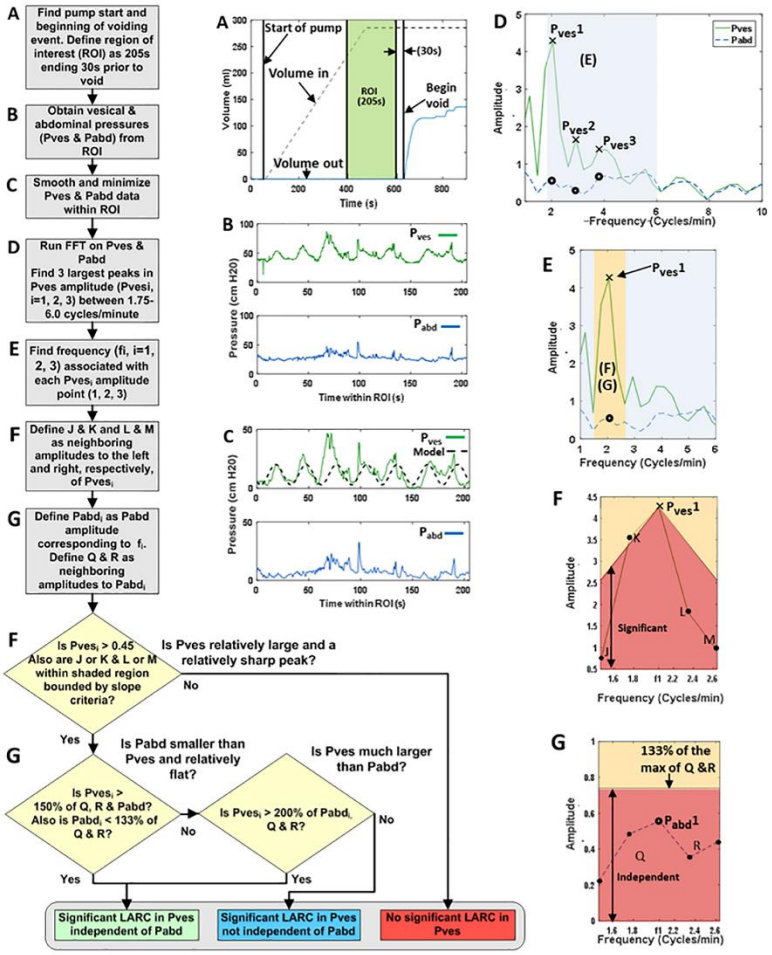

Fig 2. Flowchart for the FFT LARC algorithm. (A) UDS volume data showing time ROI. (B & C) raw and smoothed P_{ves} and P_{abd} data from the time ROI. (C dashed) Model of an ideal sine wave with a frequency of 2.05 cycles/min and a peak-to-peak amplitude of 17.12 cm-H2O, derived from the FFT results in panel F. The model peak-to-peak amplitude is 4 times the FFT output amplitude due to a factor of 2 from the FFT windowing and factor of 2 due to the two halves of the sine wave. (D) FFT of P_{ves} and P_{abd} from the ROI with the 1.75–6 cycle/min frequency range of interest shaded. (E) gray shaded region from panel D for $P_{ves}1$ with range of neighboring points shaded orange. (F) Significance test: $P_{ves}1$ is a sharp "significant" peak if J and/or K, and L and/or M are within the red region and if $P_{ves}1 > 0.45$. (G) Independence test: a significant $P_{ves}1$ peak is "independent" of $P_{abd}1$ if $P_{abd}1$ is relatively flat compared to points Q & R (within the red region below 133% of the max of Q & R) and if $P_{ves}1 > 150\%$ of $P_{abd}1$ (F & G).

https://doi.org/10.1371/journal.pone.0201594.g002

DO vs. idiopathic DO (Table 1). A two-tailed, two-sample, equal variance t-test was used to determine whether there was a significant difference in the ages of the two outcome groups (Table 1). Sensitivity and specificity analysis was performed on the algorithm, noting that an

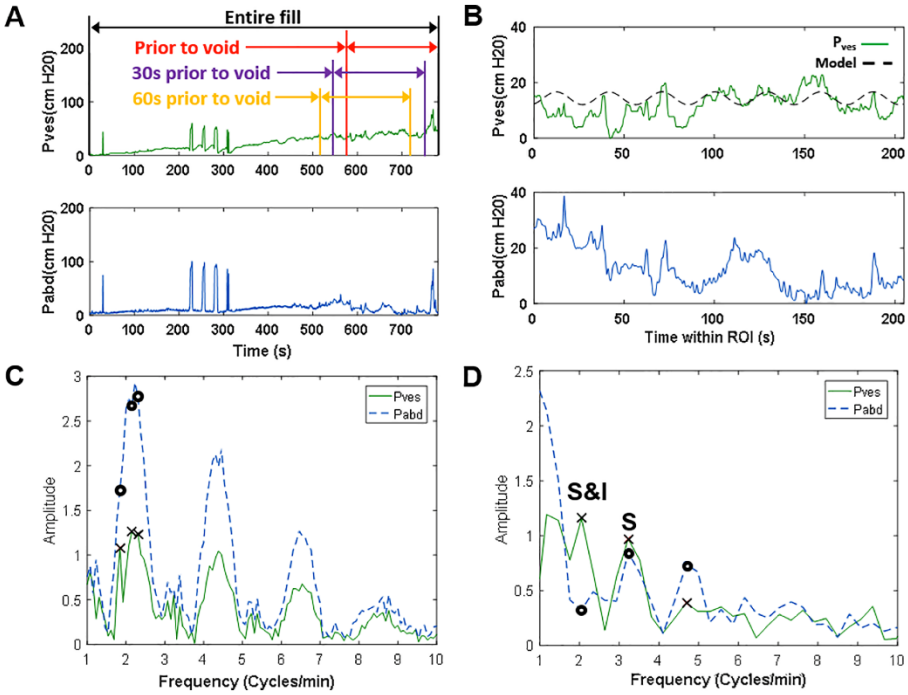

Fig 3. Examples of pressure tracings and corresponding FFT results. (A) Example P_{ves} and P_{abd} tracings for an entire UDS fill illustrating the 3 ROIs analyzed in this study. (B) P_{ves} and P_{abd} data for 205 seconds of filling illustrating the "30s prior to void" ROI with an overlaid sine wave model (dashed) derived from the FFT results in panel D. (C) FFT of P_{ves} and P_{abd} for the entire fill from panel A, demonstrating an increased frequency resolution (smaller spacing between the points) compared to (D), the FFT for the 205 second region in panel B with the frequency resolution used throughout this study. "S" indicates a significant P_{ves} peak that was not independent of P_{abd} and "S&I" indicates a significant P_{ves} peak independent of any corresponding P_{abd} peak.

https://doi.org/10.1371/journal.pone.0201594.g003

Table 2. Algorithm sensitivities and specificities. P-values showing significant association between S&I and DO (Fisher's exact).

Analysis Range	Significant and Independent	Observed DO	No Observed DO	Total	p-value	Sensitivity	Specificity
Prior to void	S&I	16	1	17	0.0003	0.3077	0.9767
	not S&I	36	42	78			
	Total	52	43	95			
30s prior to void	S&I	14	0	14	**<0.0001**	**0.2692**	**1.0000**
	not S&I	38	43	81			
	Total	52	43	95			
60s prior to void	S&I	13	0	13	0.0002	0.2500	1.0000
	not S&I	39	43	82			
	Total	52	43	95			
Any 3 ranges	S&I	22	1	23	<0.0001	0.4528	0.9333
	not S&I	30	42	72			
	Total	52	43	95			

https://doi.org/10.1371/journal.pone.0201594.t002

Appendix

ideal test would have a high specificity (only identifying LARC in patients with DO) and a specificity below 50% (highlighting the algorithm's effectiveness to identify a DO subgroup with LARC). All continuous data are reported as means ± standard error. A p-value less than 0.05 was considered significant.

Results

The LARC algorithm was implemented for the three ROIs (immediately prior to void, 30 seconds prior to void and 60 seconds prior to void, Fig 3A), and the results are provided in Table 2. The region 30 seconds prior to void provided 100% specificity. For this region, the algorithm identified significant and independent LARC in 14 of the 52 patients with DO and none of the 45 patients without DO, resulting in 100% specificity, 27% sensitivity and a significant association (Fischer's exact test, $p<0.0001$). The average slowest S&I LARC frequency was 3.20±0.34 cycles/min with an amplitude of 8.40±1.30 cm-H_2O in this region. Of the 14 individuals with DO identified with S&I LARC in this ROI, there were no significant differences based on sex, age or classification of DO as neurogenic or idiopathic (Table 1, $p>0.05$). The average infused volume for these 14 individuals was 464±58 ml, which was not different from the average infused volume of 552±31 ml for the 81 patients without S&I LARC ($p>0.05$). The average fill rate for all patients was 42±1 ml/min.

Additional analysis was performed to identify patients with an S&I frequency in any of the three ROIs (Table 2, "Any 3 ranges"). Out of the 52 patients with DO, 22 were identified with LARC, while 1 out of 43 patients without DO were identified with LARC, corresponding to a specificity of 93%.

Discussion

Clinical relevance

This study demonstrates that UDS data can be automatically analyzed for the presence of LARC using a custom-made FFT algorithm. The algorithm was purposefully designed to analyze retrospectively collected "real world" UDS data in order to demonstrate broad applicability. In addition, comparisons were made in a blinded fashion to eliminate bias. This represents a significant advance from our previous publication and first ever study showing the use of FFT in human UDS.[4] In that study, visually-identified LARC was objectively quantified, but this required direct inspection of each urodynamic tracing and the introduction of potential investigator bias.[4] The automated nature of the present algorithm eliminates this potential bias. Furthermore, the new algorithm can automatically analyze a single UDS in less than 5 sec, allowing for real-time data interpretation. Another recent study,[14] utilized wavelet analysis (as opposed to FFT) to automatically identify DO in human UDS. However, this study focused on improvement in the diagnosis of DO compared to visual inspection by the urodynamicist and did not specifically attempt to identify a DO subgroup with LARC.

The key finding of the current study is that a new DO subgroup with LARC with a frequency of 3.11±0.34 cycles/min with an amplitude of 8.24±1.24 cm-H_2O can readily be identified with 100% specificity. The sensitivity of 27% is consistent with our expectations and demonstrates that about one quarter of DO patients are characterized as being part of a LARC subgroup. Currently, according to ICS standardization,[15] the identification of DO is subjective and limited to the presence or absence of involuntary detrusor contractions and whether or not the DO is phasic or terminal. The advantage of an automated algorithm is that it allows for an objective determination of the presence of periodic LARC, distinct from non-periodic non-voiding contractions, and for an objective quantification of LARC frequency and amplitude.

Appendix

Relation to preclinical studies

Several previous studies have used FFT and other methods to quantify LARC in preclinical animal models.[2, 3, 7, 11, 16–21] Streng *et al.* observed LARC with a slow frequency of approximately 4 cycles/minute in anesthetized rats,[18] Byrne et al, identified a slow LARC frequency of 1.8 cycles/minute in rabbit detrusor strips,[7] and Lentle *et al.* observed LARC with a frequency of 3.55 cycles/minute in isolated pig bladders.[11] In addition, Colhoun *et al.* identified an average rhythmic frequency of 1.97 cycles/minute in human detrusor strips, which was similar to the 2.34 cycles/minute frequency of UDS LARC identified in that study and the 3.11 cycles/minute identified in the present study.[4]

Spontaneous rhythmic contractions in detrusor strips typically have relatively low amplitudes of ~5–15% of a maximal KCl-induced contraction [2, 22, 23]. In the present study, the average LARC amplitude was 8.24±1.24 cm-H_2O, and the average increase in P_{det} for a voiding contraction in the patients with S&I LARC was 82.65±16.62 cm-H_2O (n = 12, 2 of the 14 patients with S&I LARC did not void), which corresponds to a ratio that is consistent with the preclinical findings.

Frequency range selection

Frequencies of approximately 1.8–2.6 cycles/minute were identified in the tension tracings presented by Biers *et al.* in a study of spontaneous contractions in human detrusor strips.[5] In addition, Drake *et al.* measured micromotion between sensors placed on a balloon that was filled inside of the bladder during UDS, and frequencies of 2–5 cycles/minute were identified from their micromotion tracings.[9] Based on these studies of human bladder LARC, a frequency range of 1.75–6 cycles/minute was selected for the FFT algorithm in the current investigation. This range includes all frequencies identified in the previous studies and is slower than normal respiration.

Selection of ROI location and duration

A ramp-up of contractile activity may occur immediately prior to voiding (Fig 3A, last 30 seconds). Therefore, three ROI locations, ending immediately prior to the start of the void, 30 seconds prior to void or 60 seconds prior to void (Fig 3A), were tested with the algorithm. In terms of duration, in order to ensure a consistent bin width/frequency resolution for all patients, a constant range of 205 seconds of data was analyzed for each patient. Analysis of an entire fill longer than 205 seconds resulted in more narrow frequency bands (compare Fig 3C to 3D) and would require different algorithm thresholds for significance and independence. Also, multiple peaks might be identified at approximately the same frequency (Fig 3C, three X symbols near 2 cycles/min), which are identified as a single frequency when using the 205 sec ROI (Fig 3D, X at 2.05 cycles/min).

UDS with at least 7 minutes of filling were selected for analysis because we originally planned to analyze and compare LARC in low and high volume regions of 3.5 minutes each. We chose 3.5 minutes because we expected to find LARC frequencies of approximately 2 cycles/min [4] and wanted to analyze a range that could include several LARC cycles. Ideal implementation of FFT analysis uses data sets with a number of points equal to a power of 2, and we chose to examine 2048 points (2^{11}) taken at 10 Hz, which corresponds to 204.8 seconds, or 3.5 minutes. Furthermore, we expected that examining the latter halves of UDS fills of at least 7 minutes would ensure that the analyses were performed on data from bladders that had adequate infused volume.

P_{ves} independence from P_{abd}

Each significant P_{ves} peak was compared to the corresponding P_{abd} to ensure that any bladder activity was independent of abdominal activity. For example, translated abdominal events (i.e. coughs, Valsalvas, movements) produce peaks in both the P_{ves} and P_{abd} tracings (Fig 4A), and the LARC algorithm was designed to readily identify peaks in P_{ves} that are significant but not independent of P_{abd} (Fig 4B). In addition, non-translated abdominal events (i.e. rectal contractions) produce peaks in P_{abd} and P_{det} tracings, but not P_{ves} (Fig 4C), and by analyzing P_{ves}, the algorithm can determine that these events are not significant (Fig 4D). These examples provide rationale for the analysis of P_{ves} and not P_{det}. Another advantage of analyzing P_{ves} and P_{abd} separately is that S&I LARC may be identified from UDS data in which P_{ves} and P_{abd} have not be completely equalized (Fig 5).

Feasibility of implementation

The present algorithm was implemented by downloading data from the UDS machine, importing it as ASCII text into MATLAB, and implementing the custom LARC algorithm. This entire process takes only a couple of minutes, and once a data file has been loaded into MATLAB, the algorithm can analyze a single UDS and produce plots similar to those shown in Fig 4A and 4B in less than 5 seconds. In the future, this algorithm could be directly

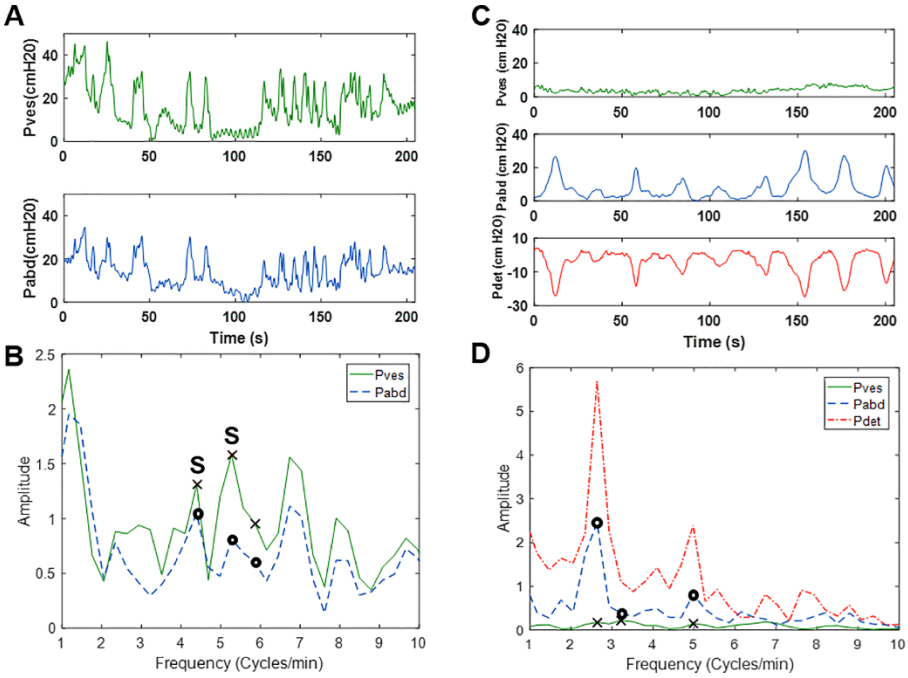

Fig 4. (A) Example P_{ves} and P_{abd} tracings for the final 205s of a UDS fill showing translated abdominal events and (B) the corresponding FFT output. "S" indicates a significant P_{ves} peak that was not independent of P_{abd}. (C) Example P_{ves}, P_{abd} and P_{det} tracings for the final 205s of a UDS fill illustrating abdominal event that was not translated to P_{ves} but appears in P_{det}, and (D) the corresponding FFT output.

https://doi.org/10.1371/journal.pone.0201594.g004

Appendix

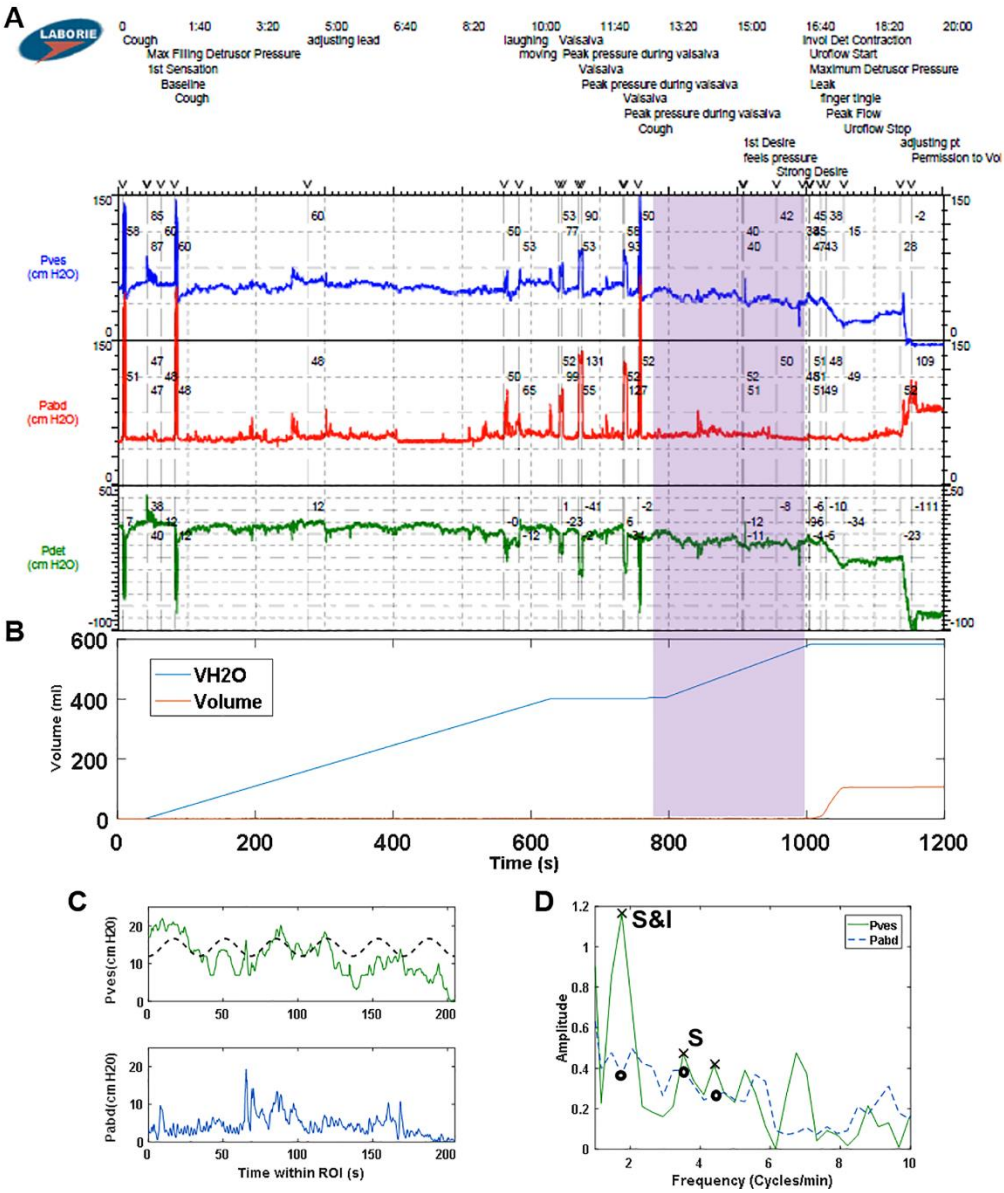

Fig 5. (A) Example of a UDS pressure data with P_{abd} and P_{ves} not equalized (cough at ~1.3 min) (B) corresponding infused (VH2O) and voided volumes. (C) P_{ves} and P_{abd} from the ROI (shaded region in A & B) and corresponding sine wave model (dashed) derived from FFT results in panel D. (D) FFT results of the ROI in panel C.

https://doi.org/10.1371/journal.pone.0201594.g005

implemented using the UDS machine to provide timely analysis for clinical use. The sine wave model with the identified LARC frequency and amplitude could be displayed along with the pressure data, as in Figs 2C, 3C and 5C, to permit immediate analysis and interpretation by the clinician. Furthermore, the system could be designed to allow the clinician to select any desired ROI for LARC analysis.

Study limitations

The present study was limited by the use of retrospective data and potential selection bias in the exclusion of studies with multiple voids/leaks (i.e. in the setting of Valsalva testing for stress urinary incontinence). However, the goal of this initial investigation was to use "real world" UDS data (performed for multiple indications and replete with artifacts and technical irregularities) to demonstrate broad applicability of the algorithm. Furthermore, the determination of "DO" was made by a neurourologist and expert urodynamicist in a blinded fashion and the algorithm was completely automated. Another issue was that the algorithm thresholds for S&I were determined iteratively using a small subset (~15 studies) of the data. In addition, because DO implies an "involuntary" contraction, the timing of a "permission to void" command is important. However, exported data from the UDS system does not include the time at which "permission to void" is granted. Incorporation of the algorithm directly into the UDS system would eliminate this limitation. A next step in the clinical implementation of this algorithm will be optimization of thresholds using prospective data obtained in different institutions and on more thoroughly characterized patient populations.

Conclusion

This is the first study demonstrating the use of an automated FFT algorithm to identify and quantitate a DO subgroup with LARC in human UDS. The algorithm can determine if a patient with DO has periodic LARC distinct from non-periodic non-voiding contractions, identifying a DO subgroup with LARC (27% of the DO group in this study) in a matter of seconds. The algorithm was tested on retrospective UDS to be broadly applicable to real-world situations. Clinical trials using pharmacotherapies, medical devices, and behavioral treatments could be designed to analyze this unique DO subgroup with LARC to help improve treatment outcomes.

Supporting information

S1 Data. Participant ages, infused volumes, infusion rates and rhythmic contraction amplitudes and frequencies.
(XLSX)

Author Contributions

Conceptualization: Adam P. Klausner, John E. Speich.

Data curation: Zachary E. Cullingsworth, Brooks B. Kelly, Nicholas A. Deebel, Andrew F. Colhoun, Adam P. Klausner, John E. Speich.

Formal analysis: Zachary E. Cullingsworth, Brooks B. Kelly, Nicholas A. Deebel, Andrew F. Colhoun, Adam P. Klausner, John E. Speich.

Funding acquisition: Adam P. Klausner, John E. Speich.

Methodology: Zachary E. Cullingsworth, Anna S. Nagle, Adam P. Klausner, John E. Speich.

Project administration: Adam P. Klausner, John E. Speich.

Software: Zachary E. Cullingsworth, John E. Speich.

Supervision: Adam P. Klausner, John E. Speich.

Writing – original draft: Zachary E. Cullingsworth, Andrew F. Colhoun, Anna S. Nagle, Adam P. Klausner, John E. Speich.

Writing – review & editing: Zachary E. Cullingsworth, Brooks B. Kelly, Nicholas A. Deebel, Andrew F. Colhoun, Anna S. Nagle, Adam P. Klausner, John E. Speich.

References

1. McCarthy CJ, Zabbarova IV, Brumovsky PR, Roppolo JR, Gebhart GF, Kanai AJ. Spontaneous contractions evoke afferent nerve firing in mouse bladders with detrusor overactivity. J Urol. 2009; 181 (3):1459–66. https://doi.org/10.1016/j.juro.2008.10.139 PMID: 19157431; PubMed Central PMCID: PMCPMC2899488.
2. Shenfeld OZ, McCammon KA, Blackmore PF, Ratz PH. Rapid effects of estrogen and progesterone on tone and spontaneous rhythmic contractions of the rabbit bladder. Urol Res. 1999; 27(5):386–92. PMID: 10550529.
3. Szell EA, Somogyi GT, de Groat WC, Szigeti GP. Developmental changes in spontaneous smooth muscle activity in the neonatal rat urinary bladder. Am J Physiol Regul Integr Comp Physiol. 2003; 285 (4):R809–16. https://doi.org/10.1152/ajpregu.00641.2002 PMID: 12750150.
4. Colhoun AF, Speich JE, Cooley LF, Bell ED 3rd, Barbee RW, Guruli G, et al. Low amplitude rhythmic contraction frequency in human detrusor strips correlates with phasic intravesical pressure waves. World J Urol. 2016. https://doi.org/10.1007/s00345-016-1994-0 PMID: 28025660.
5. Brading AF. A myogenic basis for the overactive bladder. Urology. 1997; 50(6A Suppl):57–67; discussion 8–73. PMID: 9426752.
6. Kinder RB, Mundy AR. Pathophysiology of idiopathic detrusor instability and detrusor hyper-reflexia. An in vitro study of human detrusor muscle. Br J Urol. 1987; 60(6):509–15. PMID: 3427334.
7. Byrne MD, Klausner AP, Speich JE, Southern JB, Habibi JR, Ratz PH. Fourier transform analysis of rabbit detrusor autonomous contractions reveals length dependent increases in tone and slow wave development at long lengths. J Urol. 2013; 190(1):334–40. https://doi.org/10.1016/j.juro.2013.02.071 PMID: 23485511.
8. Komari SO, Headley PC, Klausner AP, Ratz PH, Speich JE. Evidence for a common mechanism for spontaneous rhythmic contraction and myogenic contraction induced by quick stretch in detrusor smooth muscle. Physiol Rep. 2013; 1(6):e00168. https://doi.org/10.1002/phy2.168 PMID: 24400167; PubMed Central PMCID: PMCPMC3871480.
9. Drake MJ, Harvey IJ, Gillespie JI, Van Duyl WA. Localized contractions in the normal human bladder and in urinary urgency. BJU Int. 2005; 95(7):1002–5. https://doi.org/10.1111/j.1464-410X.2005.05455.x PMID: 15839921.
10. Hulls CM, Lentle RG, King QM, Reynolds GW, Chambers JP. Spatiotemporal analysis of spontaneous myogenic contractions in the urinary bladder of the rabbit: timing and patterns reflect reported electrophysiology. Am J Physiol Renal Physiol. 2017; 313(3):F687–F98. https://doi.org/10.1152/ajprenal.00156.2017 PMID: 28539334.
11. Lentle RG, Reynolds GW, Janssen PW, Hulls CM, King QM, Chambers JP. Characterisation of the contractile dynamics of the resting ex vivo urinary bladder of the pig. BJU Int. 2015; 116(6):973–83. https://doi.org/10.1111/bju.13132 PMID: 25808089.
12. Vince R, Tracey A, Deebel NA, Barbee RW, Speich JE, Klausner AP, et al. Effects of vesical and perfusion pressure on perfusate flow, and flow on vesical pressure, in the isolated perfused working pig bladder reveal a potential mechanism for the regulation of detrusor compliance. Neurourol Urodyn. 2017. https://doi.org/10.1002/nau.23362 PMID: 28745836.
13. Parsons BA, Drake MJ, Gammie A, Fry CH, Vahabi B. The validation of a functional, isolated pig bladder model for physiological experimentation. Front Pharmacol. 2012; 3:52. https://doi.org/10.3389/fphar.2012.00052 PMID: 22479248; PubMed Central PMCID: PMCPMC3315789.
14. Niederhauser T, Gafner ES, Cantieni T, Grämiger M, Haeberlin A, Obrist D, et al. Detection and quantification of overactive bladder activity in patients: Can we make it better and automatic? Neurourology and Urodynamics. n/a-n/a. https://doi.org/10.1002/nau.23357 PMID: 28745806

Appendix

15. Abrams P, Cardozo L, Fall M, Griffiths D, Rosier P, Ulmsten U, et al. The standardisation of terminology of lower urinary tract function: report from the Standardisation Sub-committee of the International Continence Society. Neurourol Urodyn. 2002; 21(2):167–78. PMID: 11857671.

16. Klausner AP, King AB, Byrne MD, Habibi JR, Li K, Sabarwal V, et al. A new and automated method for objective analysis of detrusor rhythm during the filling phase. World J Urol. 2014; 32(1):85–90. https://doi.org/10.1007/s00345-013-1084-5 PMID: 23633125.

17. Gillespie JI, Rouget C, Palea S, Granato C, Birder L, Korstanje C. The characteristics of intrinsic complex micro-contractile activity in isolated strips of the rat bladder. Naunyn Schmiedebergs Arch Pharmacol. 2015; 388(7):709–18. https://doi.org/10.1007/s00210-015-1131-4 PMID: 26004385.

18. Streng T, Hedlund P, Talo A, Andersson KE, Gillespie JI. Phasic non-micturition contractions in the bladder of the anaesthetized and awake rat. BJU Int. 2006; 97(5):1094–101. https://doi.org/10.1111/j.1464-410X.2006.06137.x PMID: 16643498.

19. Clavica F, Choudhary M, van Asselt E, van Mastrigt R. Frequency analysis of urinary bladder pre-voiding activity in normal and overactive rat detrusor. Neurourol Urodyn. 2015; 34(8):794–9. https://doi.org/10.1002/nau.22664 PMID: 25201641.

20. Smith PP, DeAngelis A, Simon R. Evidence of increased centrally enhanced bladder compliance with ageing in a mouse model. BJU Int. 2015; 115(2):322–9. https://doi.org/10.1111/bju.12669 PMID: 25116343.

21. Anderson UA, Carson C, Johnston L, Joshi S, Gurney AM, McCloskey KD. Functional expression of KCNQ (Kv7) channels in guinea pig bladder smooth muscle and their contribution to spontaneous activity. Br J Pharmacol. 2013; 169(6):1290–304. https://doi.org/10.1111/bph.12210 PMID: 23586426; PubMed Central PMCID: PMCPMC3746117.

22. Ratz PH, Miner AS. Length-dependent regulation of basal myosin phosphorylation and force in detrusor smooth muscle. Am J Physiol Regul Integr Comp Physiol. 2003; 284(4):R1063–70. https://doi.org/10.1152/ajpregu.00596.2002 PMID: 12626367.

23. Collins C, Klausner AP, Herrick B, Koo HP, Miner AS, Henderson SC, et al. Potential for control of detrusor smooth muscle spontaneous rhythmic contraction by cyclooxygenase products released by interstitial cells of Cajal. J Cell Mol Med. 2009; 13(9B):3236–50. https://doi.org/10.1111/j.1582-4934.2009.00714.x PMID: 19243470; PubMed Central PMCID: PMCPMC4516481.

Appendix B – Neurourology and Urodynamics Dynamic Elasticity Paper

Received: 16 July 2019 | Accepted: 6 December 2019
DOI: 10.1002/nau.24255

Check for updates

ORIGINAL CLINICAL ARTICLE

Neurourology Urodynamics ICS SUFU WILEY

Comparative-fill urodynamics in individuals with and without detrusor overactivity supports a conceptual model for dynamic elasticity regulation

Zachary E. Cullingsworth BS[1] | Adam P. Klausner MD[2] | Rui Li PhD[1] | Anna S. Nagle PhD[1] | Ashley W. Carroll MD[3] | John T. RosemanII MD[2] | John E. Speich PhD[1]

[1]Department of Mechanical and Nuclear Engineering, College of Engineering, Virginia Commonwealth University, Richmond, Virginia

[2]Division of Urology, Department of Surgery, Virginia Commonwealth University School of Medicine, Richmond, Virginia

[3]Department of Obstetrics and Gynecology, Virginia Commonwealth University School of Medicine, Richmond, Virginia

Correspondence
John E. Speich, PhD, Department of Mechanical and Nuclear Engineering, Virginia Commonwealth University, 401 West Main St, Richmond, VA 23284.
Email: jespeich@vcu.edu

Funding information
National Institute of Diabetes and Digestive and Kidney Diseases, Grant/Award Number: R01-DK101719

Abstract

Aims: Dynamic elasticity was previously identified in individuals with overactive bladder (OAB) using comparative-fill urodynamics (UD) and is a biomechanical mechanism for acutely regulating detrusor wall tension. On the basis of this data, a conceptual model of dynamic elasticity regulation mediated through a balance of passive mechanisms and active contractions was constructed. The present study tested this model by determining whether individuals with detrusor overactivity (DO) exhibit less dynamic elasticity than individuals without DO.

Methods: Individuals with and without urgency based on International Consultation on Incontinence Questionnaire-OAB surveys were prospectively enrolled in a comparative-fill UD study. An initial fill defined the presence or absence of DO and determined cystometric capacity. Three additional fills were employed with either passive emptying via a catheter or active voiding. To identify dynamic elasticity, average filling pressures (P_{ves}) were compared for fill 1 (before strain softening), fill 2 (after strain softening), and fill 3 (after active void). A dynamic elasticity index was defined.

Results: From 28 participants, those without DO showed decreased P_{ves} during filling after strain softening and restored P_{ves} during filling following active voiding, revealing dynamic elasticity. Participants with DO did not show dynamic elasticity. A dynamic elasticity index less than 1.0 cmH_2O/40% capacity was identified in 2 out of 13 participants without DO and 9 out of 15 with DO, revealing a significant association between DO and reduced/absent dynamic elasticity ($P = .024$).

Conclusions: This study supports a conceptual model for dynamic elasticity, a mechanism to acutely regulate detrusor wall tension through a balance of competing active contractile and passive strain mechanisms. Improved understanding of this mechanistic model may help us to identify novel treatment strategies for OAB.

KEYWORDS
bladder biomechanics, bladder compliance, cystometry, overactive bladder

1 | INTRODUCTION

Urinary urgency, the key symptom of overactive bladder (OAB), may be associated with alterations in detrusor wall tension in some individuals because tension-sensitive afferent nerves are in-series with detrusor smooth muscle cells.[1] Detrusor wall tension is a function of bladder volume, pressure, shape, and its material properties[2] that cannot be directly measured using standard urodynamic techniques; rather, it can be roughly estimated by calculating bladder compliance, defined as the ratio of the change in volume to the change in pressure during a urodynamic (UD) fill.[3] Previously, detrusor compliance was believed to be a static property that could only be altered through chronic, pathologic conditions, such as bladder outlet obstruction.[4]

However, a comparative-fill UDs protocol, in which multiple UD fill-void cycles were performed and compared in a single setting, was recently used to demonstrate that bladder compliance can be acutely regulated through a process known as dynamic elasticity.[5] Dynamic elasticity is characterized by a reduction in vesical pressure (P_{ves}) (loss of elasticity) during a bladder fill due to strain-induced stress softening (strain softening) caused by previous filling and passive emptying of the bladder through the UDs catheter, and a return of P_{ves} (restoration of elasticity) during a fill caused by previous active voiding.[5] A loss of elasticity associated with filling and passive emptying can also be seen by stretching a latex balloon before inflating it. This stretching breaks connections between latex polymers, resulting in a loss of wall tension during subsequent filling. However, unlike a latex balloon in which the loss of tension is irreversible, active voiding of the bladder re-establishes broken actin-myosin connections which lead to restored tension.[6-9] Thus, dynamic elasticity represents a biomechanical mechanism to acutely regulate detrusor wall tension.

Dynamic elasticity is the clinical correlate of adjustable preload tension, which has been identified in preclinical studies using detrusor strips in rabbits[6,7,9] and humans[10] and isolated whole bladders from mice.[8] Detrusor strips from animals[11,12] and humans[13,14] exhibit spontaneous rhythmic contractions that have been shown to regulate adjustable preload tension likely through active re-establishment of actin-myosin connections.[6,7] Furthermore, spontaneous rhythmic contractions, also called micomotion[15] or autonomous activity,[12] are elevated in detrusor muscle from patients with detrusor overactivity (DO)[14] and elevations in localized micromotions have been associated with urgency.[16]

Together, these studies suggest a mechanistic link between dynamic elasticity and DO. In this regard, a conceptual biomechanical model, similar to that proposed by van Duyl,[17] was constructed (Figure 1A) in which bladder dynamic elasticity is regulated by a balance of mechanisms. In this model, dynamic elasticity is decreased by passive forces, such as stretch during filling, which breaks or cause the release of actin-myosin connections, and dynamic elasticity is increased by active contractions, which re-establish actin-myosin connections and that provide restored tension during subsequent filling. During normal filling, subclinical micromotions regulate tension to maintain optimal bladder biomechanics. However, in pathologic conditions, increased micromotions, manifesting as DO, may alter the balance and lead to increased wall tension. The aim of the present study was to test the hypothesis of this conceptual model by determining whether individuals with DO exhibit less dynamic elasticity than individuals without DO.

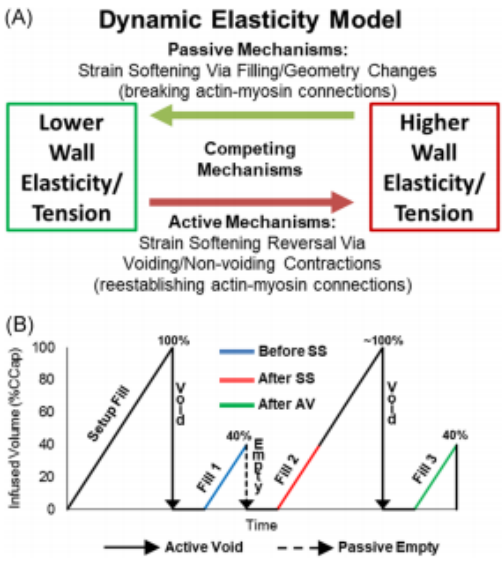

FIGURE 1 A, Conceptual model of dynamic elasticity with competing mechanisms for regulating detrusor wall tension. Passive mechanisms (stretch due to filling or geometry changes) cause strain softening by breaking actin-myosin cross bridges leading to lower wall tension during the next fill. Active contractions (voiding or nonvoiding detrusor overactivity) reverse strain softening by re-establishing actin-myosin cross bridges leading to increase wall tension during subsequent filling. B, Comparative-fill urodynamics protocol. Following a setup fill and active void (solid arrow), fill 1 was to 40% capacity and emptied by syringe aspiration (dashed black arrow). Fill 2 was to ~100% capacity and followed by an active void. Fill 3 was to 40% capacity. Vesical pressures (P_{ves}) were measured between 0% and 40% capacity for fill 1 (blue line—before strain softening—SS]), fill 2 (red line—after strain softening due to fill 1), and fill 3 (green line —after active void—AV])

Appendix

2 | MATERIALS AND METHODS

2.1 | Participants

Adults over the age of 21 years with and without OAB were enrolled in this prospective comparative-fill UD study which was approved by the Institutional Review Board. Participants were categorized as having "high urgency" or "no urgency" based on question 5a ("Do you have to rush to the toilet to urinate?") of the International Consultation on Incontinence Questionnaire-OAB.[18] Participants scoring 3 ("most of the time") or 4 ("always") were categorized as having high urgency and participants scoring 0 ("never") were categorized as no urgency. Participants completed a 3-day void diary before UD testing and relevant demographic data were collected. Participants were analyzed based on the presence or absence of DO based on UDs as this was a more objective criterion than patient-reported survey scores.

2.2 | UDs testing and setup fill

A comparative-fill UD protocol (Figure 1B) was used to test for dynamic elasticity based on an initial pilot study.[5] Multichannel pressure and flow data were acquired at 10 Hz using an Aquarius TT UD system (Laborie, Toronto, Canada). An initial "setup" UD fill-void cycle was performed to (a) determine maximum cystometric capacity, (b) identify any DO, and (c) confirm an active void and sufficient emptying (Figure 1B "setup"). The setup fill was at a rate of 10% of patient-reported maximum voided volume per minute based on the 3-day void diary. The filling was stopped when the patient reached the sensory threshold, defined by reaching 100% on a tablet-based sensation meter[19] or when involuntary voiding occurred. Participants were then given permission to void, and any post-void residual (PVR), in this fill and all subsequent fills, was removed via syringe aspiration and confirmed using a three-dimensinal ultrasound (Voluson E8; GE Healthcare, Zipf, Austria). Cystometric capacity was defined as the sum of the voided volume and any PVR from the setup fill. Participants with a PVR greater than 20% of cystometric capacity for any active void in the protocol were excluded from the data analysis.

For the calculation of compliance, any fill with a decrease in pressure or change in pressure of less than 1 cmH_2O was assigned a value of 1 cmH_2O and was calculated as the ratio of the infused volume to the change in filling pressure in the setup fill. The presence or absence of DO was determined based on the review of the setup UD tracings by a blinded neurourologist/urodynamicist following International Continence Society standards as the presence of any "involuntary detrusor contractions during the filling phase."[3]

2.2.1 | Quantification of dynamic elasticity

To quantify dynamic elasticity, it is necessary to compare multiple fills because the effect of strain softening or its reversal in one fill can only be observed in a subsequent fill. In this way, each individual acts as their own control, limiting inherent physiologic variability between participants. Therefore, three comparative fills were completed at a rate of 10% cystometric capacity/min (Figure 1B) as follows.

- *Fill 1—before strain softening:* Fill to 40% capacity (Figure 1B, blue line) and passively empty via syringe aspiration through the catheter. This provides baseline pressure from 0% to 40%. P_{ves1} was defined as averaged P_{ves} from 0% to 40%.
- *Fill 2—after strain softening:* Fill to 40% capacity (Figure 1B, red line) and then continue filling to 100% and permit active voiding. Pressures measured from 0% to 40% show the effect of strain softening induced by fill 1. P_{ves2} was defined as averaged P_{ves} from 0% to 40%.
- *Fill 3—after active void:* Fill back up to 40% capacity (Figure 1B, green line). Pressures measured from 0% to 40% show the effect of strain softening reversal induced by active voiding following fill 2. P_{ves3} was defined as averaged P_{ves} from 0% to 40%.

Averaged P_{ves} values from 0% to 40% capacity for fills 1 to 3 were compared to quantify dynamic elasticity as previously described[5] and averaged data from abdominal pressure (P_{abd}) were calculated for comparison. Each participant's P_{ves} data was shifted by subtracting the overall minimum value from fills 1 to 3 from all data to minimize the effects of any high baseline. Dynamic elasticity loss, dynamic elasticity gain, and a dynamic elasticity index were calculated as the change in pressure over the change in volume

$$\text{Dynamic elasticity loss} = (P_{ves2} - P_{ves1})/40\%\ \text{capacity}.$$

Dynamic elasticity gain was calculated similarly as

$$\text{Dynamic elasticity gain} = (P_{ves3} - P_{ves2})/40\%\ \text{capacity}.$$

A dynamic elasticity index was defined as

$$\text{Dynamic elasticity index} = ((P_{ves1} - P_{ves2}) + (P_{ves3} - P_{ves2}))/40\%\ \text{capacity}.$$

Using this formula, a higher dynamic elasticity index would correspond to more dynamic elasticity, that is, a

Appendix

larger loss in elasticity due to strain softening and/or a larger restoration in elasticity due to strain softening reversal through active voiding. In contrast, a lower dynamic elasticity index would correspond to reduced or absent dynamic elasticity.

2.2.2 | Statistical analyses

To determine the minimum number of participants needed for this study, a power analysis was performed based on the results of the previous pilot study.[5] Linear interpolation of the normalized data for strain softening to 30% capacity and 60% capacity in the pilot study indicated an expected difference in means of 32% for strain softening to 40% capacity. The power analysis determined that a sample size of eight participants per group was needed to identify a statistical difference between groups with a power level of .8 and $\alpha = .05$.

Continuous variables (P_{ves}, P_{abd}, dynamic elasticity lost or restored, dynamic elasticity index, age, compliance, and bladder volumes) were compared using paired or unpaired Student t tests, as appropriate. In addition, compliance and dynamic elasticity index were checked for normality using the Shapiro-Wilk's test, and a Pearson's correlation coefficient was computed to assess the relationship between compliance and dynamic elasticity index in participants with and without DO. Categorical variables (dynamic elasticity index above or below a threshold value and the presence or absence of DO) were compared using a Fisher's exact test. Significance was defined as $P < .05$, and all values were reported as mean ± standard error.

3 | RESULTS

Forty-three consecutive participants completed the study protocol and 28 were included in the analysis. Fifteen were excluded because of high PVRs (including 7 out of 22 normal participants without urinary urgency). Participant characteristics are listed in Table 1. The average ages of the groups with and without DO were not different (Table 1; $P = .73$). Maximum voided volumes on 3-day void diaries were not different for the groups of participants with and without DO (Table 1; $P = .76$, one participant with DO did not complete a void diary); however, the average capacity for the UD setup fill was different for the groups with and without DO (Table 1; $P = .03$).

TABLE 1 Participant characteristics

	DO+	DO−	*P* value
Participants	15	13	---
Female	10	11	---
Male	5	2	---
High urgency	10	3	---
No urgency	5	10	---
Age, y	39 ± 5	36 ± 5	.73
3-d Dairy max voided volume, mL	554 ± 60	530 ± 35	.76
Cystometric capacity, mL	443 ± 74	667 ± 61	.03

Abbreviations: −, negative; +, positive; DO, detrusor overactivity.

3.1 | Quantification of dynamic elasticity

Examples of P_{ves} tracings for an individual with DO and an individual without DO are shown in Figure 2. In these examples, a loss of dynamic elasticity was observed in the participant without DO (Figure 2A, blue line to red line) but not in the individual with DO (Figure 2B, blue line to red line). Furthermore, a gain (restoration) of dynamic elasticity after active voiding was observed in the participant without DO (Figure 2A, red line to green line) but not in the participant with DO (Figure 2B, red line to green line). Similar findings were identified for averaged data from the "without DO" and "with DO" groups (Figure 3A). In addition, there was no change in P_{abd} for any of the fills regardless of the presence or absence of DO, indicating that the observation of dynamic elasticity loss and gain was not due to abdominal activity (Figure 3B).

The group without DO demonstrated a significant loss of dynamic elasticity from fill 1 to fill 2 (Figure 4A, elasticity loss) and a statically significant gain of dynamic elasticity from fill 2 to fill 3 (Figure 4A, elasticity gain). Furthermore, the magnitude of the loss was not different from the magnitude of the gain (Figure 4A, without DO). The group with DO did not show a loss or gain of elasticity (Figure 4A, with DO). Furthermore, the dynamic elasticity index was significantly less for the group with DO (Figure 4B).

Furthermore, a threshold value of 1.0 cmH_2O over the 40% capacity range of strain softening in the present protocol was selected for dividing participants into a group with greater dynamic elasticity (index ≥ 0.025 cmH_2O/%capacity) and a group with reduced or absent dynamic elasticity (index < 0.025 cmH_2O/%capacity). A dynamic elasticity index of less than 0.025 cmH_2O/%capacity was identified in 2 out of 13 (15%) participants without DO and 9 out of 15 (60%) participants with DO, and there was a significant association between DO and reduced/absent dynamic elasticity ($P = .024$).

Appendix

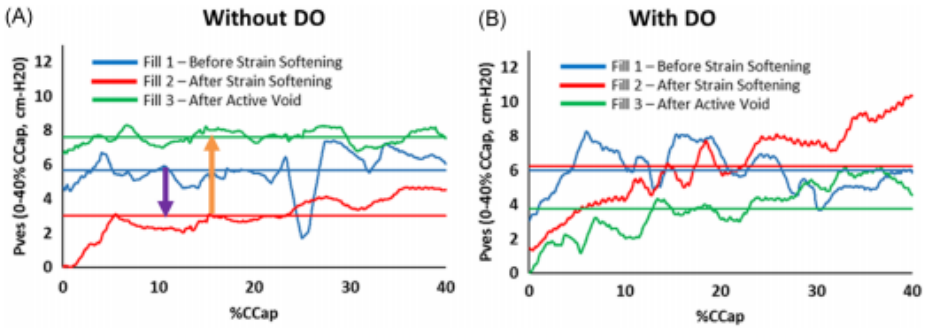

FIGURE 2 P_{ves} examples for a participant without DO (A) and a participant with DO (B). Traces represent smoothed P_{ves} data and straight lines represent averaged data from 0% to 40% capacity. In the example participant without DO, P_{ves} values from 0% to 40% capacity decreased (A, purple arrow) from fill 1 (baseline, before strain softening—blue lines) to fill 2 (after strain softening—red lines) demonstrating a loss of dynamic elasticity, and P_{ves} returned toward baseline (A, orange arrow, beyond baseline in this example) in fill 3 (after active voiding—green lines) demonstrating restored dynamic elasticity. Dynamic elasticity was not observed in the individual with DO (B, no decrease from blue to red lines and no increase from red to green lines). DO, detrusor overactivity

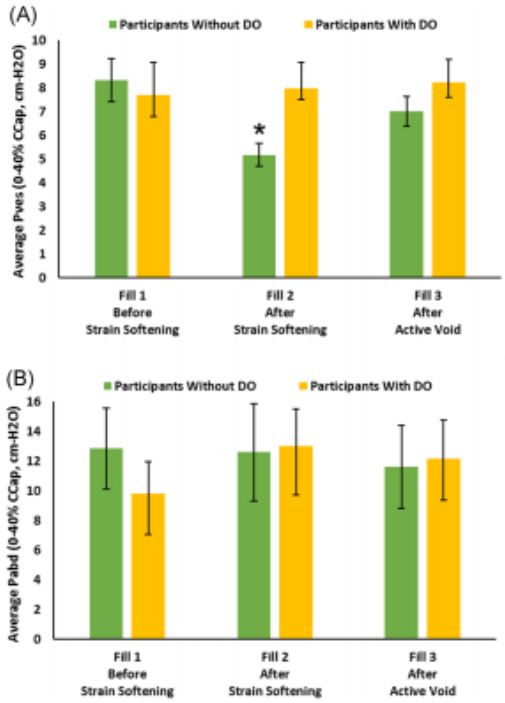

FIGURE 3 A, Average P_{ves} between 0% and 40% capacity for the participants with and without DO. P_{ves} significantly decreased from baseline fill 1 before strain softening to fill 2 after strain softening in the participants without DO (green bars, n = 13 and $^*P = .004$) but not in the participants with DO (yellow bars, n = 15 and $P = .862$). Average P_{ves} in the participants without DO returned to baseline after active voiding in fill 3 (green bars, fill 3 not different from fill 1 and $P = .172$). B, Average P_{abd} between 0% and 40% capacity for the participants with and without DO. Fills 2 and 3 were not different from fill 1 ($P > .25$). A, B, Bars indicate standard errors and * indicates a value significantly different from fill 1. DO, detrusor overactivity

Appendix

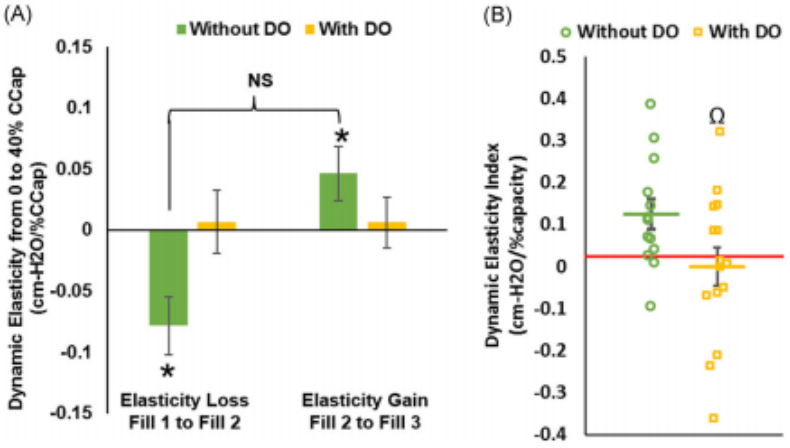

FIGURE 4 A, Dynamic elasticity in participants with and without DO. In the participants without DO (green bars), there was a significant loss in elasticity after strain softening (elasticity loss, n = 13 and *$P = .004$) and a significant gain after active voiding (elasticity gain, *$P = .045$). In addition, there was no difference in the magnitude of the loss and gain (NS; $P = .171$) demonstrating the reversibility of dynamic elasticity in participants without DO. In the participants with DO (yellow bars), there was not a significant loss (n = 15 and $P = .862$) or gain in elasticity ($P = .777$). B, The average dynamic elasticity index was significantly less in participants with DO (yellow line) vs without DO (green line, Ω and $P = .045$). A threshold index of 0.025 cmH_2O/%capacity (red line) was selected to differentiate between a group with greater dynamic elasticity and a group with reduced or absent dynamic elasticity. A total of 2 out of 13 participants without DO (green circles) and 9 out of 15 participants with DO (yellow squares) were below this threshold, indicating a significant association of DO with reduced or absent dynamic elasticity ($P = .024$). DO, detrusor overactivity; NS, not significant

Within-fill compliance values for participants with DO were less than participants without DO (268 ± 51 vs 486 ± 81 mL/cmH_2O; $P = .027$); however, compliance values for participants with a dynamic elasticity index less than 0.025 cmH_2O/%capacity was not different than for participants with an index greater than this threshold (320 ± 65 vs 400 ± 71 mL/cmH_2O; $P = .44$; n = 11 and n = 17). Both compliance and the dynamic elasticity index were normally distributed, as assessed by the Shapiro-Wilk's test ($P > .05$), and there were no outliers. There was no statistically significant correlation between compliance and dynamic elasticity index for all participants ($r(26) = -.045$, $P = .819$). In addition, compliance and the dynamic elasticity index correlation were examined using the Pearson correlation test independently on the groups with DO and without DO, and no statistically significant correlation was identified ($r(13) = -.225$, $P = .420$ and $r(11) = -.293$, $P = .331$, respectively). Together, these results indicate that standard compliance measurements from a single UD fill would not be sufficient to identify the presence or absence of dynamic elasticity.

4 | DISCUSSION

This study demonstrated that dynamic elasticity identified during a comparative-fill UD protocol was mainly observed in individuals without DO. This finding supports the conceptual model in Figure 1A, in which detrusor wall tension, and therefore compliance, can be acutely and actively regulated. According to this model, passive mechanisms that stretch the bladder wall, such as bladder filling or bladder compression,[20] break or release actin-myosin connections which reduce elasticity and result in reduced wall tension during subsequent filling. In contrast, active mechanisms, such as voiding contractions or DO, act to re-establish these actin-myosin connections and restore wall tension during subsequent filling.[6,7] In this regard, the purpose of spontaneous rhythmic contractions that have been identified in both preclinical studies[14] and in human UD,[16] may be to regulate the balance between tone and accommodation in an environment where the bladder is continuously subjected to passive forces (filling, body movement, Valsalva, bowel activity, external compression, etc). However, an imbalance in passive forces and active contractions (ie when subclinical micromotions become clinically significant DO) could contribute to OAB. This hypothesis is supported by the results of the present study, which showed a significantly lower dynamic elasticity index in participants with DO.

Studies of detrusor wall tension have been limited by a lack of minimally invasive technologies to

Appendix

directly measure this biomechanical property. However, several investigators have made strides in the development of novel technologies to measure detrusor wall tension in a minimally invasive fashion. Fatemi et al[21] developed a bladder vibrometry method in which ultrasonic shear waves were used to measure wall elasticity. Likewise, Sturm et al[22] were able to achieve similar results using bladder elastography. In addition, Nagle et al[23] have developed a method to calculate real-time detrusor wall tension during UD filling using ultrasound-derived metrics. However, none of these studies have compared detrusor wall tension to the presence or absence of DO to provide a potential mechanism to explain how acute regulation of detrusor wall tension might relate to clinical conditions such as OAB.

It is important to mention that the protocol in this study differs from our previous pilot investigation in which two separate fills with passive emptying (to 30% capacity and then to 60% capacity) were used to identify dynamic elasticity in individuals with OAB. In the current study, a single passive emptying fill to 40% capacity was employed for simplicity and because linear interpolation of the strain-softening data from 30% capacity and 60% capacity in the original pilot study indicated that filling to 40% capacity would be expected to produce statistically significant dynamic elasticity in the subjects from that study ($P = .033$ for interpolated data).[5]

On the basis of preclinical studies in detrusor strips showing that active contraction at short muscle lengths reverse strain softening,[7] we expected that strain softening might not be reversed in participants that did not actively void to a sufficiently small volume. As a result, participants with a PVR greater than 20% of cystometric capacity for the active voids following the setup fill or fill 2 were excluded. A PVR of 20% of cystometric capacity is equivalent to half of the 40% capacity volume used to strain soften the bladder in fill 1. Thus, to be included in the study, the participant must have achieved an active voiding contraction that emptied the bladder to a volume that included at least half of the range of the strain softening.

A limitation of the current investigation was the lack of more objective metrics to identify and quantify DO. However, new techniques to objectively identify DO with automated fast Fourier transforms[24] or wavelet analysis[25] have recently been developed and could make the process far more objective for future investigations. Another limitation of the current study was the relatively large number of participants were excluded because of high PVRs. However, this finding is consistent with an earlier study that identified high PVRs in some healthy participants during UDS.[26]

5 | CONCLUSION

This study presents a conceptual model for dynamic elasticity, a mechanism to acutely regulate detrusor wall tension through a balance of competing active contractile and passive strain mechanisms. Dynamic elasticity was found to be associated with participants without DO. The absence of dynamic elasticity in most participants with DO supports the model and suggests that DO may produce an imbalance in the regulation of detrusor wall tension. Improved understanding of this mechanistic model may help us to identify novel treatment strategies for OAB.

ACKNOWLEDGMENTS

The authors would like to thank Kimberly Bradley, Meagan Miller, and Sandy Smith for their contributions to this study. This study was supported by a grant from the National Institutes of Health (R01-DK101719).

ORCID

Zachary E. Cullingsworth http://orcid.org/0000-0002-4087-9764
Adam P. Klausner http://orcid.org/0000-0003-3849-7131
Rui Li http://orcid.org/0000-0003-0006-818X
Anna S. Nagle http://orcid.org/0000-0001-9960-4864
John T. Roseman http://orcid.org/0000-0001-6031-4595
John E. Speich http://orcid.org/0000-0002-8824-4098

REFERENCES

1. Andersson KE. Detrusor myocyte activity and afferent signaling. *Neurourol Urodyn*. 2010;29(1):97-106.
2. Habteyes FG, Komari SO, Nagle AS, et al. Modeling the influence of acute changes in bladder elasticity on pressure and wall tension during filling. *J Mech Behav Biomed Mater*. 2017;71:192-200.
3. Abrams P, Cardozo L, Fall M, et al. The standardisation of terminology of lower urinary tract function: report from the standardisation sub-committee of the International Continence Society. *Neurourol Urodyn*. 2002;21(2):167-178.
4. Metcalfe PD, Wang J, Jiao H, et al. Bladder outlet obstruction: progression from inflammation to fibrosis. *BJU Int*. 2010; 106(11):1686-1694.
5. Colhoun AF, Klausner AP, Nagle AS, et al. A pilot study to measure dynamic elasticity of the bladder during urodynamics. *Neurourol Urodyn*. 2017;36(4):1086-1090.
6. Ratz PH, Speich JE. Evidence that actomyosin cross bridges contribute to "passive" tension in detrusor smooth muscle. *Am J Physiol Renal Physiol*. 2010;298(6):F1424-F1435.
7. Speich JE, Borgsmiller L, Call C, Mohr R, Ratz PH. ROK-induced cross-link formation stiffens passive muscle: reversible

Appendix

strain-induced stress softening in rabbit detrusor. *Am J Physiol Cell Physiol*. 2005;289(1):C12-C21.
8. Speich JE, Southern JB, Henderson S, Wilson CW, Klausner AP, Ratz PH. Adjustable passive stiffness in mouse bladder: regulated by Rho kinase and elevated following partial bladder outlet obstruction. *Am J Physiol Renal Physiol*. 2012;302(8):F967-F976.
9. Southern JB, Frazier JR, Miner AS, Speich JE, Klausner AP, Ratz PH. Elevated steady-state bladder preload activates myosin phosphorylation: detrusor smooth muscle is a preload tension sensor. *Am J Physiol Renal Physiol*. 2012;303(11):F1517-F1526.
10. Colhoun AF, Speich JE, Dolat MT, et al. Acute length adaptation and adjustable preload in the human detrusor. *Neurourol Urodyn*. 2016;35(7):792-797.
11. Byrne MD, Klausner AP, Speich JE, Southern JB, Habibi JR, Ratz PH. Fourier transform analysis of rabbit detrusor autonomous contractions reveals length dependent increases in tone and slow wave development at long lengths. *J Urol*. 2013;190(1):334-340.
12. Drake MJ, Hedlund P, Harvey IJ, Pandita RK, Andersson KE, Gillespie JI. Partial outlet obstruction enhances modular autonomous activity in the isolated rat bladder. *J Urol*. 2003; 170(1):276-279.
13. Colhoun AF, Speich JE, Cooley LF, et al. Low amplitude rhythmic contraction frequency in human detrusor strips correlates with phasic intravesical pressure waves. *World J Urol*. 2016;35:1255-1260.
14. Kinder RB, Mundy AR. Pathophysiology of idiopathic detrusor instability and detrusor hyper-reflexia. An in vitro study of human detrusor muscle. *Br J Urol*. 1987;60(6):509-515.
15. Drake MJ, Kanai A, Bijos DA, et al. The potential role of unregulated autonomous bladder micromotions in urinary storage and voiding dysfunction; overactive bladder and detrusor underactivity. *BJU Int*. 2017;119(1):22-29.
16. Drake MJ, Harvey IJ, Gillespie JI, Van Duyl WA. Localized contractions in the normal human bladder and in urinary urgency. *BJU Int*. 2005;95(7):1002-1005.
17. van Duyl WA. A model for both the passive and active properties of urinary bladder tissue related to bladder function. *Neurourol Urodyn*. 1985;4(4):275-283.
18. Abrams P, Avery K, Gardener N, Donovan J, Advisory Board ICIQ. The International Consultation on Incontinence Modular Questionnaire:www.iciq.net. *J Urol*. 2006;175(3 pt 1):1063-1066.
19. Nagle AS, Speich JE, De Wachter SG, et al. Non-invasive characterization of real-time bladder sensation using accelerated hydration and a novel sensation meter: an initial experience. *Neurourol Urodyn*. 2017;36(5):1417-1426.
20. Balthazar A, Cullingsworth ZE, Nandanan N, et al. An external compress-release protocol induces dynamic elasticity in the porcine bladder: a novel technique for the treatment of overactive bladder? *Neurourol Urodyn*. 2019;38:1222-1228.
21. Bayat M, Kumar V, Denis M, et al. Correlation of ultrasound bladder vibrometry assessment of bladder compliance with urodynamic study results. *PLoS One*. 2017;12(6):e0179598.
22. Sturm RM, Yerkes EB, Nicholas JL, et al. Ultrasound shear wave elastography: a novel method to evaluate bladder pressure. *J Urol*. 2017;198(2):422-429.
23. Nagle AS, Klausner AP, Varghese J, et al. Quantification of bladder wall biomechanics during urodynamics: a methodologic investigation using ultrasound. *J Biomech*. 2017;61: 232-241.
24. Cullingsworth ZE, Kelly BB, Deebel NA, et al. Automated quantification of low amplitude rhythmic contractions (LARC) during real-world urodynamics identifies a potential detrusor overactivity subgroup. *PLoS One*. 2018;13(8):e0201594.
25. Niederhauser T, Gafner ES, Cantieni T, et al. Detection and quantification of overactive bladder activity in patients: can we make it better and automatic? *Neurourol Urodyn*. 2018; 37(2):823-831.
26. Leitner L, Walter M, Sammer U, Knupfer SC, Mehnert U, Kessler TM. Urodynamic investigation: a valid tool to define normal lower urinary tract function? *PLoS One*. 2016;11(10):e0163847.

How to cite this article: Cullingsworth ZE, Klausner AP, Li R, et al. Comparative-fill urodynamics in individuals with and without detrusor overactivity supports a conceptual model for dynamic elasticity regulation. *Neurourology and Urodynamics*. 2020;39:707–714. https://doi.org/10.1002/nau.24255

Appendix C – Neurourology and Urodynamics Compression Paper

Received: 14 March 2019 | Accepted: 14 March 2019

DOI: 10.1002/nau.23992

ORIGINAL BASIC SCIENCE ARTICLE

WILEY Neurourology Urodynamics ICS SUFU

An external compress-release protocol induces dynamic elasticity in the porcine bladder: A novel technique for the treatment of overactive bladder?

Andrea Balthazar MD[1] | Zachary E. Cullingsworth[2] | Naveen Nandanan MD[1] | Uzoma Anele MD[1] | Natalie R. Swavely MD[1] | John E. Speich PhD[2] | Adam P. Klausner MD[1]

[1]Department of Surgery/Division of Urology, Virginia Commonwealth University School of Medicine, Richmond, Virginia

[2]Department of Mechanical and Nuclear Engineering, Virginia Commonwealth University College of Engineering, Richmond, Virginia

Correspondence
Adam P. Klausner, MD, Division of Urology, VCU Medical Center, Richmond, VA 23298-0118.
Email: adam.klausner@vcuhealth.org

Funding information
National Institute of Diabetes and Digestive and Kidney Diseases, Grant/Award Number: R01-DK101719; Virginia Commonwealth University, Grant/Award Number: School of Medicine Summer Research Fellowship Prog; NIH

Abstract

Introduction: Dynamic elasticity is an acutely regulated bladder material property through which filling and passive emptying produce strain softening, and active voiding restores baseline pressure. The aim of this study was to test the hypothesis that strain softening produced by filling-passive emptying is equivalent to that produced by compression-release in a porcine bladder model.

Methods/materials: Latex balloons and ex vivo perfused pig bladders were used for a series of alternating fill-passive emptying ("Fill") and external compress-release ("Press") protocols. For the Fill protocol balloons/bladders were (1) filled to defined volumes (prestrain softening), (2) filled to capacity to strain soften (reference), and (3) passively emptied to the original volume (poststrain softening). For the Press protocol, balloons/bladders were (1) filled to defined volumes (prestrain softening), (2) externally compressed to reference pressure and then released for five cycles (poststrain softening). After each protocol, bladders were voided with high-KCl buffer to induce "active" voiding.

Results: In both balloons and porcine bladder, both the Fill and Press protocols produced significant strain softening ($P < 0.05$) and poststrain softening pressures were not different for Fill and Press protocols ($P > 0.05$), indicating a similar degree of strain softening with both methods.

Conclusions: Repeated external compression can induce bladder strain softening similar to filling and passive emptying. This technique may represent a means to acutely regulate bladder compliance and potentially be used as a mechanical treatment for urinary urgency.

KEYWORDS
animal model, biomechanics, bladder, compliance, elasticity, overactive bladder, urodynamics

1 | INTRODUCTION

Overactive bladder (OAB) is defined as urinary urgency with or without urgency urinary incontinence, often

Zachary E. Cullingsworth contributed equally as first author.

accompanied by frequency and nocturia, in the absence of urinary tract infection or other obvious pathology.[1] OAB is a common condition that affects over 38 million Americans.[2] The impact of OAB is far reaching with significant effects on physical and mental health as well as high socioeconomic cost.[3]

Dynamic elasticity is a biomechanical property of the bladder that was identified using a comparative-fill urodynamics protocol in patients with OAB.[4] Dynamic elasticity is a material property of detrusor smooth muscle responsible for the acute changes in wall tension that can happen from one fill to another.[4] Dynamic elasticity is lost due to strain-induced stress softening ("strain softening") caused by bladder filling and passive emptying, and results in reduced intravesical pressure during subsequent filling.[4] The reduction in stiffness in a latex balloon that has been repeatedly stretched and released before inflation is a common example of strain softening and results in decreased wall tension and pressure throughout inflation, thus making the balloon easier to inflate. Once the balloon has been stretched or inflated, it will not regain the original wall tension for a given volume because the strain softening is not fully reversible. However, detrusor in both humans[5] and other mammalian species[6–14] demonstrates reversible and acutely regulated strain softening. Active voiding restores the stiffness,[6–14] and as a result, the subsequent filling pressure returns to baseline.[4] This property of acutely reversible strain softening is termed "dynamic elasticity."[4]

The repeat fill and passive empty protocol used to identify dynamic elasticity required placement of an invasive urethral catheter to facilitate passive emptying.[4] This protocol also required instillation of fluid into the bladder through the catheter, which may increase the risk of infection and cause mucosal irritation. The present study utilizes an innovative external bladder compression protocol to test the hypothesis that dynamic elasticity can be manipulated in a noninvasive manner. The aim of this study was to determine if strain softening produced by repeated noninvasive isovolumetric compression-release cycles is equivalent to strain softening produced by filling and passive emptying in an isolated perfused pig bladder model.[15,16] As a result, this study may represent an essential step toward the development of a novel, noninvasive technique to identify dynamic elasticity and to reduce intravesical pressure and possibly urinary urgency.

2 | MATERIALS AND METHODS

2.1 | Latex balloon protocol

Before testing in bladders, a latex balloon protocol was designed and implemented to test the hypothesis that strain softening accomplished through repeated application of external compression ("Compress" protocol) would be equivalent to that accomplished through repeated filling and passive emptying ("Fill" protocol). Nine-inch latex balloons were obtained from a local party supply store. An Aquarius TT urodynamics unit (Laborie Inc., Mississauga, Ontario) and an air-charged 7F single sensor catheter were used for infusion and continuous monitoring of intraluminal pressure. A catheter was inserted into each new balloon and secured to ensure the system was watertight. Balloons were divided into equal groups for the "Fill" and "Press" protocols. The balloons in the Fill group were filled to a series of volume increments at 50 mL/minute, and the quasi-steady-state intraluminal pressure (P) was recorded after a 5-minute equilibration period at each volume (Figure 1A). The prestrain-softening pressure was recorded at 1500 mL (Figure 1A; P_{pre}). The balloon was then strain-softened by increasing the fill volume to 3000 mL, and the peak pressure was recorded as a reference (Figure 1A, P_{ref}). Half the volume was removed from the balloon via syringe aspiration (back to 1500 ml), and the poststrain-softening pressure was recorded (Figure 1A; P_{post}). The Press protocol was implemented on a separate group of new balloons (Figure 1B). These balloons were filled to 1500 mL as described in the Fill protocol, and prestrain-softening pressure was recorded (Figure 1B; P_{pre}). Then balloons were subjected to an external compression and release protocol (Figure 1B) in which external force was applied to the surface of the balloon using the base of a graduate cylinder to evenly distribute the force. To strain-soften to a similar degree level as seen in the Fill protocol, external compression was increased until the pressure was equivalent to the average P_{ref} from all balloons in the Fill protocol. Five press and release cycles were performed with 15 seconds of compression and 15 seconds of release in each cycle, and the average maximum pressure during compression (P_{max}) was recorded. The poststrain-softening pressure (Figure 1B; P_{post}) was recorded after the final release, and the balloon was then emptied via syringe aspiration. The degree of strain softening induced by each protocol was determined by comparing the poststrain softening vs prestrain softening pressures (P_{post} vs P_{pre}).

2.2 | Porcine bladder protocol – harvest and preparation

Bladders from adult male (castrated) and female pigs were obtained from local abattoirs immediately after slaughter. As previously described, the dissection included removal of the bladder, urethra, ureters, and vascular tree including a section of the aorta, iliac arteries, branching vesical arteries, and corresponding venous system.[15,16] The aorta was cannulated and cold-perfused with heparinized Krebs-Henseleit (KH) buffer.[15,16] Tissues were stored in

Appendix

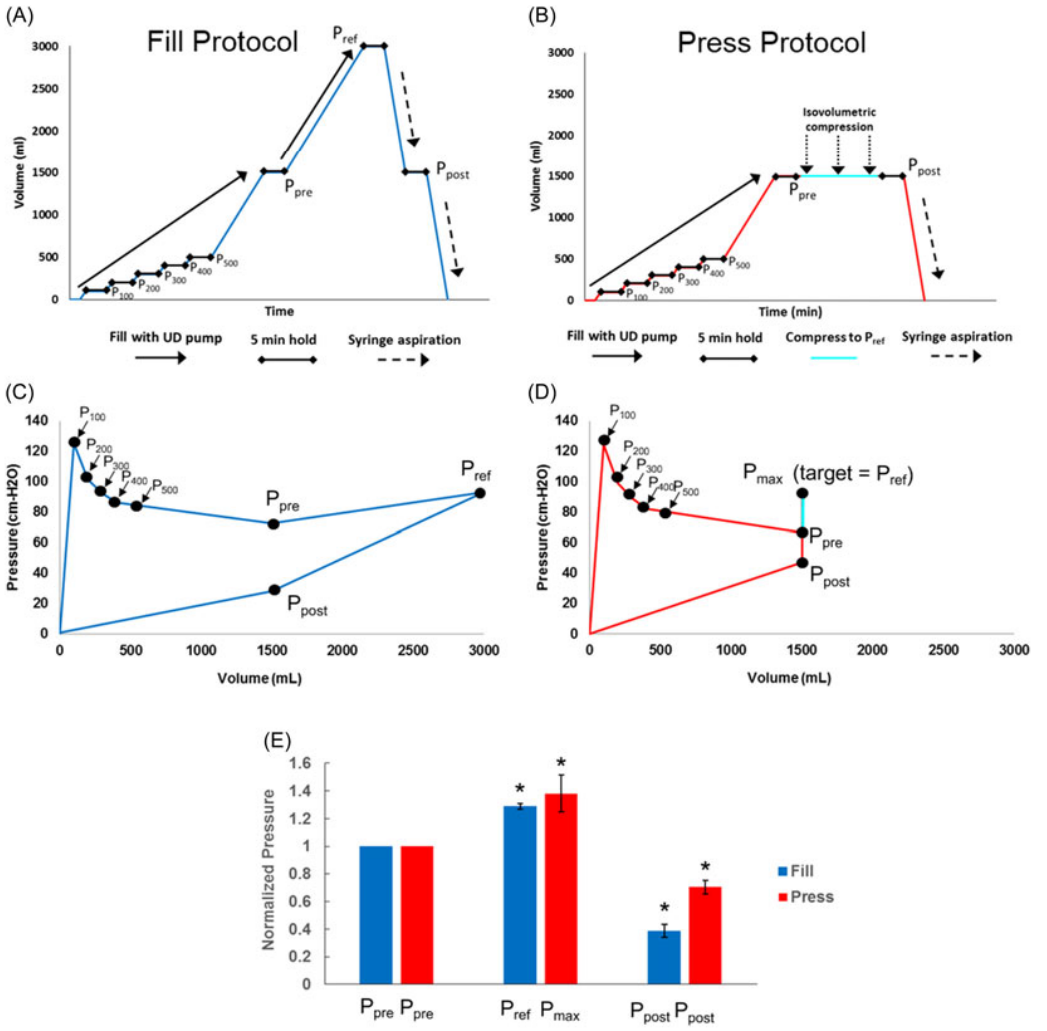

FIGURE 1 Fill (A) and Press (B) protocols for balloons. Pressures ($P_{100\text{-}500}$) were recorded at increasing volumes (100-500 mL, respectively). For each protocol, volume was increased to 1500 mL, and prestrain softening pressures (P_{pre}) were recorded. In the Fill protocol (A), volume was increased to 3000 mL to strain soften and peak pressure (P_{ref}) was recorded. Poststrain-softening (P_{post}) was recorded after syringe aspiration back to 1500 mL. In the Press protocol (B), balloons were compressed five times to P_{max} and poststrain softening pressures (P_{post}) were recorded. Average pressure values for the Fill (C) and Press (D) protocols are presented as a series of pseudo-steady-state pressure values with connecting lines to illustrate their sequence. (E) Normalized prestrain softening, maximum and poststrain softening pressures for the Fill and Press protocols (*indicates a value significantly different from 1.0, n = 5 for each protocol; $P < 0.05$). Poststrain softening pressures were significantly less than the prestrain softening pressures for both the Fill and Press methods (E; $P < 0.05$)

3-(N-morpholino) propanesulfonic acid (MOPS) based buffer and transported to the lab for use within approximately 3 hours or stored for use within 48 hours.[15,16] Excess tissue was removed and vesical arteries were cannulated at their branch points in the aorta using polyethylene tubing. Both ureters were suture-ligated and urethra was cannulated with both a 16F straight catheter to permit drainage and a 7F Laborie urethral catheter that was connected to the Aquarius TT urodynamics system for infusion and pressure monitoring. Bladders were filled with 50 mL of 0.9% normal saline,

perfused with KH buffer at 4 mL/minute, and warmed to a physiologic temperature in a customized chamber (Figure 2) during a 45-minute equilibration period as previously described.[15]

2.3 | Porcine bladder protocol – perfusion and data acquisition

Using the previously developed system (Figure 2), bladders were perfused with KH buffer gassed with 95%/5% O_2/CO_2 in a humidified and heated reservoir.[15] Perfusate was pumped through an in-line Transpac IV pressure transducer (ICU Medical, San Clemente, CA) and an in-line ultrasonic flowmeter (IUF-1000; Radnoti LLC, Coniva, CA) as previously described.[15] A buffer was pumped through the bilaterally cannulated vesical arteries, and perfusion was maintained at 4 mL/minute based on prior study data.[15] A T-DOC 7F single sensor air-charged bladder catheter permitted both measurement of intravesical pressure and bladder filling at 50 mL/minute. Data acquisition was performed using the Aquarius TT and a BIOPAC MP150 transducer with AcqKnowledge 4.2 software (BIOPAC Systems).

2.4 | Porcine bladder protocol – fill and press

As in the balloon study, fill-passive emptying ("Fill"; Figure 3A) and external compress-release ("Press"; Figure 3B) protocols were developed. Each pig bladder was subjected to two Fill and two Press protocols in the following sequence: Fill1 → Press1→ Fill2 → Press2. For both protocols, pressure recordings were made after 5 minute periods of equilibration.

For the Fill protocol (Figure 3A), after an initial 45-minute equilibration period at a volume of 50 mL, each bladder was filled to 250 mL using the urodynamics pump, and the prestrain softening pressure was recorded (Figure 3A; P_{pre}). Next, bladder volume was increased to 500 mL to strain soften the bladder, and the peak (reference) pressure was recorded (Figure 3A; P_{ref}). Then, the bladder was passively emptied to 250 mL and the poststrain softening pressure was recorded (Figure 3A; P_{post}). Passive emptying was performed via syringe aspiration using a single action pump system (Boston Scientific, Marlborough, MA). Finally, an "active void" was performed by bathing the bladder in a potassium-enriched (110 mM KCl) solution (Figure 3A). This active void was performed to remove the remaining volume through the 16F urethral catheter and to reverse strain softening based on previous studies.[4–6,9]

The Press protocol (Figure 3B) was performed after the Fill protocol by filling the same bladder to 250 mL and measuring the prestrain softening pressure (Figure 3B; P_{pre}). Then, the bladder was strain-softened using manual external compression to deform (strain) the bladder and increase the pressure to the peak pressure recorded at 500 mL (P_{ref}) during the previous Fill protocol. This pressure was held and released for 15 seconds intervals, and the compression-release cycles were repeated five times. The average maximum pressure was recorded (P_{max}). Then, as in the Fill protocol, the poststrain softening pressure was recorded (Figure 3B; P_{post}). Finally, an "active void" was performed to remove the remaining volume and reverse strain softening (Figure 3B) as described in the Fill protocol. The degree of strain softening was determined by comparing the intravesical pressures pre vs. poststrain softening in both the Fill and Press protocols.

2.5 | Statistics

Statistical analyses of the data were performed via a two-way, paired Student *t* test. Significance was defined as $P < 0.05$, and all values were reported as a mean ± SEM with n representing the number of balloons or bladders used in each comparison.

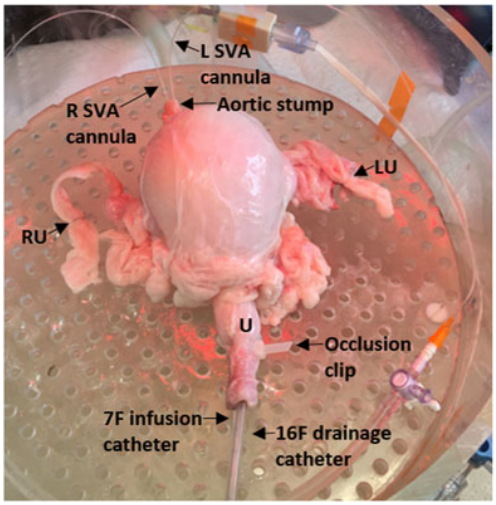

FIGURE 2 Photo of a porcine bladder perfused in an apparatus designed to maintain physiologic conditions. The picture shows the left and right superior vesical artery (SVA) cannulas through the aortic stump, ligation of both the right (RU) and left (LU) ureters, a 7F Laborie catheter for filling and pressure monitoring and a 16F urethral catheter for drainage in the urethra (U). An occlusion clip on the urethra prevents any leakage from around the catheters

Appendix

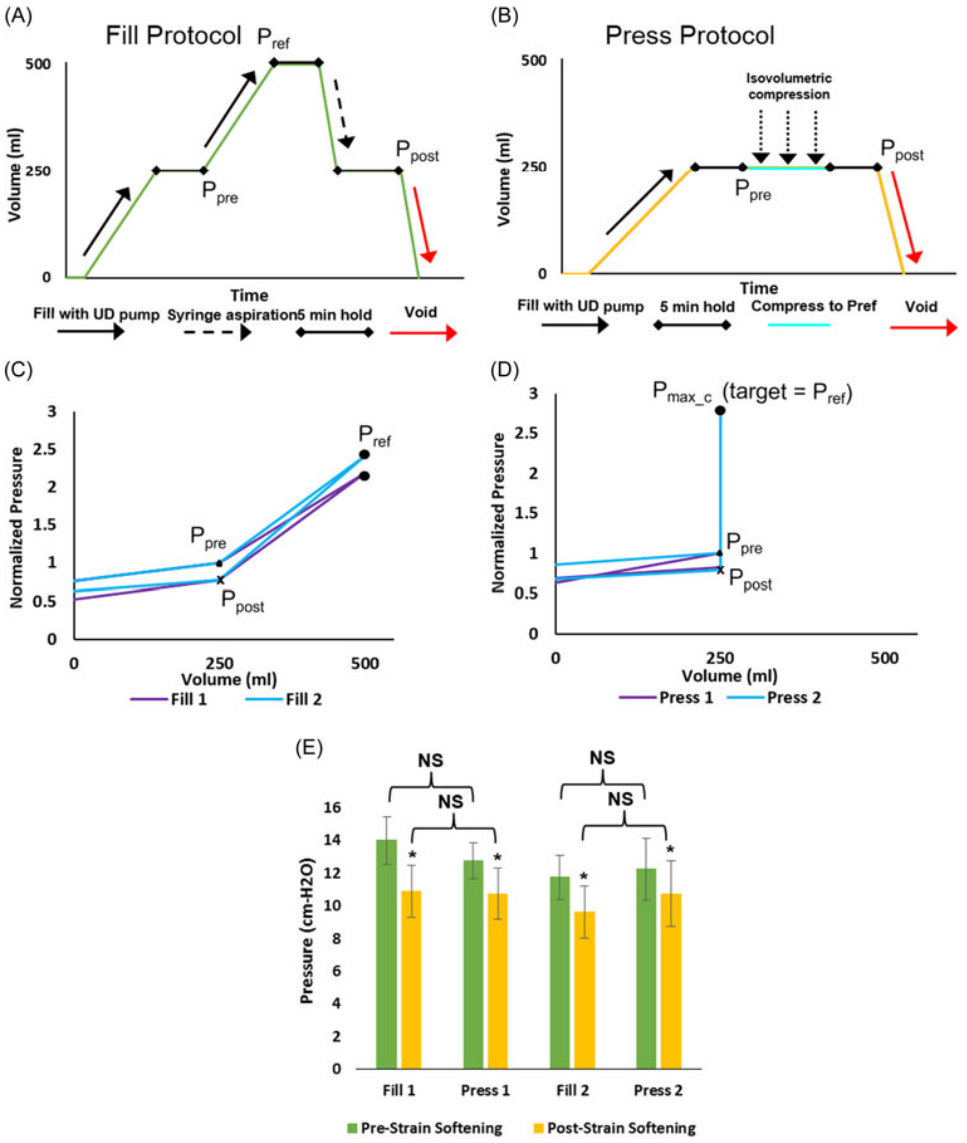

FIGURE 3 Fill (A) and Press (B) protocols for the porcine bladder model. For each protocol, the bladder was filled to 250 mL, and prestrain softening pressures (P_{pre}) were recorded. In the Fill protocol (A), volume was increased to 500 mL to strain soften and peak pressure (P_{ref}) was recorded. Poststrain softening pressure (P_{post}) was recorded after syringe aspiration back to 250 mL. In the Press protocol (B), bladders were compressed five times to P_{max} and poststrain softening pressures (P_{post}) were recorded. At the end of each protocol, a high-KCl buffer was used to induce an active void (A-B, red arrows). Average pressure values for the Fill (C) and Press (D) protocols were normalized to P_{pre} values and presented as a series of pseudo-steady-state pressure values with connecting lines to illustrate their sequence. (E) Poststrain softening pressures were significantly less than prestrain softening pressures for both the Fill and Press protocols (E; n = 8; $^{*}P < 0.05$). Poststrain softening pressures were not significantly different for the Fill and Press methods (E; NS; $P > 0.05$), indicating a similar degree of strain softening. Strain softening was repeatable in both the Fill and Press protocols in the same bladders, indicating the reversibility of strain softening in the pig bladders (E; Fill2 and Press2). NS, nonsignificant

Appendix

2.6 | Ethical approval

The Institutional Animal Care and Use Committee at Virginia Commonwealth University approved this study.

3 | RESULTS

3.1 | Latex balloons

In the balloon study, the Fill (N = 5) and Press (N = 5) protocols both caused significant decreases in pressure when comparing poststrain-softening pressure (P_{post}) to prestrain softening pressure (P_{pre}) (Figure 1C-E; $P = 0.0002$). These results indicate that both the Fill and Press protocols caused strain softening in the balloon and motivated similar studies in porcine bladders.

3.2 | Porcine bladders

In porcine bladders (N = 8), strain softening occurred in both the Fill and Press protocols (Figure 3C-E; $P < 0.05$). In addition, poststrain-softening pressures were not different for the Fill and Press protocols (Figure 3C-E; $P > 0.05$), suggesting a similar degree of strain softening was induced by each method. Prestrain-softening pressures were restored during each fill after active voiding (Figure 3E; $P > 0.05$), demonstrating reversible strain-softening, and both the Fill and Press results were repeatable in the same bladders (Figure 3E; "Fill2" and "Press2").

4 | DISCUSSION

Reversible strain-softening has been quantified as dynamic elasticity during comparative-fill urodynamics in patients with OAB,[4] and reveals that elasticity during bladder filling can be acutely regulated as a function of recent strain and contractile activity. Tension sensors in the bladder wall are responsible for the afferent nerve activity associated with the sensation of urgency when bladder volume increases[17]; therefore, any defect in the mechanisms that regulate dynamic elasticity could contribute to OAB. The novel contribution of the present study is the quantification of reversible strain-softening in an ex vivo porcine model through both a filling and passive emptying protocol and an isovolumetric compression protocol. These findings are important because pig bladders may provide a valuable model for studying the mechanisms responsible for dynamic elasticity, and the Press protocol demonstrates the feasibility of manipulating dynamic elasticity in humans using noninvasive abdominal compression.

Dynamic elasticity can be quantified during urodynamics,[4] but the procedure involves invasive catheter placement that may cause anxiety and discomfort and has an increased risk of urinary tract infection. The American Urological Association has guidelines regarding the treatment of OAB and lists noninvasive pelvic floor muscle therapy (PFMT) as a conservative first-line therapy. The conservative first-line therapy includes behavioral therapy, such as bladder training, lifestyle changes, dietary changes, PFMT, and biofeedback. The first-line conservative therapies have potential benefits and are associated with little to no risk of adverse effects.[18] In terms of PFMT, it is well-established that this therapy is associated with improved urinary incontinence. In 2015 a Cochrane review complied level 1 evidence supporting supervised PFMT for the treatment of urge, stress, and mixed incontinence in women.[19] Potential benefits of PFMT include improved pelvic floor muscle strength, endurance, and coordination through improved control and muscle strength.[20]

The compression-release protocol developed in this study represents a noninvasive form of PFMT that could potentially be used to reduce urgency by decreasing the load on tension sensors in the bladder wall associated with sensation. It was previously proposed that derangements in the processes regulating in dynamic elasticity may contribute to the pathophysiology of OAB as the alterations could be responsible for increased urgency at lower bladder volumes.[4] The present study demonstrates intravesical pressure could be decreased using strain softening induced by repeated compression of the bladder. Therefore, we hypothesize that repeated applications of external compression and release applied to the bladder could induce strain softening, lower bladder pressure, prolong the filling phase of micturition and reduce urgency associated with OAB.

A limitation of the present study is that the ex vivo pig model may not be representative of human bladder function; however reversible dynamic elasticity has been identified in multiple mammalian species, including humans.[4] Further studies are warranted, including in vivo porcine studies to refine and characterize the manipulation of dynamic elasticity using compression. Another limitation of a theoretical use of compression as both a diagnostic or therapeutic technique for OAB is that applying abdominal compression may exacerbate the need void. Thus, studies to identify the magnitude of compression are needed, and the optimal timing and volume at which to apply compression would be required.

5 | CONCLUSIONS

A prior study identified dynamic elasticity in patients with OAB during urodynamics.[4] The present study

Appendix

demonstrated that both filling and isovolumetric compression produce measurable strain softening in a balloon model and in an ex vivo perfused porcine bladder model. The study also showed that strain softening in the porcine model is acutely reversible. The novel, noninvasive compress-release technique has potential diagnostic and therapeutic applications. External compression may have diagnostic value as a means to induce strain softening without an invasive urodynamics catheter. Furthermore, a reduction in intravesical pressure through a compress-release technique may allow prolonged filling and lead to a reduction in symptoms associated with OAB.

ACKNOWLEDGMENTS

Dr. Martin Mangino provided valuable advice regarding the experimental setup, and College of Engineering students Sydney Roberts and Ryan Musselman assisted with the experimental protocols. This work was funded by the NIH (R01-DK101719) and from the Virginia Commonwealth University School of Medicine Summer Research Fellowship Program.

ORCID

Zachary E. Cullingsworth http://orcid.org/0000-0002-4087-9764
John E. Speich http://orcid.org/0000-0002-8824-4098
Adam P. Klausner http://orcid.org/0000-0003-3849-7131

REFERENCES

1. Haylen BT, de Ridder D, Freeman RM, et al. An International Urogynecological Association (IUGA)/International Continence Society (ICS) joint report on the terminology for female pelvic floor dysfunction. *Int Urogynecol J*. 2010;21(1):5-26.
2. Stewart WF, Van Rooyen JB, Cundiff GW, et al. Prevalence and burden of overactive bladder in the United States. *World J Urol*. 2003;20(6):327-336.
3. Durden E, Walker D, Gray S, Fowler R, Juneau P, Gooch K. The economic burden of overactive bladder (OAB) and its effects on the costs associated with other chronic, age-related comorbidities in the United States. *Neurourol Urodyn*. 2018;37(5):1641-1649.
4. Colhoun AF, Klausner AP, Nagle AS, et al. A pilot study to measure dynamic elasticity of the bladder during urodynamics. *Neurourol Urodyn*. 2017;36(4):1086-1090.
5. Colhoun AF, Speich JE, Dolat MT, et al. Acute length adaptation and adjustable preload in the human detrusor. *Neurourol Urodyn*. 2016;35(7):792-797.
6. Speich JE, Borgsmiller L, Call C, Mohr R, Ratz PH. ROK-induced cross-link formation stiffens passive muscle: reversible strain-induced stress softening in rabbit detrusor. *Am J Physiol Cell Physiol*. 2005;289(1):C12-C21.
7. Speich JE, Quintero K, Dosier C, Borgsmiller L, Koo HP, Ratz PH. A mechanical model for adjustable passive stiffness in rabbit detrusor. *J Appl Physiol*. 2006;101(4):1189-1198.
8. Speich JE, Dosier C, Borgsmiller L, Quintero K, Koo HP, Ratz PH. Adjustable passive length-tension curve in rabbit detrusor smooth muscle. *J Appl Physiol*. 2007;102(5):1746-1755.
9. Ratz PH, Speich JE. Evidence that actomyosin cross bridges contribute to "passive" tension in detrusor smooth muscle. *Am J Physiol Renal Physiol*. 2010;298(6):F1424-F1435.
10. Almasri AM, Ratz PH, Bhatia H, Klausner AP, Speich JE. Rhythmic contraction generates adjustable passive stiffness in rabbit detrusor. *J Appl Physiol*. 2010;108(3):544-553.
11. Almasri AM, Ratz PH, Speich JE. Length adaptation of the passive-to-active tension ratio in rabbit detrusor. *Ann Biomed Eng*. 2010;38(8):2594-2605.
12. Speich JE, Southern JB, Henderson S, Wilson CW, Klausner AP, Ratz PH. Adjustable passive stiffness in mouse bladder: regulated by Rho kinase and elevated following partial bladder outlet obstruction. *Am J Physiol Renal Physiol*. 2012;302(8):F967-F976.
13. Southern JB, Frazier JR, Miner AS, Speich JE, Klausner AP, Ratz PH. Elevated steady-state bladder preload activates myosin phosphorylation: detrusor smooth muscle is a preload tension sensor. *Am J Physiol Renal Physiol*. 2012;303(11):F1517-F1526.
14. Speich JE, Wilson CW, Almasri AM, Southern JB, Klausner AP, Ratz PH. Carbachol-induced volume adaptation in mouse bladder and length adaptation via rhythmic contraction in rabbit detrusor. *Ann Biomed Eng*. 2012;40(10):2266-2276.
15. Anele UA, Ratz PH, Colhoun AF, et al. Potential vascular mechanisms in an ex vivo functional pig bladder model. *Neurourol Urodyn*. 2018;37:2425-2433.
16. Vince R, Tracey A, Deebel NA, et al. Effects of vesical and perfusion pressure on perfusate flow, and flow on vesical pressure, in the isolated perfused working pig bladder reveal a potential mechanism for the regulation of detrusor compliance. *Neurourol Urodyn*. 2018;37(2):642-649.
17. Kanai A, Andersson KE. Bladder afferent signaling: recent findings. *J Urol*. 2010;183(4):1288-1295.
18. Winters JC, Dmochowski RR, Goldman HB, et al. AUA/SUFU Guidelines: Urodynamics. 2012. http://www.auanet.org/education/guidelines/adult-urodynamics.cfm
19. Dumoulin C, Hay-Smith J, Habee-Seguin GM, Mercier J. Pelvic floor muscle training versus no treatment, or inactive control treatments, for urinary incontinence in women: a short version Cochrane systematic review with meta-analysis. *Neurourol Urodyn*. 2015;34(4):300-308.
20. Willis-Gray MG, Dieter AA, Geller EJ. Evaluation and management of overactive bladder: strategies for optimizing care. *Res Rep Urol*. 2016;8:113-122.

How to cite this article: Balthazar A, Cullingsworth ZE, Nandanan N, et al. An external compress-release protocol induces dynamic elasticity in the porcine bladder: A novel technique for the treatment of overactive bladder? *Neurourology and Urodynamics*. 2019;1-7. https://doi.org/10.1002/nau.23992